Chem Soc Rev

Directing Evolution of Novel Ligands by mRNA Display

Journal:	*Chemical Society Reviews*
Manuscript ID	CS-SYN-02-2021-000160.R2
Article Type:	Review Article
Date Submitted by the Author:	21-May-2021
Complete List of Authors:	Kamalinia, Golnaz; USC Dana and David Dornsife College of Letters, Arts and Sciences, Chemical Engineering and Materials Science, and Molecular and Computational Biology Grindel, Brian J; UT MD Anderson Cancer Center, Cancer Systems Imaging Takahashi, Terry; University of Southern California, Department of Chemistry Millward, Steven; Univerisity of Texas MD Anderson Cancer Center, Cancer Systems Imaging Roberts, Richard W.; USC Dana and David Dornsife College of Letters, Arts and Sciences, Chemical Engineering and Materials Science, and Molecular and Computational Biology

Directing Evolution of Novel Ligands by mRNA Display

Golnaz Kamalinia[1], Brian J. Grindel[2], Terry T. Takahashi[1,*], Steven W. Millward[2,*], Richard W. Roberts[3,4*]

1. Department of Chemistry, University of Southern California, Los Angeles, CA
2. Department of Cancer Systems Imaging, University of Texas MD Anderson Cancer Center, Houston, TX
3. Department of Chemistry and Mork Family Department of Chemical Engineering and Materials Science, University of Southern California, Los Angeles, CA.
4. USC Norris Comprehensive Cancer Center, Los Angeles, CA.

*To whom correspondence should be addressed: tttakaha@usc.edu, smillward@mdanderson.org, richrob@usc.edu

Abstract

mRNA display is a powerful biological display platform for the directed evolution of proteins and peptides. mRNA display libraries covalently link the displayed peptide or protein (phenotype) with the encoding genetic information (genotype) through the biochemical activity of the small molecule puromycin. Selection for peptide/protein function is followed by amplification of the linked genetic material and generation of a library enriched in functional sequences. Iterative selection cycles are then performed until the desired level of function is achieved, at which time the identity of candidate peptides can be obtained by sequencing the genetic material.

The purpose of this review is to discuss the development of mRNA display technology since its inception in 1997 and to comprehensively review its use in the selection of novel peptides and proteins. We begin with an overview of the biochemical mechanism of mRNA display and its variants with a particular focus on its advantages and disadvantages relative to other biological display technologies. We then discuss the importance of scaffold choice in mRNA display selections and review the results of selection experiments with biological (e.g., fibronectin) and linear peptide library architectures. We then explore recent progress in the development of “drug-like” peptides by mRNA display through the post-translational covalent macrocyclization and incorporation of non-proteogenic functionalities. We conclude with an examination of enabling technologies that increase the speed of selection experiments, enhance the information obtained in post-selection sequence analysis, and facilitate high-throughput characterization of lead compounds. We hope to provide the reader with a comprehensive view of current state and future trajectory of mRNA display and its broad utility as a peptide and protein design tool.

Keywords: mRNA display, directed evolution, *in vitro* selection, non-natural amino acids, macrocyclization, next generation sequencing

1 Overview

New functional proteins and peptides can aid in the development of new therapeutics to treat human disease or function as molecular tools to help solve biological and chemical problems. Despite recent advances in the rational design of proteins,[1] directed evolution remains an important and robust functional solution to engineer new protein and peptide function. In directed evolution, a large library of diverse proteins is first partitioned for a desired function and the functional molecules are subsequently amplified. This process is repeated until most to all of the pool is highly enriched in molecules that perform the desired task (**Figure 1**).

A key requirement for directed evolution is that the genotype (i.e., DNA or RNA) and phenotype (function) of the molecules must be linked, otherwise amplification of the "fittest" sequences is impossible. The directed evolution of proteins presents a challenge: once a protein is synthesized during translation, its sequence information is lost; no current methods are capable of reverse translation nor can the protein be directly amplified through a process analogous to polymerase chain reaction (PCR). Several "display" methods have been developed to link a protein to its encoding genetic material including phage display (PD)[2, 3], mRNA display,[4] ribosome display,[5] peptides-on-plasmids,[6] and CIS display.[7] For a comprehensive discussion of biological display technologies, the reader is directed to these reviews.[8-12]

Of these display methods, mRNA display has several unique advantages over other display techniques including the ability to generate the most diverse peptide libraries and the ability to engineer drug-like peptides containing unnatural amino acids. Over the last 20 years, mRNA display has been used to develop high affinity ligands against a wide range of targets including intracellular proteins, extracellular proteins, membrane proteins, and RNA. In this review, we first introduce basic mRNA display principles, mechanisms, and variants. We define mRNA display as any technique using puromycin to link genetic information to proteins and/or peptides. We discuss the application of mRNA display to engineer new proteins, peptides, and drug-like peptides and efforts to use these new molecules as tools for chemical biology, molecular imaging, and therapy. Finally, we highlight recent technological advances to improve mRNA display, including increasing speed and depth of post-selection analysis.

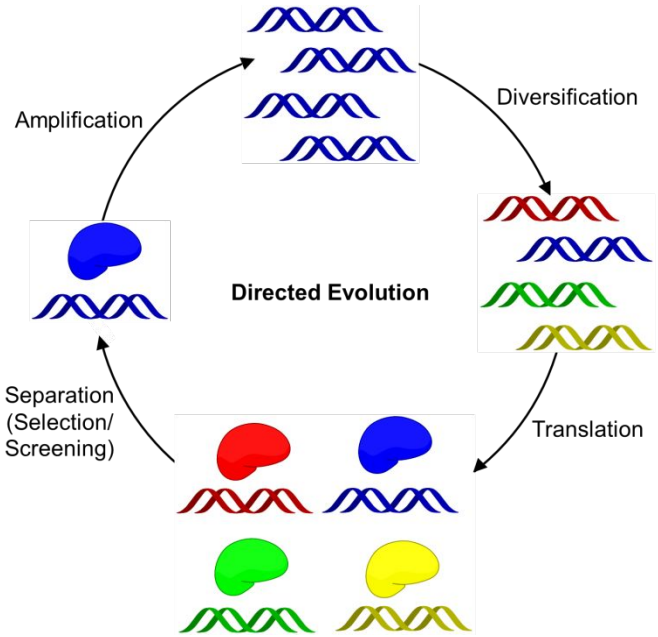

Figure 1. Directed evolution process. In directed evolution, a library of molecules is subjected to a selective step that separates functional and non-functional molecules. Functional molecules are then amplified to generate a library for the next round of selection. This process is repeated until the library is dominated by functional molecules. Directed evolution requires that the genotype (e.g., DNA or RNA) is linked to its corresponding phenotype (function).

mRNA display is an elegant solution to the display problem as it involves simply linking a protein to its encoding mRNA.[4] This is accomplished by appending puromycin to the 3' end of an mRNA via a molecular spacer (**Figure 2**). Puromycin is an antibiotic that mimics the 3' end of an aminoacylated tRNA (**Figure 3**) and acts as a bridge between mRNA and protein. The resulting fusion of mRNA and protein (i.e., an mRNA-protein fusion) generates a molecular "Rosetta Stone," allowing the sequence of the peptide to be recovered by reverse transcription/PCR of the linked nucleic acid followed by DNA sequencing.

A typical mRNA display *in vitro* selection cycle is shown in **Figure 4**. A DNA library, obtained from synthetic or natural sources, is first transcribed into mRNA. A linker containing puromycin is attached to the 3' end of the mRNA and the resulting mRNA-puromycin template is translated *in vitro*. The resulting mRNA-protein fusion is typically reverse transcribed into a cDNA/mRNA duplex, which prevents the inadvertent selection of RNA aptamers. The pool of mRNA-peptide fusions is then subjected to a selective step, typically binding to an immobilized macromolecular target, which separates functional and non-functional sequences. Non-functional sequences are washed away and cDNA from functional sequences is amplified by PCR, generating a dsDNA library enriched in functional

sequences. This library can either be used for more rounds of selection or sequenced to identify the functional protein sequences.

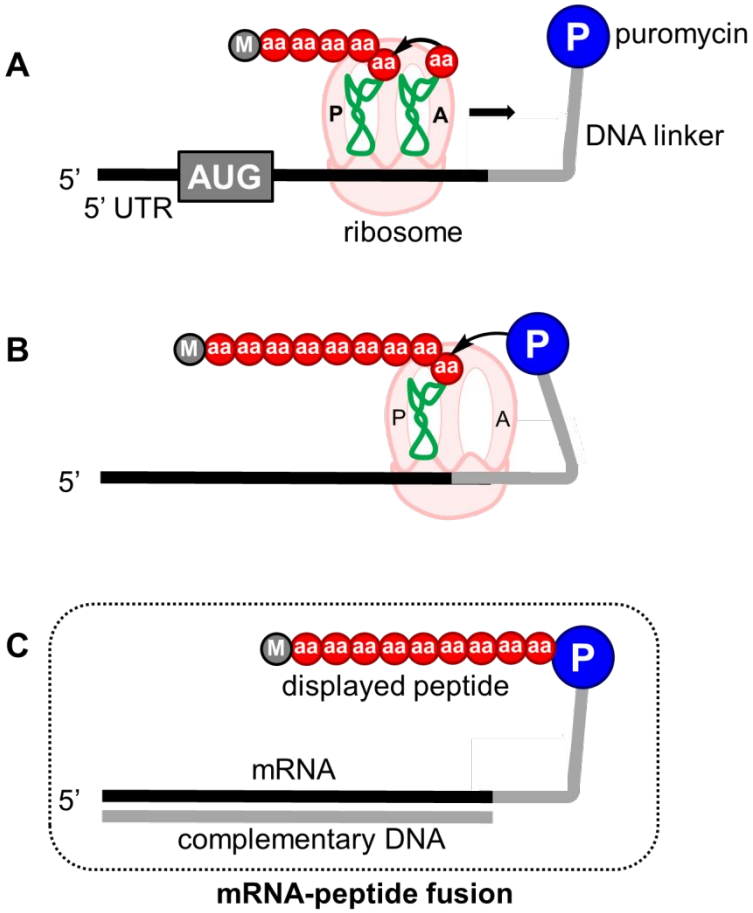

Figure 2. mRNA-peptide fusion formation. (A) puromycin-ligated mRNA is translated by the ribosome (pink) *in vitro*. **(B)** When the ribosome reaches the mRNA/DNA junction, puromycin enters the A site of the ribosome, forming a covalent bond with the C-terminus of the nascent peptide, generating an mRNA-peptide fusion. **(C)** The mRNA strand is reverse transcribed into cDNA, enabling sequence amplification and identification, and eliminating RNA secondary structure.

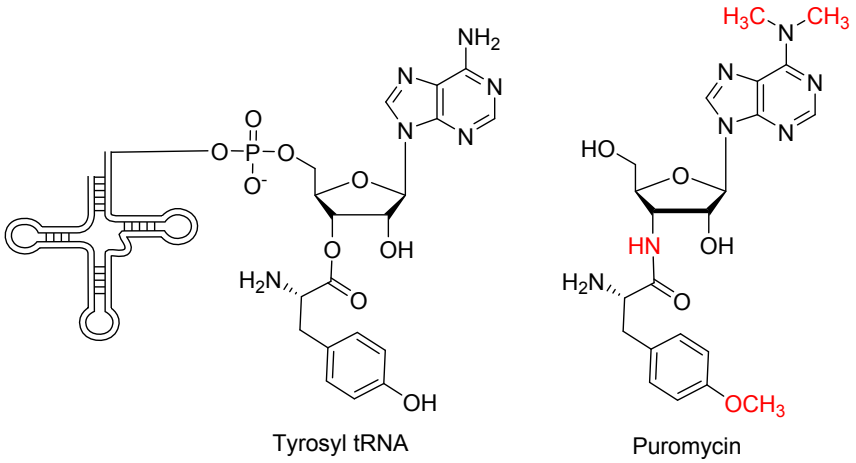

Figure 3. Structures of Tyrosyl tRNA and puromycin. Puromycin is a structural mimic of the 3' end of aminoacylated tRNA. The differences between puromycin and tyrosyl tRNA are highlighted in red

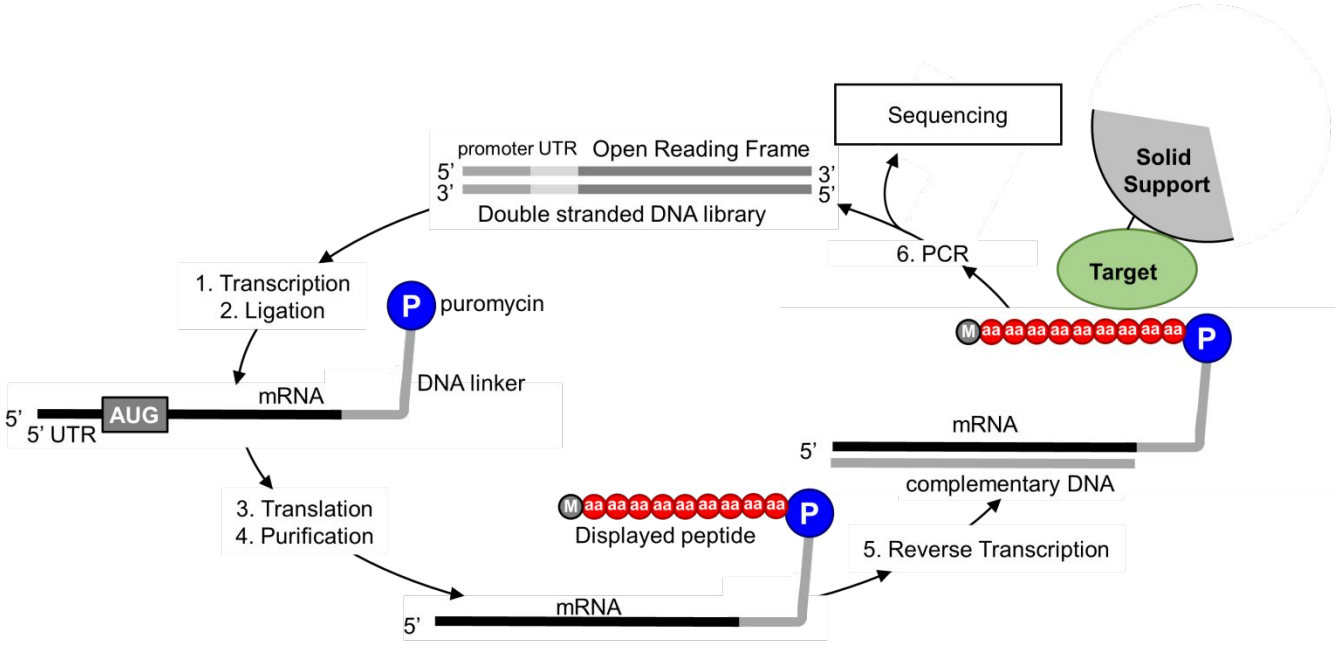

Figure 4. mRNA display cycle. A library of dsDNA consisting of a 5' promoter and 5' untranslated region (UTR) is PCR amplified and transcribed into an mRNA library which is subsequently ligated to a puromycin-linker. The ligated mRNA library is then translated *in vitro* to form a library of mRNA-peptide fusion molecules. The mRNA-peptide fusion library is then reverse transcribed and panned against the target of interest to isolate functional sequences. PCR amplification regenerates the DNA library, which can be used for another round of selection or sequenced to identify functional peptides.

2 mRNA Display

2.1 mRNA Display Mechanism

All mRNA display formats require a DNA library with a 5' promoter for transcription (e.g., for T7 RNA polymerase), a 5' untranslated region (UTR) for the preferred cell-free translation system, start

codon, open reading frame (ORF; usually containing a mix of fixed and random codons), and a 3' UTR used for RT-PCR amplification. Libraries can be constructed to include an affinity purification tag (e.g., His tag, FLAG tag, hemagglutinin (HA)-tag, etc.) or chemical moiety for purification.

The *in vitro* translation systems used in mRNA display can be bacterial, eukaryotic, or a synthetic reconstitution of selected proteins from either source. The current model for fusion formation involves translation of an mRNA template until the ribosome reaches the RNA/DNA junction and stalls. There, puromycin enters the A-site and the peptidyl transferase activity of the ribosome catalyzes the formation of an amide bond between the primary amino group of puromycin and the C-terminus of the nascent protein chain in the P-site (**Figure 2**). This fusion formation reaction must occur "in cis," i.e., an mRNA template must be fused to the protein that it encodes. A "trans" reaction – an mRNA fused to a protein translated by another mRNA – would result in a mixed message, preventing directed evolution. Early experiments showed that translation of two templates of different lengths resulted in only the correctly fused products. No mixed products were observed, supporting a cis fusion formation model.[4, 13] Experiments optimizing the linker length between mRNA and puromycin also support a model for cis fusion formation. Increasing the linker length beyond ~30 nucleotides (which roughly spans a distance corresponding to that between the mRNA decoding site and the peptidyl transferase center) results in decreased fusion formation efficiency, suggesting that trans products would be unlikely to form.[13] Lastly, many new ligands have been engineered using mRNA display, which would not be possible unless the fidelity of fusion formation between mRNA and protein within the same ribosome is preserved.

Ribosomal stalling at the mRNA/DNA junction also seems to play an important role in fusion formation. In a study to determine where puromycin can enter the ribosome, Starck *et al.* used a biotinylated derivative of puromycin to pull-down puromycin-terminated products.[14] Rather than observing random puromycin entry at many sites in the sequence, this group observed that puromycin only terminated translation at distinct sites in the protein sequence. This observation suggested that these sites corresponded to ribosomal pause points during translation of the mRNA, supporting the idea that a pause during translation in mRNA display is important for puromycin entry. When the mRNA template is linked to puromycin through a DNA linker (typically poly-dA), the DNA-RNA junction provides an efficient pause site.[13] In TRAP display (Transcription−Translation coupled with Association of Puromycin linker), a UAG stop codon is placed at the 3' end of the ORF to induce ribosomal pausing.[15]

2.2 mRNA Display Variants

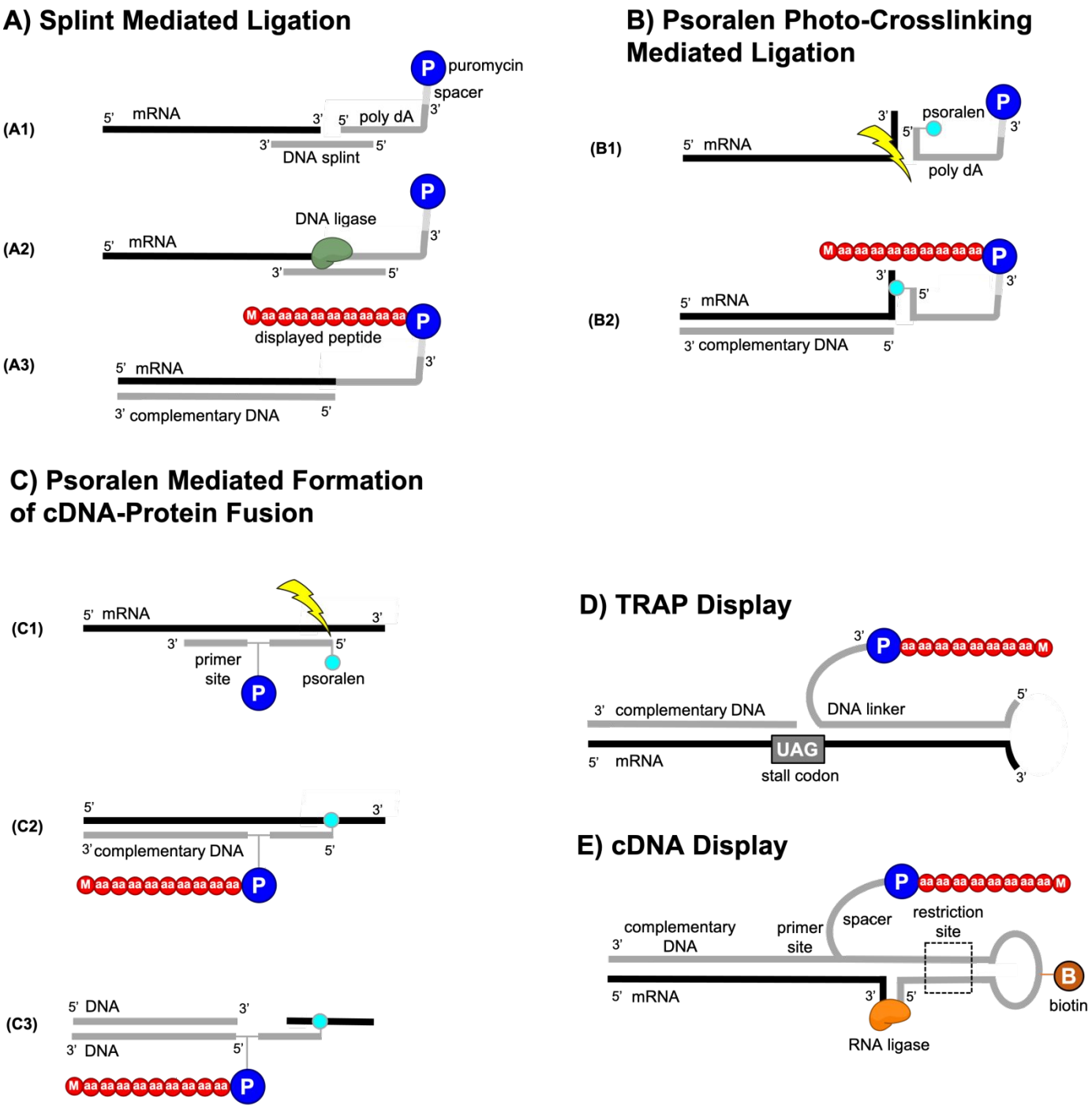

Figure 5. mRNA Display Variants. All mRNA display systems use puromycin to conjugate a protein to its encoding mRNA. How the puromycin linker is attached to the mRNA differs between mRNA display variants. DNA is represented by grey lines while RNA is represented by black lines. **(A)** Classical mRNA display uses a DNA splint in the ligation between mRNA and the linker. The puromycin linker contains a poly dA stretch to stall the ribosome for puromycin entry and serve as an affinity handle for poly-deoxythymidine (dT) purification after fusion formation. Psoralen mediated photo-crosslinking can also be used to form (**B**) mRNA-protein fusions or **(C)** cDNA-protein fusions. **(D)** In TRAP display, the puromycin linker is not covalently attached to the mRNA and the mRNA 3' UTR contains a UAG codon to stall the ribosome and enhance puromycin entry.

(E) In cDNA display, the puromycin linker consists of four main parts including a ligation site, a restriction site, a reverse transcription primer site, and a biotin site.

Several variants of mRNA display have been developed, all of which use puromycin as the means to link mRNA and protein (**Figure 5**). These technologies include Profusion™,[16] *in vitro* virus (IVV) display,[17] cDNA display,[18] and TRAP display.[15] The main difference in these variants lies in the structure of the puromycin linker that bridges mRNA and protein. The original mRNA display linker consisted of a simple deoxyadenosine spacer (5' – dA_{27}dCdC**P** – 3', where **P** = puromycin),[4] which was trademarked as Profusion™ technology.[13, 16] Subsequent optimization experiments showed that increased flexibility in the linker, introduced via incorporation of polyethylene glycol spacers (Spacer 9), resulted in higher rates of fusion formation between mRNA and translated protein.[13] In both cases, these puromycin linkers were ligated to mRNA using T4 DNA Ligase in the presence of a DNA splint (**Figure 5A**).[19] Alternatively, the puromycin linker can be added to the mRNA using photo-crosslinking by incorporating a psoralen[20, 21] (**Figure 5B**) or a 3-cyanovinylcarbazole nucleoside (^{CNV}K).[22] The advantage of psoralen ligation is that the ligated product can be directly translated without a gel purification step, whereas splint-mediated ligation requires gel purification to eliminate the DNA splint that can lead to RNase H-mediated degradation of the mRNA.[23] Similarly, a branched puromycin linker containing both psoralen and a reverse transcription primer (**Figure 5C**) can be used to create a cDNA-protein fusion or a dsDNA-protein fusion, which both show higher stability versus mRNA-protein fusions in environments where RNase is present.[20]

The IVV approach to mRNA display was named for an mRNA-protein fusion's similarity to a simple retrovirus.[17] In this system, puromycin is attached to mRNA via a DNA/RNA chimera nucleotide termed a "P-acceptor" and a 105 nucleotide DNA spacer linking protein and mRNA.[17] A second generation IVV was generated through simple hybridization of a puromycin linker containing 2'-OMe nucleotides, leading to a non-covalent peptide fusion.[24] A more recent version, TRAP display, uses a non-covalent hybridized DNA-containing puromycin linker and incorporates a UAG codon into the mRNA to stall the ribosome and enhance puromycin entry (**Figure 5D**).[15] This format was found to reduce the time required for a single selection round to <3 hours.

Several other technologies using splint-less ligation methods have also been developed. A Y-ligation method uses a puromycin linker that hybridizes to the mRNA, after which short single-stranded sections of the mRNA and linker are ligated in the presence of T4 RNA ligase to form a small single-stranded loop.[25, 26] This strategy has been further developed to synthesize cDNA-fusions using a linker similar to the branched psoralen linker described above, except that instead of using psoralen

crosslinking, the Y-ligation strategy is used.[18, 27, 28] This branched Y-ligation linker contains a reverse transcription primer for generation of a covalently linked cDNA-peptide fusion. In some versions of this technique, this linker also incorporates a restriction site and biotin group, allowing for immobilization of the ligated mRNA followed by solid-phase translation and reverse transcription (**Figure 5E**). This approach effectively eliminates the need for intermediate purification steps[27] and the subsequent cDNA-peptide fusions can be released from the solid phase by restriction enzyme cleavage.[18] A recent well-controlled study comparing mRNA display and cDNA display showed that both mRNA and cDNA display are comparable in enriching functional sequences, though mRNA display showed higher enrichment versus cDNA display, possibly due to higher non-specific binding of the cDNA display fusions.[29] However, this effect was only seen when gel purification steps were included during library synthesis.

3 Advantages and Disadvantages of mRNA Display

As with any technology, mRNA display has a number of inherent advantages and disadvantages that should be considered. As an entirely *in vitro* technology, virtually any library can be constructed ranging from a totally random peptide library to those based on a complex protein scaffolds (e.g., antibodies. The covalent link between mRNA and protein allows a wider range of temperatures, buffers, binding conditions, and incubation times during selection compared to ribosome display, where a non-covalent ternary complex must be maintained throughout the selection. Flexibility in buffer conditions is also an advantage of *in vitro* selection systems, as display systems involving cells, such as yeast display (YD) or *E. Coli* display (ED), require conditions that keep cells viable and intact. Finally, the covalent link between peptide and protein, coupled with the minimized peptide-nucleic acid structure of the mRNA-protein fusion allows for the possibility of post-translational chemical modification which dramatically enhances the potential chemical complexity of mRNA display libraries.

mRNA display also has a number of disadvantages. One general limitation of many mRNA display selections (and all selections using biochemically purified targets) is that targets are often presented on a solid-phase support, which may not recapitulate the conformation of the target in a native biological context. For example, if a target can adopt multiple conformations, not all of these conformations may be sampled on the solid support. Also, by selecting against an immobilized target, *in vitro* selections partition molecules based purely on their binding affinity or binding kinetics (i.e., K_D, k_{on}, and/or k_{off}) as it is difficult to devise a method to partition molecules based on their activity. As a result, some selections result in molecules that can bind to a target *in vitro*, but show no activity in biological systems or cannot bind the target in a biological context (see, for example, Sections 5.2.2, 5.2.4, or 6.2.1). An

alternative strategy is to overexpress a target on the cell surface and select for binding against these cells. However, ensuring that the selection results in ligands to the target of interest is often difficult, even if cells without overexpressed target are used as a negative selection step. Lastly, the mRNA portion of an mRNA-protein fusion can help to solubilize the linked protein, allowing marginally soluble proteins to be selected. As a result, downstream expression or synthesis of the selected proteins or peptides can be challenging.

3.1 Diversity

mRNA display[4] and ribosome display libraries[30] are effectively the largest peptide libraries that are experimentally accessible. While it is physically possible to construct even larger libraries, such efforts are impractical requiring kilograms of genetic material. Up to 10^{15} unique sequences can be synthesized using mRNA display (**Figure 6**) and even a single copy of a functional sequence can be PCR amplified following *in vitro* selection. In contrast, *in vivo* display technologies, such as PD, are typically limited to a practical diversity of approximately 10^9 sequences owing to the obligate *in vivo* transformation step and resulting loss of diversity. mRNA display libraries are orders of magnitude larger than the immune system (~10^9 unique molecules), one-bead-one-compound (OBOC) libraries[31] (~10^7 unique molecules), and non-ribosomal peptide synthetase (NRPS) or polyketide synthetase (PKS) libraries[32, 33] (~10^3 unique molecules).

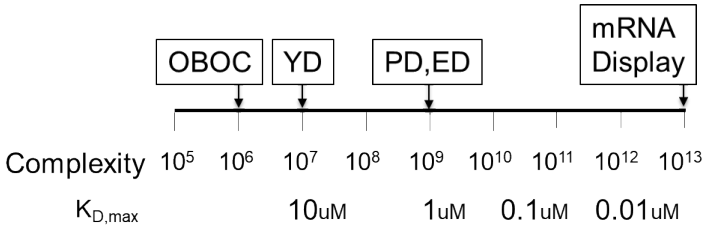

Figure 6. Biological display platforms including one-bead-one-compound (OBOC), yeast display (YD), phage display (PD), *E. coli* display (ED) and mRNA display libraries. The platforms are compared based on their complexity and the maximum dissociation constant ($K_{D,max}$) that can be achieved for the highest affinity ligand for a given library complexity. Ribosome display libraries have the same complexity as mRNA display. $K_{D,max}$ values were roughly estimated according to Reference [34] (not to scale).

In general, library size is directly correlated with the probability of obtaining a functional sequence of desired affinity.[34, 35] A theoretical study by Rosenwald[36] found that the degree of binding site complementarity is correlated to the size and complexity of the ligand, e.g., the more topologically complex the ligand, the more interactions it can make with a topologically complex binding site, such as a protein surface. There is also a correlation between the initial diversity of the library and the

probability of obtaining a ligand of a given dissociation constant (K_D), and for every log of increased complexity in the starting library, a log of decreased K_D is obtained. An example of the effect of library size on affinity is shown by comparing selections against streptavidin using mRNA display and PD. Using mRNA display, Wilson *et al.* discovered 20-amino acid peptide sequences that bound to streptavidin with dissociation constants ranging from 110 nM to as low as 2.4 nM.[37] In comparison, a PD selection against streptavidin resulted in a single peptide that bound with 13 μM affinity.[38, 39] While different libraries were used in these selections, these results suggest that large mRNA display libraries may yield higher affinity compounds than PD.

Despite the advantages of highly diverse libraries, there are some notable drawbacks. For example, if a high diversity library is constructed so that there is only one copy of each sequence, it is possible that functional sequences could be lost stochastically in the first round of selection. Therefore, the copy number of each random sequence in the library should be carefully considered.[40] In addition, because there are more total sequences in a high diversity library, more non-functional sequences must be removed in order to identify the functional sequences. This implies more rounds required for convergence in mRNA display (4 to >10) as compared with PD (generally, <3). In addition to requiring more time, additional selection cycles can result in contamination or selection failure. In the end, high diversity display libraries generated by selection platforms like mRNA display offer the potential for identifying high affinity compounds which must be considered alongside the increased selection time and technical difficulty.

3.2 Biases in Display Technology

All display technologies suffer from some bias and no display technology will generate a truly unbiased library. In a translation-based *in vitro* selection (e.g., mRNA display, ribosome display, PD, YD, etc.) the codon bias of the translation machinery, mRNA secondary structure, and post-translational processing are well-known sources of library bias.[41, 42] Finally, differential efficiencies in the amplification and transcription of the fused genetic material may also introduce significant bias into the final protein library.

In PD, proteins are displayed on the surface of a micrometer-long bacteriophage with a negative surface charge [MW > 1 X 10^8 Da] raising the possibility of non-selective target binding through interactions between the phage and target. In ribosome display, the ribosome, mRNA, and translated peptide form a stable ternary complex. Although smaller than phage, the ribosome is still a ~2,000,000 Da particle, raising the possibility of steric occlusion and/or non-selective binding driven by the nucleic acid and protein components of the ribosome. In other display technologies, peptide or protein libraries are linked to even larger molecules such as cells (ED or YD) or plasmids. mRNA display, on the other

hand, only contains mRNA linked to peptide or protein,[43] and is the minimal set of elements needed for protein or peptide display. The effect of the display scaffold on the quality of selection results or scaffold bias has been discussed elsewhere[44, 45] and is an important source of background binding and false-positive hits.

Display technologies that require an *in vivo* transformation step (e.g., PD, YD, etc.) introduce additional library biases. In the case of PD, peptides are most commonly displayed as fusions with Gene III (5 copies) or Gene VIII (thousands of copies). Multiple copies of a peptide displayed on phage can result in selection for weaker binding peptides due to avidity effects that prevent discrimination between moderate and high affinity clones.[46] In mRNA display, proteins are presented in a strictly monomeric context, avoiding avidity effects and allowing the selection of high affinity sequences. The insertion of a peptide or protein into Gene III can also interfere with the infectivity of the phage particle. If phage amplification is biased by a peptide sequence, the abundance of a clone might reflect a clone's infectivity and amplification rather than its binding to target. Lastly, during the process of phage assembly and export, known biases against certain sequences prevent display of some peptides (e.g., basic peptides).[47-49]

3.3 Simultaneous Optimization of Multiple Positions

The stepwise optimization of a peptide sequence is a relatively straightforward strategy – starting with a single functional sequence, the best amino acid at a single position is determined and repeated for each position in the sequence. Once the optimal amino acids are known at each position, they are then combined into one sequence. While a stepwise optimization strategy can be successful, it is often difficult to achieve in practice since changing an amino acid can result in unpredictable changes in binding affinity or specificity. One example is a study where Fiacco and co-workers attempted to introduce N-methyl amino acids into a peptide binding to the G-protein, Gαi1.[50] Each position in this peptide was systematically substituted for its corresponding N-methyl amino acid, with many substitutions resulting in dramatic increases in protease resistance. However, almost all substitutions resulted in a decrease in affinity and one substitution resulted in a change in binding specificity from Gαi1 to Gα12.

The best amino acid at one position in a sequence can also change depending on the context of the surrounding positions. mRNA display offers a powerful solution for optimization of a sequence since multiple positions of a sequence can be optimized simultaneously. One example is where mRNA display was used to engineer a peptide that could not be achieved through stepwise modifications.[51] In this study, the authors developed a macrocyclic peptide that bound Gαi1. Unlike the parental sequence, this peptide contained two N-methyl Alanine residues and was highly protease resistant.

However, substitution of either residue with alanine lead to a 100-1,000-fold decrease in protease stability. In a hypothetical stepwise optimization experiment, adding N-methyl amino acids in a stepwise fashion to the original peptide would have resulted in peptides with no increase in stability and these peptides would have been discarded. As a result, it seems highly unlikely that a stepwise optimization strategy could have resulted in the discovery of the selected Gαi1-binding peptide. Furthermore, only 20% of the original natural amino acids of the parental peptide were retained in the selected peptide. This indicates that a leap of about 8 independent steps would have been required in a stepwise modification strategy beginning with the parental peptide and ending at the protease-resistant selected peptide.[51]

3.4 Simultaneous Optimization of Multiple Properties

An additional advantage of mRNA display is that it can also be used to optimize multiple biophysical properties of a sequence simultaneously. For example, Howell *et al*., developed a multi-step selection for binding and for protease resistance.[52] This was achieved by first incubating an mRNA display library with chymotrypsin, thereby selecting for sequences that were protease resistant, followed by incubation of the library with target. A 100- to 400-fold increase in protease resistance was observed, while still retaining binding for target. Selections for thermostability have also been performed similarly.[53] These examples illustrate the powerful ability of mRNA display to optimize properties along multiple fitness axes.

4 Results from mRNA Display Selections

In the ~20 years since its inception, mRNA display has successfully been used to engineer novel ligands against a wide variety of targets. In this section, we review the results of these selections and observe some common themes and results. These selections fall into two broad categories: 1) Protein selections, where the resulting ligands are folded and contain a buried hydrophobic core, and 2) Peptide selections, where no explicit structural constraints or contexts are imposed on the initial library. We will begin with a discussion of selections in the first category where known biological scaffolds (e.g., fibronectin) are partially randomized to generate mRNA display libraries from which folded, functional ligands can be identified. We will then review the selection of linear, natural peptides by mRNA display and their application as chemical tools. We will conclude by surveying the recent literature describing the use of cyclization and non-proteogenic amino acids to generate non-ribosomally synthesized peptide (NRSP)-like mRNA display libraries and their application to the selection of drug-like peptides. We note that while mRNA display libraries can be constructed from cDNA, we refer the reader to other publications for more information.[54, 55]

5 Biological Scaffolds in mRNA Display

There is great interest in engineering novel proteins for a number of applications, including therapeutics,[56] imaging agents,[57] diagnostics,[58] and tools for biological/biochemical research. One difficulty encountered when engineering proteins is that it is impossible to exhaustively search the entire sequence space of even the smallest proteins. Sequence space is immeasurably large: the number of possible sequence combinations increases by a factor of 20 with each additional amino acid that is added to a protein chain. Thus, even using libraries of 10^{15} unique molecules, only a maximum of ~11-12 amino acids can be exhaustively searched by *in vitro* display technologies. As a result, it is often necessary to design and constrain a library to specific regions within the primary sequence. Many protein libraries are based on a protein "scaffold," which remains constant and acts to support randomized regions that will be selected to interact with a target of interest. Often, the scaffold's hydrophobic core is kept constant so that randomization of loops or surface residues will not result in unfolding, aggregation, or loss of solubility.[59, 60]

The choice of scaffold and if a scaffold is even needed should be carefully considered before embarking on an mRNA display selection. Matching the biophysical properties of a potential scaffold to the final intended end application is important, as each scaffold has both advantages and disadvantages. In general, scaffolds are thought to result in higher affinity ligands relative to peptides. Peptides are generally unstructured in solution and must pay a large entropic penalty upon binding resulting in weaker binding affinities.[61] In contrast, random regions within a scaffold are comparatively fixed in place by the scaffold topology and lose less conformational entropy upon binding, resulting in improved affinity.[62] Structured proteins are also generally more resistant to proteolytic degradation relative to linear peptides making them an attractive starting point for *in vivo* applications.[63]

These advantages must be weighed against the disadvantages of protein scaffolds. In mRNA display, longer proteins have a reduced efficiency of fusion formation,[64] which can increase the technical difficulty of successfully completing an mRNA display selection and result in decreased effective library sizes. Likewise, scaffold-based proteins will be selected for *both* foldedness *and* function, which can potentially reduce the number of winning sequences. For example, Keefe and Szostak estimated that ATP-binding proteins selected from a random 80-mer library occurred at frequency of roughly 1 in 10^{11} molecules.[65] They hypothesized that this surprising low frequency of ATP binders could have been due to the difficulty of forming a folded protein with a buried hydrophobic core from a totally random library. Additionally, longer random protein libraries often have increased chances of stop codons or frameshifts due to library construction, increasing the probability of aborted translation products.[66] Lastly, larger protein scaffolds, such as the fibronectin and single chain fragment variable

(scFv) domains, may suffer from reduced tissue/tumor penetration due to poor extravasation rates and rapid systemic clearance.[67]

In mRNA display, several scaffolds have been used in successful *in vitro* selections including nanobodies,[68] SH3 domains,[69] fragment antigen binding (Fab) domains,[70] scFv domains, and fibronectin[71] scaffolds. Of these, the two most common scaffolds are scFvs (~27 kDa) and fibronectin-based scaffolds (~10 kDa) (**Figure 7)**. While both scaffolds are substantially larger than small peptides (~1-2 kDa), they are still approximately 1/5 to 1/10 the size of monoclonal antibodies (mAbs), facilitating binding to molecular crevices that antibodies are too large to access. Despite their smaller size, however, they are still capable of modulating protein function and can be more effective at blocking protein-protein interactions than small peptides.[72, 73]

5.1 Antibody Scaffolds

Antibodies are the gold standard for protein ligands and can bind to protein targets with high affinities and specificities. mAbs are among the most promising therapeutics and have revolutionized the pharmaceutical industry, with up to $200 billion in annual revenue predicted by 2022.[74] Although hybridoma technology has been effectively used to generate thousands of new mAbs,[75] this technology is over 40 years old and has a number of disadvantages. mAb production is laborious and little control can be exerted over the binding conditions and the stringency under which a mAb is generated, potentially resulting in mAbs with poor affinity and/or selectivity.[76] mRNA display using antibody and antibody-like scaffolds is an attractive alternative for generating novel antibodies and antibody-like

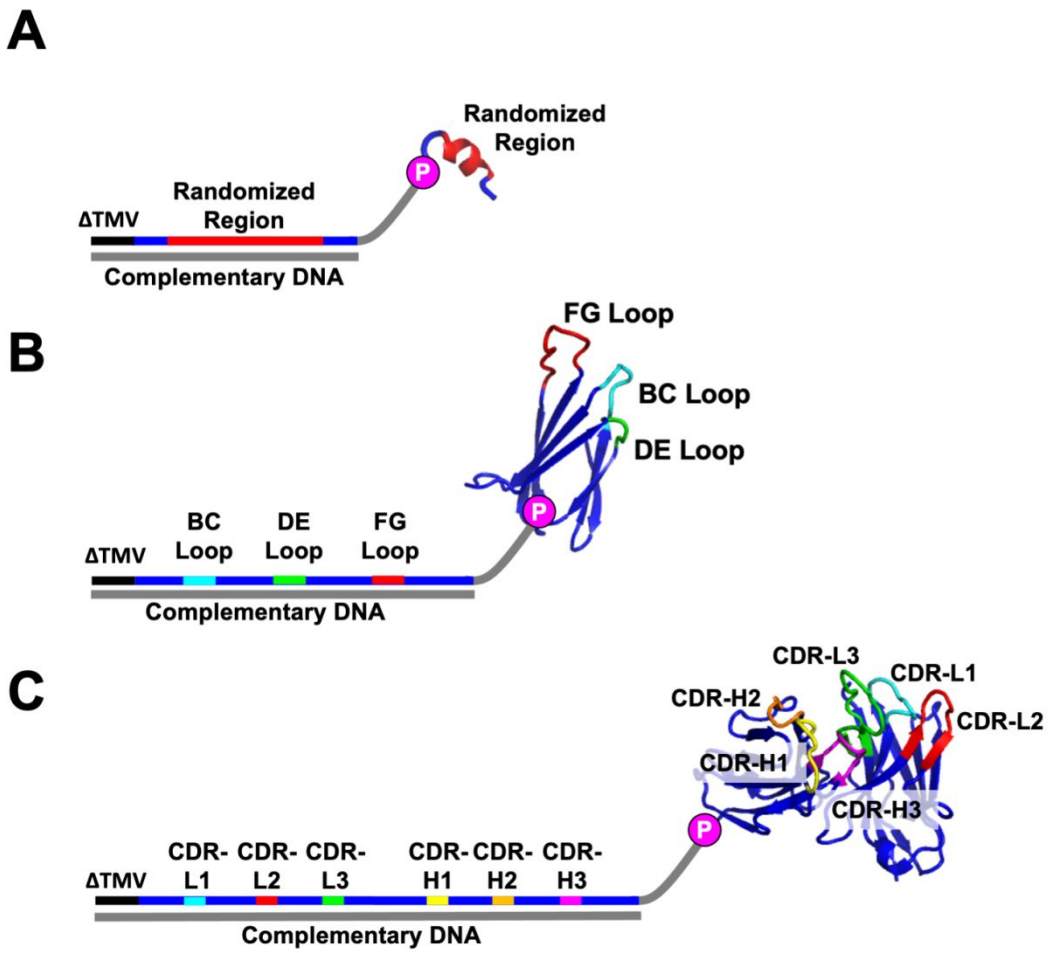

compounds, as the larger library size (**Figure 6**) and precise control over selection conditions can yield antigen-binding ligands with antibody-like affinity and specificity. In the following section, we review the use of mAb scaffolds (antibody) as well as Fab and scFv scaffolds (antibody-like) in mRNA display experiments.

Figure 7. Schematic of various mRNA-protein fusions. (**A**) A 13-amino acid peptide attached to its encoding mRNA. Randomized regions (for mRNA and peptide) are red. (**B**) A fibronectin fusion with three randomized loops (BC (cyan), DE (green), and FG (red) attached to its encoding mRNA. Random regions in the mRNA are colored while the constant scaffold is dark blue. (**C**) An scFv attached to its encoding mRNA. Constant scaffold regions are dark blue while CDRs are colored accordingly.

Structurally, immunoglobulin variable domains (Fv) consist of two sandwiched β-sheets. Antigen specificity is conferred by loops that connect β-strands called complementarity determining regions (CDRs). CDRs vary with each antibody and comprise the antigen-binding surface.[77] In mRNA display, as with the immune system, CDR loops are commonly randomized in order to create antibody and antibody-like libraries.[71] Antibodies are composed of variable heavy (V_H) and variable light (V_L) chains, which contain both intermolecular (between V_H and V_L chains) and intramolecular (within a V_H or V_L chain) disulfide bonds.[78] Because these disulfide bonds potentially make antibody folding and assembly difficult, mRNA display methods have been developed to increase the folded fraction of the library.[79] Alternative translation conditions can also mitigate folding issues. For example, the PURE (**P**rotein synthesis **U**sing **R**ecombinant **E**lements) system was used to select a disulfide-containing scFv targeting insulin.[80] Reticulocyte-based systems have used protein disulfide isomerase and other disulfide-forming enzymes to translate and properly fold antibodies.[81] Lastly, assembling an antibody that retains V_H/V_L pairing throughout a selection is difficult because the chains are encoded separately. Despite a method using emulsion PCR to retain Fab fragment V_H/V_L pairs,[70] Fab fragments are uncommon in mRNA display.

For the past 20 years, the scFvs have been most frequently used antibody scaffold in mRNA display. The scFv scaffold balances the challenges associated with *in vitro* library development and expression (e.g., incorporating disulfide bonds) with the benefits of the antibody scaffold. scFvs are derived from V_H and V_L chains of antibodies where the chains are linked by glycine-serine repeats (**Figure 8**). Encoding the V_H/V_L pairs in a single protein chain simplifies mRNA display library construction and selection, making scFvs the preferable scaffold for antibody selection.

mRNA display using scFv scaffolds has resulted in several successful selections. A selection against Mouse Double Minute 2 homolog (MDM2) and p53 combining Surface Plasmon Resonance (SPR) and an off-rate selection converged after two rounds to yield scFvs with 4.3 nM and 12 nM K_D values, respectively.[82] scFv selections using mRNA display were also performed against Tumor Necrosis Factor α Receptor (TNFR),[83] fluorescein (0.95 nM K_D),[84] and Receptor Activator of Nuclear Factor κB (RANK).[85]

While scFvs may be better suited for mRNA display, full-length mAbs that include both the Fv and the Fc (Fragment crystallizable) constant regions are important for therapeutic purposes. These regions mediate antibody-dependent cell-mediated toxicity (ADCC), activation of complement, and are responsible for long serum half-lives.[86]

Unfortunately, as discussed above, full-length mAbs are extremely challenging to adapt to mRNA display library design and selection workflows. One strategy to create full-length mAbs is to first perform an mRNA display selection with an scFv library then graft the selected CDR loop sequences onto a full-length mAb scaffold. In one such study, scFvs obtained by mRNA display were used to design over 100 mAbs against 15 antigens.[81] However, this strategy is only successful in some circumstances as many of the grafted antibodies showed loss of specificity/affinity. This phenomenon was also observed when scFvs were selected using PD.[87, 88] These observations suggest that the scFv scaffold may not present the CDR loops in the same context/structure as an intact antibody.[81]

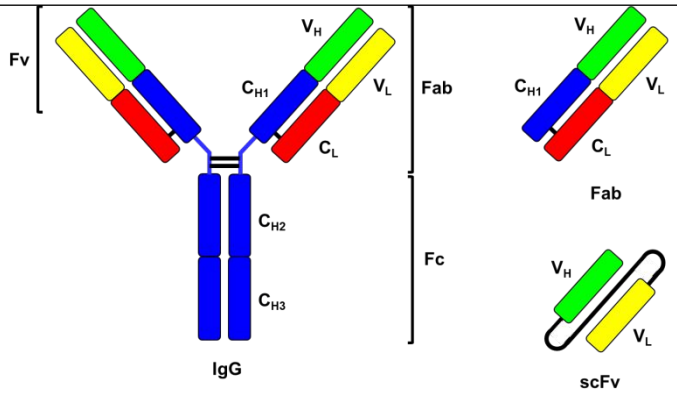

Figure 8. Antibody based scaffolds (scFv and Fab) compared to full IgG antibody (Fv: immunoglobulin variable domain, Fc: fragment crystallizable domain, Fab: antigen-binding fragment, V_H: variable heavy, V_L: variable light, C_L: constant light, C_H: constant heavy, scFv: single chain fragment variable)

5.2 Fibronectin-Based Scaffolds

While antibody and antibody-like scaffolds are leading sources of biological therapeutics, alternative scaffolds are being developed for the next generation of therapeutic proteins.[89] Disulfides in antibodies can cause structural heterogeneity and instability due to isomerization/alternative disulfide pairing, interconversion, and/or reduction.[90, 91] Antibodies are also unstable in the reducing intracellular environment, making the use of antibodies inside the cell (i.e., intrabodies) more challenging. During mRNA display, disulfide bond-mediated protein folding also poses an additional challenge that can decrease the library complexity and impair selection robustness. As a result, alternative scaffolds that

structurally mimic antibody variable chains without disulfide bonds have been developed for use in mRNA display selections. The most common of these is the fibronectin scaffold.

Fibronectin is a large extracellular matrix protein responsible for interfacing cells with the stromal environment.[92] Three types of modules or domains (Type I, II, and III) are found in fibronectin and each type contains two anti-parallel β-sheets that form a β-sandwich. Type I and II domains contain disulfide bonds while the Type III domain lacks disulfide bonds, making the Type III domain an attractive scaffold for mRNA display. The 10th subunit of human Fibronectin is a Type III domain (^{10}Fn3) that is widely used as a scaffold in mRNA display (trademarked as Adnectins™ by Bristol-Myers Squibb, or also called "monobodies").[62] Wild type ^{10}Fn3 has several biophysical properties that are attractive for a biological scaffold: it has high solubility (>15 mg/mL), is highly thermostable (Tm >90 °C) even without disulfide bonds,[62, 71, 93] and expresses well in bacterial systems (50 mg/L).[94] The 94-amino acid ^{10}Fn3 scaffold contains three loops (BC, FG, DE), analogous to nanobodies, which are based on the single variable domain camelid antibody V_{HH} CDRs (**Figure 9A and Figure 9B**).[95] The FG loop is the longest and most flexible of the three loops and is involved in endogenous RGD-mediated binding of wild type ^{10}Fn3 with integrins.[92] Randomization of the BC and FG loops does not affect ^{10}Fn3 stability, allowing the BC and FG loops to form a contiguous molecular surface for target binding.[62] mRNA display-generated ^{10}Fn3 ligands have been used to as ligands for extracellular proteins in molecular imaging, immune regulation, crystallization, and therapeutic applications.[96-98] ^{10}Fn3 probes for intracellular targets (intrabodies) have also been developed for dynamic *in vivo* imaging.[99] A comprehensive list of fibronectin-based ligands selected by mRNA display is presented in **Table 1**.

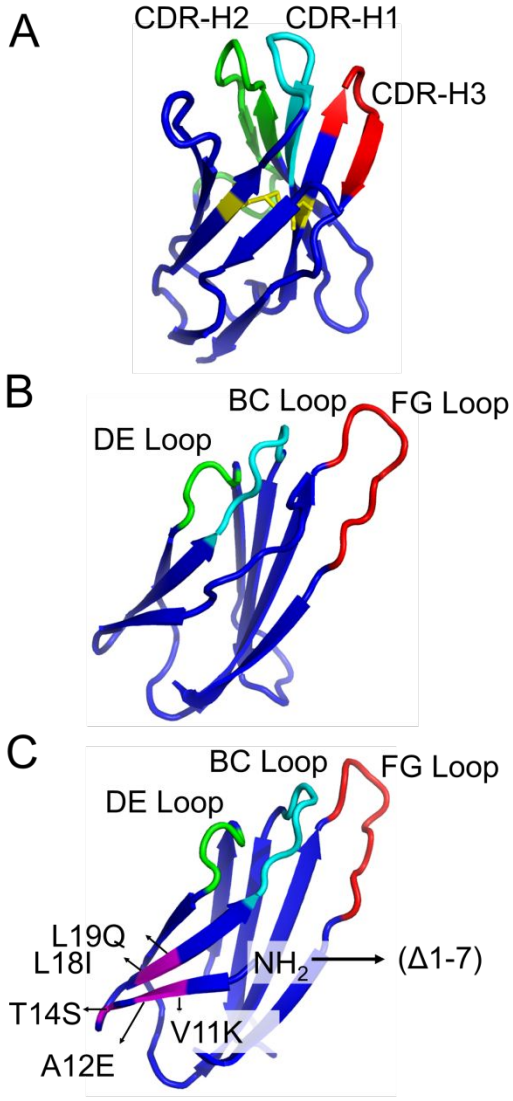

Figure 9. The tertiary structure of (A) Llama V_{HH} domain (PDB accession number 1TTG), (B) wild-type human ^{10}Fn3 domain (PDB accession number 1HCV) and (C) truncated human ^{10}Fn3 domain carrying structural mutations (PDB accession number 1HCV). The Llama V_{HH} domain and human ^{10}Fn3 domain show comparable folding into β-sandwiches. (^{10}Fn3: 10th subunit of Fibronectin type III), with the BC, DE, and FG of the ^{10}Fn3 domain resembling the CDR loops of the Llama V_{HH} domain. The complementarity determining regions (CDR) in the V_{HH} domain and the randomized loops in the ^{10}Fn3 domain are showed in green, cyan and red. The disulfide bond formed between cysteines 22 and 92 in the V_{HH} domain is highlighted in yellow. In the truncated human ^{10}Fn3 domain, the mutated residues are highlighted in magenta.

5.2.1 Initial mRNA Display Selections with the ^{10}Fn3 Scaffold

In 1998, Koide *et al*. designed the first ^{10}Fn3-based scaffold library.[62] Using PD, they isolated a single clone with moderate specificity and affinity towards ubiquitin (reported IC_{50}: 5 μM). The first mRNA display selection using an ^{10}Fn3 scaffold was against Tumor Necrosis Factor α (TNFα).[71] In this selection, three libraries were constructed: one library randomizing the FG loop only, one randomizing

the BC and FG loops, and one randomizing the BC, DE, and FG loops. Using these three libraries, the selection yielded ligands with K_D values ranging from 1 to 24 nM, with over 90% of the clones originating from the third, three-loop library. Subsequent affinity maturation that included random mutagenesis, high temperature incubations to select for protein stability, and extended washing for increased binding affinity, resulted in improved variants with K_D values as low as 20 pM. Biophysical characterization of the two winning sequences showed they were monomeric, could be expressed in *E. coli*, and were resistant to proteolytic digestion at room temperature. However, the selected molecules showed lower thermostability than wild type ^{10}Fn3 and suffered from low to moderate bacterial expression efficiencies.[71] The authors hypothesized that the higher affinity and larger number of functional sequences resulting from the selection (~100 total) was due to the larger mRNA display library (10^{12} independent sequences) versus the less diverse PD library (10^8) in the original ubiquitin selection.

A second study described extensive biophysical and biochemical characterization of the fibronectin scaffold. In this study, Olson and co-workers synthesized a library similar to the two-loop library above, where the DE loop was kept constant while the BC and FG loops were randomized. The first seven amino acids of the ^{10}Fn3 scaffold were removed in this library because structural analysis showed these N-terminal residues threaded between the randomized BC and FG loops, potentially affecting binding. Supporting this hypothesis was the observation that removal of the first eight residues of ^{10}Fn3 fibronectins selected against Kinase insert domain receptor (KDR)/vascular endothelial growth factor receptor-2 (VEGFR2) improved binding by ~3-fold on average.[73] The wild type and Δ1-7 mutant were equally stable in unfolding studies, suggesting that these seven N-terminal amino acids were not important for folding and stability. The authors also determined the folded fraction of the library by screening clones from the ^{10}Fn3 library expressed with Green Fluorescent Protein (GFP) fused to its C-terminus. GFP fluorescence is highly dependent on the solubility and tertiary stability of the fused N-terminal protein.[100] GFP reporter fluorescence showed that ~45% of the naïve fused library was correctly translated in-frame and lacked stop codons. These data supported the hypothesis that the fibronectin library is able to tolerate loop randomization and can display these random loops without significant effects on stability or folded structure.[94]

5.2.2 Targeting Extracellular Proteins with ^{10}Fn3 Selections

Extracellular proteins are a common target in ^{10}Fn3-based mRNA display selections. Each selection described below employed slightly different selection pressures and antigen presentation strategies. Engineered ^{10}Fn3 scaffolds termed Adnectins were selected against interleukin-23 (IL-23) and epidermal growth factor receptor (EGFR).[101] Both Adnectins bound their targets with a K_D of 2 nM

and inhibited either EGFR receptor phosphorylation (IC_{50} = 50 nM) or IL-23/IL-23R binding (IC_{50} = 1 nM).[96] Co-crystallization of the Adnectins with their targets revealed they bound epitopes distinct from previously identified mAbs, suggesting their small size allowed them to bind to concave, antibody-inaccessible sites while still being able to sterically hinder receptor/agonist interactions.[96] The ability to recognize distinct epitopes from mAbs could make fibronectin scaffolds useful in situations where critical protein surfaces cannot be effectively targeted with larger scaffolds.

The dendritic cell-specific ICAM3-grabbing non-integrin receptor (DC-SIGN) was targeted with a fibronectin mRNA display library containing two random loops. The authors hypothesized a DC-SIGN specific fibronectin would enable targeted delivery of antigens to dendritic cells, promoting a more effective immune response. After seven rounds of selection, several fibronectin ligands were obtained, with the most promising ^{10}Fn3 ligand showing a reported K_D of 19 nM.[102] While all fibronectins were able to bind to recombinant DC-SIGN in biochemical assays, only one sequence bound to DC-SIGN expressed on the surface of cells. It is unclear if many of these sequences did not bind because the binding epitope for the non-functional sequences is occluded on the cell surface. These results highlight the utility of having multiple potential ligands to screen for function in downstream experiments. Lastly, when this DC-SIGN specific fibronectin was coupled with vaccine antigens, the fibronectin-antigen conjugate resulted in greater DC antigen presentation and enhanced $CD8^+$ cytotoxic T-cell activation.[102]

Bispecific biologics were also generated using ^{10}Fn3 mRNA display selections. Adnectins were first engineered separately against EGFR and insulin-like growth factor-I receptor (IGF-IR). Optimized ^{10}Fn3 clones were integrated into a bispecific construct through a glycine-serine cross-linker to create the EI-Tandem Adnectin that inhibited EGFR and IGF-IR phosphorylation with IC_{50} values from 0.1 to 113 nM and triggered receptor degradation. A polyethylene glycol (PEG)ylated version of EI-Tandem increased serum half-life while only minimally impacting affinity for either target. In a preclinical nude mouse model of pancreatic cancer where EGFR and IGF-IR are overexpressed, administration of the EI-Tandem Adnectin resulted in significant tumor growth inhibition.[72] Notably, the EI-Tandem Adnectin was more effective than co-administered monomeric EGFR and IGF-IR Adnectins, indicating that bispecific presentation is crucial for enhanced effectiveness. The EGFR binding Adnectin was also adapted for chimeric antigen receptor (CAR) adoptive T-cell transfer.[98] This Adnectin demonstrated comparable effectiveness when compared to established scFv molecules derived from EGFR binding mAbs, indicating the ^{10}Fn3 scaffold could provide a simpler and faster route to produce a larger repertoire of CARs.[98] Adnectins have also been combined with traditional mAbs or other biologics. For example, a mouse IL-23 specific Adnectin (PEGylated Adnectin K_D for IL-23 = 234 pM) was combined

with an IL-17 mAb and/or IL-17 decoy receptor.[103] Administering both Adnectin and mAb resulted in decreased inflammation with an enduring response in an autoimmune mouse model that was more effective than administration of either inhibitor alone.[103]

Adnectins targeting immune checkpoint ligands have been developed as well. Notably, the Adnectin BMS-986192 binds programmed death ligand 1 (PD-L1) with a K_D = 35 pM even after radiolabeling with ^{18}F.[99] ^{18}F-BMS-986192 has also been shown to discriminate dynamic levels of PD-L1 in murine xenograft models,[104] and was used to assess PD-L1 expression in patients with advanced stage non-small cell lung cancer.[105] Alternative radiolabeling (^{68}Ga chelation) was also successful in preclinical mouse models.[106] Adnectins were also developed to inhibit human immunodeficiency virus (HIV) infection by binding to CD4 (K_D = 3.9 nM).[107] In one study, a gp41-binding Adnectin was tethered to a CD4-targeted Adnectin, resulting in enhanced inhibition of HIV replication (EC_{50} = 37 pM).[108] Mutagenesis and addition of a membrane fusion blocking peptide further improved the bispecific Adnectin.[109]

A two-loop fibronectin library was used to develop ligands against the extracellular domain of the α1-Nicotinic Acetylcholine Receptor. [53] These ligands, called FANGs (**F**ibronectin **A**ntibody-mimetic **N**icotinic acetylcholine receptor **G**enerated ligands) were selected under conditions to improve thermostability (by incubating at 65 °C), protease resistance (by incubating with Proteinase K), and improved affinity (through selection for sequences with slower off-rates). As a result, these FANGs were highly thermostable and bound to the α211 subunit of α1 nicotinic acetylcholine receptor (K_D = 670 pM) with the receptor in monomeric and heteropentameric forms in cell culture.[53] One of these fibronectins, α1-FANG3, was able to compete directly with the bungarotoxin for nicotinic acetylcholine receptor binding.[53]

Engineered fibronectins have also been used as targeting agents to deliver cytotoxic drugs in the form of fibronectin-drug conjugates.[110] Pharmacokinetically, the smaller size of Adnectins (~10 kDa) results in much faster clearance than antibodies, which could expand the therapeutic window by reducing cytotoxic exposure to normal tissue. In order to test this hypothesis, Lipovsek *et al.* first engineered an Adnectin targeting Glypican-3, which is overexpressed on hepatocellular carcinoma cells. This Adnectin was then site-specifically conjugated to the cytotoxic drug tubulysin via a C-terminal cysteine on the Adnectin. Conjugation of tubulysin had little impact on Adnectin binding (K_D = 8 nM). The group observed that the drug conjugate was effective at the xenograft tumor site, but was cleared rapidly through the kidneys, limiting systemic toxicity. Although this result supports the hypothesis that Adnectin-drug conjugates might display more favorable therapeutic safety profiles relative to antibodies, further studies will be necessary to show this in the clinic.[110]

Biologics targeting the severe acute respiratory syndrome (SARS) Coronavirus-2 (SARS-CoV-2; the virus that causes COVID-19) were rapidly developed in wake of the pandemic using TRAP display. In this study, a fibronectin library with randomized BC and FG loops was used to target the S1 subunit of SARS-CoV-2 spike protein that contains the receptor binding domain (RBD).[111] In the first round of selection, the authors added mRNA coding for the fibronectin library with a puromycin linker instead of the typical TRAP display protocol (where a DNA library is added and transcription/translation occur simultaneously) in order to increase the diversity of the library. In subsequent rounds, TRAP display was used to increase the speed of the selection. Within four days, ^{10}FN3 sequences that bound to the S1 subunit with single-digit nanomolar to sub-nanomolar K_D's were obtained. Several clones were able to block the interaction between the RBD domain of the spike protein and ACE2, some at concentrations as low as 10 nM. The set of clones that were tested also bound to three epitopes and 16 different combinations were suitable reagents for a sandwich enzyme-linked immunosorbent assay (ELISA). Clones also inhibited S1 subunit proteolytic conversion and were able to capture virions from patient nasal swabs. Finally, one clone was able to inhibit SARS-CoV-2 infection in a cell-based assay as a monomer (0.5 nM IC_{50}) or as a tandem dimer (0.4 nM IC_{50}). This work demonstrates that mRNA display-based selections can be used to discover new affinity reagents in exigent public health emergencies.

Table 1. Fibronectin Scaffolds Selected with mRNA Display. Affinities are obtained directly from the corresponding reference and are not normalized for temperature. *Refers to the stated complexity of the library in the original reference. N/S is used if this value is not provided. (Abbreviations: CFMS (Continuous flow magnetic separation); HTS (High throughput sequencing))

Target	Loop(s) Randomized	Library Diversity*	Rounds Selected	Affinity/ Solubility Maturation	Selected Scaffold Name	Final Loop Sequence(s)	Affinity/IC_{50}/Kinetic Properties	Notes	Ref
TNF-α	BC DE FG	10^{12}	14	Error-Prone PCR	M12.04 (^{10}Fn3)	BC: SMTPNWP DE: PWAS FG: HRDT (FG truncation)	K_D= 0.02 nM	-	71
VEGFR2	BC DE FG	N/S	-	Thermo-stability optimization	^{10}Fn3- 159-(A56E)	BC: RHPHFPT DE: LQPP(E) FG: MAQSGHELFT	K_D= 0.59 nM	-	112
VEGFR2 (KDR); Flk-1	BC DE FG	10^{13}	6	Error-prone PCR	VR28-E19	BC: RHPHFPT DE: LQPP FG: VERNGRHLMTP	VEGFR2: K_D = 0.06 nM Flk-1: K_D = 0.34	-	73
Phospho-IκBα	BC FG	$3x10^{13}$	10	Error-prone PCR	10C17C25 (10FnIII)	BC: PASSRWR FG: QQLHQPKWRW	K_D = 18 nM	1000x more specific for phosphorylated version; Used as intrabody FRET sensor	113
SARS nucleocapsid protein	BC FG	10^{12}	6	-	Fn-N22	BC: LNMWYNV FG: KRSFWSKSAG	K_D = 1.7 nM	Used as Intrabody	114
EGFR; IGF-1R (bispecific EI-tandem Adnectin)	BC DE FG	10^{13}	4	-	EI-tandem Adnectin	**EGFR:** BC: DSGRGSYQ; DE: GPVH; FG: DHKPHADGPHTYHES **IGF-IR:** BC: SARLKVAR DE: KNVY FG: RFRDYQ	EGFR: K_D = 10.1 nM IGF-IR: K_D = 1.17 nm	-	72
IL-6	BC FG	10^{12}	4	CFMS	eFn-4B02	BC: GNGGPLV FG: HAFSGRVAVI	K_D = 21 nM	-	115
EGFR	BC DE FG	N/S	-	-	Adnectin1 (EGFR)	BC: DSGRGSY DE: GPVH FG: DHKPHADGPHTYHES	IC_{50}= 50 nM K_D = 2 nM	IC_{50} was determined based on inhibition of EGFR phosphorylation	96
IL-23					Adnectin 2 (IL-23)	BC: EHDYPYR DE: KDVD	IC_{50}= 1 nM K_D = 2 nM	IC_{50} was determined based on IL-23 receptor competition	

						FG: SSYKYDMQYS			
IgG (Fc)	BC FG	10^9	1	CFMS/HTS	eFn-anti-IgG-1	BC: PATTYTL FG: PCNQCQLRPN	K_D = 28 nM	-	[116]
MBP					eFn-anti-MBP-2	BC: QAPHLFV FG: QFMYLLLPGR	K_D = 130 nM		
Human/ mouse DC-SIGN	BC FG	10^{12}	Mouse: 3 Human: 4	-	eFn-DC6	BC: PQPWLQV FG: YLPLTYGHYR	Human: K_D = 19 nM; Mouse: K_D = 133 nM	-	[102]
PSD-95 and Gephyrin	BC FG	10^{12}	PSD-95: 6 Gephyrin: 7	-	FingRs	-	-	Used as Intrabody	[117]
CAMKIIα	BC FG	10^{12}	7	-	CAMKIIα FingR clone 1	BC: IHHAKEI FG: TVSFAWKRVL	-	Used as intrabody	[118]
PXR Ligand Binding Domain (To compete with SRC-1)	BC DE FG	N/S	-	-	-	BC: PPPYYEGVTV DE: PYWTET FG: EMYPGSPWAGQVMDIQP	K_D = 11 nM	-	[97]
IL-23	BC DE FG	10^{12}	-	-	ATI-1221 anti-mouse IL-23p19 Adnectin	-	Parent: K_D = 0.245 nM PEGylated form: K_D=0.234 nM	-	[103]
H-RAS (G12V)	BC FG	10^{12}	6	5 additional rounds for maturation	RasIn2	BC: SIVFGKHD FG: FRWPKRRLVR	K_D = 120 nM	-	[119]
CD4	NP1 library: BC, DE, FG with N-terminal and flanked randomized residues WS1 library: CD strand FG loop with randomized flanked residues	N/S	6	Stringency and off-rate improvement	Adnectin 6940_B01	CD strand region: HSYHIQYWPLGSYQRYQVFS FG loop and flank: EYQIRVYAETGGADSDQSFG WIQIGYRTEPES	K_D = 3.9 nM	-	[107]
PD-L1	-	N/S	-	-	Adnectin BMS-986192	-	K_D = 0.035 nM	-	[99]
gp41 (N17)	BC DE FG	N/S	7	3 additional rounds for optimization	Adnectin 6200_A08	BC: EYKVHPY DE: FVLE FG: VDS	Parent Adnectin: K_D = 0.8 nM	Tethered CD4 and gp41 Adnectin to inhibit HIV (EC_{50}= 37 pM)	[108]
Glypican-3	BC DE FG	5.3×10^{13}	7	-	A2-tub	BC: SDDYHAH DE: GEHV FG: YDAEKAATDWSIS C-terminus: NYRTPC	K_D = 8 nM	-	[110]
α211 subunit of α1-Nicotinic Acetylcholine Receptor	BC FG	$\leq 10^{14}$	5	Off-rate optimization/ heat and protease stability selection	α1-FANG3	BC: PSMFGHV FG: WIHLKWLTNF	K_D = 0.67 nM	-	[53]
Subunit S1 of SARS-CoV-2	BC FG	$3x10^{13}$	6		Clone 6 monobody	BC: GGDYVGYY FG: TYNGPWIYGYEEI	K_D = 0.76 nM		[111]

5.2.3 Clinical Translation of ^{10}Fn3/Adnectin Biologics Targeting Tumor-Promoting Receptors

Fibronectin molecules selected via mRNA display have been translated to the clinic. An Adnectin targeting VEGFR-2 has advanced the furthest along the translational pathway, ending in a Phase 2 clinical trial. Several strategies were used to develop anti-VEGFR-2 ^{10}Fn3 scaffolds. Using a combination of mRNA display, affinity maturation and site-directed mutagenesis, an exceptionally stable ^{10}Fn3 derivative capable of binding VEGFR-2 with a 13 nM K_D was engineered.[112] Stability of the Adnectin was sacrificed in favor of enhanced binding affinity, which was improved by >40-fold through additional screening. Based on these two molecules, a third ^{10}Fn3 scaffold was designed that exhibited a combination of high affinity (K_D = 0.59 nM) and improved stability (T_m = 53 °C).[112] The dissociation constant was later improved by modifying the FG loop, achieving K_D values as low as 0.06 nM. These anti-VEGFR-2 Adnectins were screened against both human and murine VEGFR-2 to ensure that selected Adnectins would bind to VEGFR-2 from both species. This strategy allows the same molecule to be used in mouse preclinical studies and clinical human trials, potentially simplifying translation. These Adnectins significantly inhibited VEGF-mediated cell proliferation in a dose dependent manner.[73]

CT-322/BMS-844203, a PEGylated anti-VEGFR-2 ^{10}Fn3 derivative with a K_D of 11 nM, was tested in pre-clinical animal models.[120, 121] CT-322 entered the clinic with the goal of blocking angiogenesis in a variety of human cancers.[122-124] In a Phase 1 trial, CT-322 was well tolerated up to doses of 2 mg/kg/week, however 82% of patients developed anti-drug antibodies that were directed against the engineered fibronectin loops.[123] Surprisingly, these anti-drug antibodies did not have an effect on pharmacokinetics or biological function. CT-322 was then tested in Phase 2 trials assessing efficacy in recurrent glioblastoma as a monotherapy and in combination with camptotechin-11 chemotherapy.[125] Unfortunately, CT-322 failed to show efficacy as a monotherapy as measured by six month progression free survival, resulting in termination of the study before completion.[125] Despite its patient tolerability and potent VEGFR-2 inhibition, the CT-322 Adnectin has yet to find a clinical role.

5.2.4 Targeting Intracellular Proteins with Fibronectins

The term “intrabodies” refers to antibodies that target intracellular antigens. Intrabodies are useful as reagents for live cell imaging or for the recognition of proteins in real-time, allowing researchers to address temporal and dynamic biological questions. Historically, proteins have been monitored in live cells through fluorescent protein tagging (e.g., GFP). However, overexpressing proteins as fusions with fluorescent proteins can perturb biological systems, resulting in protein mis-localization and unintended functional effects rendering the system incapable of addressing nuanced biology.[126] Some intrabodies are based on antibody scaffolds which have been engineered to eliminate redox-labile disulfide bonds.[127] However, since the ^{10}Fn3 scaffold is disulfide free, it is well-suited for intrabody applications and these intrabodies can be generated by mRNA display.

The first mRNA display derived intrabody was engineered against the phosphorylated form of IκBα, a negative regulator of nuclear factor-κB signaling. After ten rounds of selection using a ^{10}Fn3 library to target a phosphorylated peptide derived from IκBα, a clone was found to bind phospho-IκBα (K_D = 18 nM). This clone showed >1,000-fold greater affinity for the phosphorylated peptide versus the non-phosphorylated version.[113] To increase solubility and expression, the authors performed iterative rounds of mutagenic PCR followed by a GFP solubility screen.[100] This screen resulted in the replacement of solvent-exposed hydrophobic residues with polar ones, greatly enhancing β-sheet formation and bacterial expression. The intrabody was then adapted into a fluorescence resonance energy transfer (FRET) sensor with the goal of monitoring IκBα phosphorylation within cells.[113]

A second selection by the same group was directed against the SARS nucleocapsid protein (SARS-N). The selection resulted in at least eight fibronectin intrabodies that recognized different epitopes of SARS-N; six of these recognized the C-terminal domain of SARS-N while two recognized

the N-terminal domain. Two were characterized by SPR and found to have low nanomolar dissociation constants (1.7 nM and 72 nM). At least four transfected SARS-N binding intrabodies were capable of selectively disrupting SARS virus replication inside cells.[114] These anti-SARS intrabodies have been used as affinity reagents for detection of SARS.[128]

In a follow up study, anti-SARS fibronectins were engineered to recognize the nucleocapsid protein from SARS-CoV-2.[129] The nucleocapsid protein from SARS-CoV-2 and SARS-CoV are highly similar, with 91% identity and 94% similarity. The authors performed an initial doped selection based on one N-terminal domain binding fibronectin (NN1) and one C-terminal domain binding fibronectin (NC1) from the original selection, in order to improve the affinity and stability of these first-generation fibronectins. However, since the nucleocapsid sequence from SARS-CoV-2 (SARS-CoV-2 N) was not known at the beginning of the project, nucleocapsid from SARS-CoV (SARS-N) was instead used as the target. Two second-generation fibronectins, NN2 and NC2 were isolated with binding to both SARS-N (NN2 K_D = 3.3 nM; NC2 K_D = 390 pM) and to SARS-CoV-2 N (NN2 K_D = 28 nM; NC2 K_D = 6.7 nM). Both fibronectins retained binding to the respective domain of their parental clone and were able to bind the nucleocapsid protein inside SARS-CoV-2 infected cells. These second-generation fibronectins were once again doped and selected against SARS-CoV-2 N to make third-generation fibronectins. With only a single round of selection coupled with high throughput sequencing and a machine learning approach, several fibronectins were identified. Following expression and purification from *E. Coli*, one clone, NN3-1, was found to have a K_D = 18 nM. Finally, this group engineered a sandwich ELISA-based assay for SARS-CoV-2 N detection using either a fibronectin and an antibody, or using two fibronectins, with sensitivity limits approaching 4 pg/mL in human sera.

A three-loop library was used to produce Adnectins that bound to the ligand-binding domain of a promiscuous nuclear receptor family member, human pregnane X receptor (PXR). Eight Adnectins were identified, with binding affinities ($K_{D)}$ ranging from 100 nM to sub-nanomolar values. These Adnectins bound to different epitopes with one Adnectin (K_D = 11 nM) able to compete with the endogenous PXR ligand, steroid receptor co-activator-1 (SRC-1).[97] Previously, the authors discovered a small molecule antagonist of CC Chemokine Receptor-1 (CCR1) with undesirable off-target binding to PXR. The anti-PXR Adnectin was used to obtain a co-crystal structure of the small molecule compound in complex with PXR. This co-crystal structure was important for the structure-based design of new small molecule derivatives with reduced PXR binding and off-target effects.[97] This work highlights the ability of selected fibronectin ligands to act as crystallization chaperones to enhance target crystallization efforts.[130]

The ^{10}Fn3 scaffold was also exploited to identify state-selective K- and H-Ras intrabodies. mRNA display was used to select a ^{10}Fn3 that bound GTPγS-K-Ras(G12V), a constitutively active mutant Ras commonly found in cancer. This study included selective pressure for fibronectins that recognized the active, GTP-bound state. The selection resulted in a first-generation antibody called RasIn1 (**Ras In**trabody), which had modest binding affinity (K_D = 2.1 μM) and was state selective for active GTP-Ras versus inactive GDP-Ras. Affinity maturation of RasIn1 by doping the BC loop of RasIn1 and selecting with a fully randomized FG loop resulted in RasIn2. The second generation fibronectin showed improved affinity (K_D = 120 nM) while retaining selectivity towards the GTP bound state of mutant K and H-Ras.[119] By designing and expressing RasIn-GFP variants, the authors were able to monitor the activation state of Ras in living cells.[119]

Lastly, intrabodies to explore neuronal dynamics were engineered with mRNA display. These intrabodies were termed FingRs (**F**ibronectin **In**trabodies **G**enerated with m**R**NA display) and were first selected against excitatory and inhibitory post-synaptic marker proteins, Post Synaptic Density-95 (PSD-95) and Gephyrin, respectively.[117] The authors of this study first selected for fibronectin ligands that recognized each protein. Several clones from each selection were expressed in cells and screened for their ability to colocalize with exogenously expressed target. Surprisingly, only a few fibronectins were able to colocalize in this assay, suggesting that this dual selection/screening strategy was required to identify functional FingRs. Fusing FingRs to GFP enabled live-cell imaging in dynamic protein trafficking and localization experiments. The authors note that use of these FingRs does not lead to observable changes in neurons, such as spine density, size of PSD-95 or Gephryin puncta, morphological, or electrophysiological changes.[126] In a complementary study, a similar strategy was used to develop a FingR targeting Ca^{2+}/calmodulin-dependent protein kinase II α (CaMKIIα). Dynamic changes in CaMKIIα clustering and localization in response to pH, Ca^{2+}, or glutamate could be monitored in cortical neuron somata using FingR agents.[118] These FingRs have been used in several other follow-up experiments[131-133]

6 Peptide Evolution by mRNA Display

6.1 Peptides and Peptide-Based Therapeutics

Natural peptides (e.g., hormones, neurotransmitters and growth factors) have critical roles in human physiology, specifically bind to their respective cellular receptors, and trigger a variety of downstream signals. Peptide therapeutics have been developed based on these natural peptides and as a class, have desirable safety and efficacy profiles and can have beneficial outcomes in treating

human diseases.[134] Peptides have the ability to modulate protein-protein interactions whereas few small molecules that bind tightly or disrupt protein-protein interfaces have been identified, with some exceptions.[135] One hypothesis to explain this observation is that protein interaction surfaces are typically large and flat,[135, 136] with the interface area per subunit for dimeric protein-protein interactions ranging from 350 to 4,900 angstroms.[137] Lastly, peptides also have lower production costs and reduced quality control issues compared to protein-based biopharmaceuticals therapeutics and small molecules, making them nominally attractive molecular architectures for rapid clinical translation.[134]

Unfortunately, peptides are often seen as poor therapeutic candidates because of the poor stability of unmodified natural peptides and their short circulation times. Rational peptide design approaches to improve the physiochemical properties of peptides include: 1) improving chemical and physical stability by replacing amino acid residues susceptible to oxidation, isomerization, or chemical modifications,[134, 138] 2) improving solubility by modifying the charge distribution or pI (isoelectric point),[134] 3) increasing resistance to enzymatic modification by removing potential cleavage sites from the peptide sequence or by addition of non-natural modifications (e.g., cyclization, stapling, N-methylation, etc.), and 4) extending circulation time through PEGylation, acylation or by incorporating albumin binding elements.[134, 139-141] However, as discussed above, these rational design approaches can be difficult because of context-dependent effects.

In the context of oncology, peptides are attractive alternatives to existing biologics because their tumor penetration is potentially enhanced relative to larger biologics. Tumor penetration is a complex function of molecular size, vascular permeability, affinity, diffusibility, stability, and plasma clearance.[142] A comparison of Her2 targeting therapeutics of vastly differing molecular weights demonstrated that compounds with low effective molecular weight (e.g., affibodies and peptides) and high molecular weight (e.g., antibodies) penetrated tumors much more effectively than compounds with intermediate molecular weights (e.g., Fab fragments and scFvs).[67] The higher tumor permeability of small peptides was attributed to their rapid diffusivity and interstitial transport as well as enhanced extravasation through capillary vessels of the tumor tissue.[67] High tumor penetration of extremely large molecules, such as antibodies, was attributed to their long serum half-lives (days to weeks) which provides sufficient time for slow, but continuous tumor uptake. In addition, the rate of clearance from the body is roughly inversely proportional to compound size, and as a result, peptides offer different pharmacokinetics than mAbs. Unlike antibodies the small effective molecular weight of peptides generally results in rapid renal clearance within minutes following their administration.[143] In some applications – such as imaging or treatment with compounds with small therapeutic windows – fast clearance of a compound could be desirable. Finally, peptides are generally considered less

immunogenic than proteins (though peptides may contain some immunogenic sequences[143]) and therefore are predicted to have more favorable safety profiles.[144, 145]

Peptides thus offer a different modality for treatment of disease and many efforts have focused on isolating novel peptide sequences that recognize macromolecules or making peptides more drug-like through macrocyclization and introduction of non-natural amino acids. In this section, we review mRNA display selections supporting these efforts.

6.2 Linear Peptides Selected with mRNA Display

6.2.1 RNA Binding Peptides

RNA- and DNA-binding proteins are key regulators of transcription and translation.[64] mRNA display has been used to discover novel ligands that recognize nucleic acids with high affinity and specificity.[146, 147] Engineering novel nucleic acid-binding ligands is a challenge for mRNA display since the nucleic acid target must be recognized in the context of the fused mRNA/cDNA that could cause off-target binding. Liu *et al*. showed that the λ N peptide (1-22 amino acids) synthesized as an mRNA-peptide fusion retained its ability to recognize its cognate BoxBR target.[13] Selection conditions were also optimized in order to develop a robust protocol for selection of RNA-binding peptides.[23] An important result from this work was that increasing the amount of non-specific competitor (i.e., non-target nucleic acid, such as tRNA) increased the enrichment of RNA-binding peptides, probably by increasing the selection stringency for peptides that bound to the target RNA.

Building on this work, Barrick *et al*. designed several libraries based on the λ N peptide.[146] One library randomized two positions and was selected against the BoxBR hairpin target. Surprisingly, few of the resulting peptides contained wild type residues at the randomized positions, with arginine favored at position 15 instead of the wild type glutamine. Although these peptides still bound the BoxBR target, they did so using a distinct recognition mode relative to wild type λ N peptide. A second library of 9 trillion sequences where the first ~11 amino acids of λ N peptide were fixed were while the last 10 C-terminal amino acids were randomized. This library was panned against three targets: 1) the cognate BoxBR RNA hairpin, 2) a non-cognate GNRA tetraloop, or 3) a non-cognate P22 hairpin. These targets all share the same stem as BoxBR, but differ in the hairpin loop by a single nucleotide.[23, 146] More than 80 different peptide sequences were isolated which had few similarities with the wild type sequence or to each other. As with the selection described above, Arg15 was the most conserved residue in final pools. The selected peptides all bound their targets with nanomolar K_D values and were able to distinguish between different RNA hairpins.[146] Subsequent studies further examined the function of these selected peptides as well as their affinity and specificity for different RNA targets.[148-150]

6.2.2 G-Protein Signaling

Peptides can also be used to modulate intracellular signaling. Many of the most important intracellular signaling networks are controlled by G-Protein Coupled Receptors (GPCRs).[151, 152] Binding of cognate ligands to GPCR extracellular domains results in activation of G-proteins bound to the cytosolic portion of the receptor.[153-155] There are three classes of G-protein subunits (α, β, γ), that associate in a combinatorial fashion.[156] Furthermore, G-proteins α subunits have different states (GDP-bound, GTP-bound, or apo) which dictate their biochemical and biological function.[157]

To target proteins in the Gα family, Ja *et al*. designed a library based on the G-protein regulatory motif (L19 GPR) and performed a selection using Giα1 as the target. The library fixed 10 amino acids of the L19 GPR motif to act as an "anchor" for binding to Giα1, followed by six random amino acids. The selection resulted in a peptide called R6A (K_D of 60 nM) which was selective for the GDP-bound form of Giα1. R6A was truncated to a nine amino acid version (called R6A-1) that retained a K_D of 200 nM for Giα1. Surprisingly, R6A-1 only includes two amino acids from the original GPR "anchor," suggesting that the majority of the fixed GPR residues were dispensable for binding in the context of the newly selected residues. However, R6A and R6A-1 still compete with L19 GPR for binding, suggesting that they bind the same site, though the authors could not rule out allosteric competition. In addition, both peptides inhibit the guanine nucleotide dissociation of Giα1 and compete with G$\beta\gamma$ for binding to Giα1.[153, 158]

Further studies examined the specificity profile of the selected peptides. While L19 GPR has selectivity for the Gαi class, R6A was able to bind to three Gα classes, and R6A-1 was able to bind to all four Gα classes (Gα, Go, Gq, and Gs).[159] Since truncation of R6A to R6A-1 resulted in a decrease of specificity, the authors hypothesized that performing the inverse experiment – i.e., addition of amino acids to R6A-1 – might confer binding specificity to different Gα classes. To test this hypothesis, Austin and co-workers designed a library based on R6A-1 of the form MXXXXXX**DQLYWWEYL**XXXXXX, where the central R6A-1 sequence (bold) was doped at ~50% wild type amino acids and six random amino acids (X positions) were added to the N- and C-terminus.[160] This library was used in a positive selection for Gαs(s) binding, which resulted in a peptide called GSP that was able to bind with some specificity to Gαs(s) but still retained some binding to Giα1. A second library based on the GSP sequence was used in a second selection that included a negative selection for binding to Giα1. Here, a molar excess of soluble Giα1 was added to the binding buffer to act as a decoy in the presence of

immobilized Gαs(s). This dual selection strategy resulted in highly specific Gαs(s) peptides with K_Ds in the 130-300 nM range, representing an over 8,000-fold change in specificity from Giα1 to Gαs(s).[160]

This library was also used in a second selection to generate state-specific peptides. In this selection, the library described above was targeted to Giα1-AlF (AlF_3 or AlF_4^-), which mimics the transition state of GTP hydrolysis. This selection also included a negative selection against Giα1-GDP to remove Giα1-GDP binding sequences. Two peptides with the highest ratio of binding Giα1-AlF versus Giα1-GDP (AR6-04 and AR6-05) were chosen for further characterization. Even with the negative selection, AR6-05 had a K_D of 10 nM for Giα1-GDP, blocked Gβγ binding, and enhanced the basal current of a downstream G-protein-activated inwardly rectifying potassium (GIRK) channel. AR6-04 was the only peptide that bound more strongly to Giα1-AlF versus Giα1-GDP. It also enhanced Gβγ binding to Giα1, in contrast with the AR6-05 and the parental R6A-1 peptides. One reason why Giα1-AlF-specific peptides might have not been readily found is that AR6-04 also has a much weaker K_D of 10 μM, yet was still able to decrease downstream basal GIRK current.[161]

Ja and co-workers attempted to modulate G-Protein/GPCR signaling by engineering peptides that directly target a GPCR.[162] Using mRNA display, a 27-mer random library was selected against the ectodomain of Methuselah (Mth), a *Drosophila melanogaster* GPCR associated with longevity. Several peptides in the final pool contained a [R/P]XXWXXR motif and showed dissociation constants ranging from 18 to 31 nM. These peptides antagonized Mth signaling with IC_{50} values ranging from 45 to 115 nM. Consistent with previous results showing that Mth antagonism increases fly lifespan, transgenic flies expressing one of the selected peptides showed a 38% increase in mean life span and a 26% increase in maximal life span.

6.2.3 Cell Penetrating Peptides

mRNA display has also been used to discover peptides that penetrate cell membranes and enhance the delivery of otherwise non-penetrant molecules. In many of these selections, an mRNA display library is first incubated with cells, the molecules on the outside of the cells are removed, and the cells lysed to recover mRNA-peptide fusions that successfully crossed the cell membrane. Kamide and co-workers performed such a selection using a 15-mer random library fused to a C-terminal cargo protein (a POU domain).[163] This library was selected for entry into Jurkat cells and yielded several putatively alpha helical peptides that contained a cationic helical face. One of these peptides was

labeled with fluorescein and showed higher intracellular fluorescence in CHO, HeLa, and Jurkat cells relative to the TAT peptide, a previously identified cell penetrating peptide.

In a similar study, the same library was used to select for cell penetrating peptides in the glioblastoma multiforme (GBM) cell line U87MG with the goal of using these peptides for cell-specific delivery.[164] After selection and screening of fluorescein-labeled peptides, peptide1 resulted in the highest internal fluorescence in U87MG cells. Peptide1 was specific for the U87MG cell line and could deliver a small peptidic inhibitor of p16, triggering apoptotic cell death.

Lee *et al*. used a 29-mer random library to select for peptides that would increase peptide uptake in HEK 293 and HeLa cells.[165] After selection and sequencing of the library, two peptide sequences were identified and fused to the red fluorescent protein, DsRed. Incubation of these constructs with HeLa and HEK293 cells resulted in higher intracellular fluorescence compared to a DsRed fusion tagged with Arg11, a previously identified cell penetrating peptide.

6.2.4 Epitope Mapping

mRNA display has been used as a tool to identify peptides that interact with antibodies for epitope mapping and identification of epitope mimics, or "mimotopes", to act as vaccine antigens.[166-170] One of the first examples was the selection of epitope-like motifs that bound to the 9E10 anti-c-myc antibody. 9E10 recognizes the linear epitope EQKLISEEDL and 61% of selected clones contained the "LISE" sequence, and another 25% of clones showed single homologous substitutions in this motif. A similar selection was performed against the M2 anti-FLAG antibody that binds the sequence DYKDDDDK.[29] Four different libraries of varying levels of randomization were tested using both mRNA display and cDNA display. Both techniques showed that the antibody preferred an eDYKxxDp motif (where upper case indicate strong conservation and lower case indicate weaker conservation).

mRNA display was also used to identify peptides that bind to an anti-polyhistidine mAb. A linear X_{27} library was panned against immobilized antibody yielding several peptides containing stretches of 2 to 5 histidine residues. Surprisingly, the selected sequences also revealed a high bias for arginine.[168] In order to minimize the length of the dominant peptide sequence (Peptide C), the authors constructed a deletion library and reselected against the anti-polyhistidine mAb. By aligning the fragments resulting from this second selection Peptide C (K_D = 18.5 nM) was minimized to 15 amino acids (K_D = 38 nM). Interestingly, most sequences recovered in the second selection were not homologous to Peptide C and a new consensus motif (ARRXA) was observed.

Traditional vaccine development for pathogens such as Hepatitis C Virus (HCV) has been challenging. To address this, Guo et al. performed an mRNA display selection to identify mimotopes,

or short peptides that mimic the structure of native epitopes. These mimotopes could then be used to elicit the production of neutralizing antibodies.[167] Using mRNA display, a random 27 amino acid library was sieved against the HCV-neutralizing antibody mAb41, which resulted in peptides with a common W(L/I)XX(L/I) motif. The conserved amino acids in this motif align with W437, L438, and L441 in the wild type sequence of the HCV Genotype 1a E2 protein, indicating which amino acids are important for mAb41 binding. Interestingly, a previous PD selection against mAb41 only identified peptides with W437 and L438 but not L441.[171] When administered to mice, the selected peptides elicited an immune response and the production of neutralizing antibodies similar to the original mAb41 antibody.

Mimotopes were also generated against cetuximab, an anti-human EGFR therapeutic mAb.[170] After six rounds of mRNA display, one dominant peptide, M077-A02 showed the highest level of selective binding to cetuximab. Rabbits immunized with M077-A02 conjugated to keyhole limpet hemocyanin (KLH) developed antibodies that were reactive with human EGFR. These studies indicate that mRNA display can be used to reliably generate effective peptides mimotopes against antibodies of interest.

6.2.5 Enzymatic Substrate Mapping

mRNA display also provides a powerful tool to identify the optimal sequence for enzyme substrates.[172, 173] This is typically accomplished by incubating an mRNA display library with the enzyme of interest and purifying the modified sequences. This approach was first used to determine residues critical for the interaction between *Ecballium elaterium* trypsin inhibitor two (EETI-II) and trypsin. In this study, positions 3-8 of EETI-II, which interact with trypsin, were randomized. A consensus sequence, PRXLXX, was identified, with 20% of the clones having the wild type PRILMR sequence. This study confirmed that mRNA display could be used to optimize enzyme substrates as well as target-binding ligands. mRNA display was also used to determine the consensus sequence for the substrates of the v-abl tyrosine kinase.[172] A random peptide library containing a central fixed tyrosine ($GCGGX_5$-Y-X_5GCG) was incubated with v-abl, followed by immunoprecipitation with a phosphotyrosine-specific antibody. The selection resulted in peptides closely resembling the previously known consensus sequence (I/L/V-Y-X_{1-5}-P/F). In a second selection, the authors used a cDNA library to identify cellular proteins that were substrates for v-abl.[172] In addition to identifying previously known substrate proteins of v-abl, novel v-abl substrates were also identified and may indicate a more extensive interactome for this kinase.

An mRNA display selection was also used to identify substrates of transglutaminase, an enzyme that catalyzes the crosslinking of glutamine and lysine side chains. A random 10 amino acid peptide

library was first incubated with *Streptomyces mobaraensis* transglutaminase (STG) in the presence of beads with immobilized hexalysine (K_6). Functional STG peptide substrates thus could be immobilized on the beads and amplified.[173] Two peptides were minimized to pentamers which showed selective reactivity to *Streptomyces mobaraensis* transglutaminase relative to guinea pig transglutaminase, demonstrating some specificity for the enzyme used for selection.

Fleming *et al.* used mRNA display to investigate the interaction of PaaA enzyme with its substrates and to evaluate its promiscuity, recognition mode, and processing.[174] PaaA is involved in the biosynthesis of Pantocin A, a ribosomally synthesized and post-translationally modified peptide natural product (RiPP). PaaA catalyzes a bicyclization reaction through dehydration and decarboxylation of two glutamic acids within the precursor peptide, making the bicyclic peptide products resistant to proteolytic cleavage by GluC. This property was used in a selection to probe PaaA activity where a peptide library was first incubated with PaaA, treated with GluC to remove the non-PaaA modifiable sequences, and the uncleaved sequences that were modified by PaaA were recovered. Using a 6-position library, the authors obtained a consensus sequence of XBXXRB (where B = V, L, or I), which matched a previously determined FXXBXXRB consensus sequence (underlined amino acids correspond to the randomized positions). Surprisingly, the enzyme accepts a wide range of substrates outside of residues involved in peptide binding. An analogous study by Vinogradov and co-workers was recently published and described the use of reactivity-profiling mRNA display to identify the substrate preference of the lactazole biosynthetic pathway.[175] Post-translational modification by these and other similar enzymes could be used to expand the number of unnatural structures that could be used in mRNA display selections (see the Unnatural Peptide section below).

6.2.6 Peptides Targeting Cancer Relevant Proteins

Immune surveillance provides a critical role in preventing the formation and expansion of malignant tumors. However, one of the hallmarks of cancer is the development of molecular mechanisms to evade immune surveillance.[176] The interaction between the PD-L1 receptor on tumor cell surfaces with the PD-1 receptor on T cell surfaces dampens T-cell activity and dramatically attenuates their anti-tumor activity. A dual-stage mRNA display strategy was used to identify SPAM (**S**ignal **P**eptide-based **A**ffinity **M**aturated ligand), an 18 amino acid linear peptide that binds to glycosylated and non-glycosylated human PD-L1 with dissociation constants of 67 and 119 nM, respectively.[177] SPAM was highly selective for human PD-L1 relative to murine PD-L1 and human PD-L2. SPAM was found to disrupt binding of PD-1 as well as the mAbs Atezolizumab and Avelumab, suggesting that the SPAM binding site overlaps with the native PD-1 binding interface. SPAM is also

resistant to modification in human serum, showing no proteolytic degradation after five hours in serum *ex vivo*. While additional affinity maturation of this peptide is needed for *in vivo* applications, its relative ease of synthesis and biological stability make it an attractive lead compound.

MDM2 (Mouse double minute 2 homolog) is an E3 ubiquitin ligase that ubiquitinates the p53 tumor suppressor protein, thereby tagging p53 for destruction by the proteasome. Upregulation of MDM2 is found in many tumors and represents a potential target for anticancer therapeutic development. An mRNA display selection targeting MDM2 resulted in a peptide called MIP (**M**DM2 **I**nhibitory **P**eptide) that inhibited the interaction of MDM2 or MDMX (an MDM2 homologue) with p53.[154] MIP was shown to interact with MDM2 inside cells, resulting in stabilization of p53 and reactivation of the p53 pathway. Further characterization of the peptide by NMR showed that the peptide formed an α-helical structure. Key hydrophobic residues that participate in the peptide:MDM2 interface were also identified.[178]

Several mRNA display selections have targeted the anti-apoptotic protein Bcl-x_L (B-cell lymphoma-extra large). Using a random 16-mer library and a partially randomized library based on the Bak peptide (an endogenous peptide that binds Bcl-x_L), Matsumura and co-workers selected for peptides that bound to Bcl-x_L. Two peptides called A01 and B01 showed IC_{50} values of 0.9 μM and 6.4 μM, respectively, in a competition binding assay with Bak. These peptides bound Bcl-x_L when transfected into cells as GFP fusions and could block the anti-apoptotic function of Bcl-x_L to induce cell death. Additionally, using mRNA display, 21-amino acid peptides with picomolar affinities to Bcl-x_L were also isolated from a primary selection followed by a second selection using a doped library.[179]

6.2.7 Non-biological Target Selections

While the majority of mRNA display selections have been carried out against macromolecular targets, selections have also been performed against non-biological targets. In several cases, the goal of these selections is to discover peptides that react with small molecules, enabling the selective modification of proteins and peptides without enzymatic assistance. Kawakami *et al.* developed the **D**irected **I**n **V**itro **E**volution of **R**eactive peptide tags via **S**equential **E**nrichment (DIVERSE) system to discover peptides that react with small molecules.[180] This group designed a selection where peptides that react with a p-(chloromethyl)benzamide (p-ClBz) moiety would lead to immobilization of the peptide on the solid phase resin. The selective pressure was increased throughout the selection by decreasing the reaction time between the library and the immobilized p-ClBz. After 19 rounds of selection, two cysteine-containing peptides were isolated. A second-generation peptide (WFWCPYWCCWVP) was

isolated after a maturation selection. This peptide covalently reacted with p-ClBz-containing molecule within 30 min and could be used to add fluorescent dyes the peptide. Fusion of the tag with GFP demonstrated that the conjugation reaction could be catalyzed inside living cells.

An alternate strategy was used to select for peptides that could undergo cysteine arylation with perfluoroarenes. Evans and co-workers designed an mRNA display selection where a peptide library was incubated with a biotinylated water soluble perfluoroarene, enabling peptides that successfully reacted with the perfluoroarene target to be selectively purified.[181] Previous studies had identified a FCPF sequence that performed the cysteine arylation and this sequence was doped into the library. Interestingly, the FCPF sequence was not enriched after selection, and the winning MP01 sequence instead used a cysteine encoded in the random region. The MP01 sequence was quantitatively arylated in 6-8 hours. The reaction was found to require some peptide structure, as addition of urea into the reaction significantly inhibited MP01 arylation (but did not affect the arylation of a control sequence). Addition of the MP01 sequence to Sortase A showed that the reaction was regioselective where the MP01 cysteine was arylated specifically, even in the presence of a cysteine in the active site of the enzyme. Further investigation showed many other perfluoroarene-reactive peptides, some which were predicted to have β-sheet and α-helical conformations.[182]

A similar selection was performed to isolate peptides that would react with dibenzocyclooctyne (DBCO), a strained cyclooctyne that is commonly used for copper-free click chemistry.[183] Using cDNA display, a 23 amino acid peptide was discovered that contained a single cysteine that reacted with DBCO. The peptide was shown to react with DBCO by MALDI-TOF mass spectrometry and was minimized to a 16-mer peptide called sDRP. However, the reaction yield was relatively poor as only about 20% of sDRP could be modified by DBCO. sDRP was also fused to Dihydrofolate reductase (DHFR), which could be specifically labeled with DBCO-tetramethyl rhodamine even the presence of other cysteine-containing proteins.

Peptides that bind to small molecules have also been isolated using cDNA display. Phenolphthalein was immobilized on a solid support and used as a target for a cDNA display selection.[184] In this study, the authors used a library with a higher fraction of aromatic residues at the randomized positions and selected a hydrophobic peptide called LV59 (LVFLIWWM). LV59 binds phenolphthalein at neutral pH but is eluted at alkaline pH. Control experiments where aromatic residues were mutated to alanine abrogated binding. However, LV59 showed some weak cross-reactivity with phenol, suggesting that additional selection experiments are required to develop highly selective dye-binding peptides.

Surfaces and membranes may also serve as the target in mRNA display selection.[185, 186] Artificial linear peptides that can bind to the c-face of hydroxyapatite were selected by Ono and co-workers through mRNA display. An alanine-asparagine-threonine (ANT) motif was recognized to be essential for the adsorption of the peptides on the hydroxyapatite surface.[185] Kobayashi and co-workers used liposomes as an artificial lipid bilayer target and selected for peptides that can bind to such surfaces. The selected peptide contained both cationic and amphiphilic regions and bound to a wide variety of liposomes with different compositions. One selected peptide was successfully used as an anchor to immobilize macromolecules on the liposome surface.[186]

Table 2: Linear Peptides Consisting of Canonical Amino Acids Selected By mRNA Display. Affinities are obtained directly from the corresponding reference and are not normalized for temperature. The randomized residues are underlined. (Abbreviations: SPR (Surface Plasmon Resonance); FT (Fluorescence Titration); FP (Fluorescence polarization); BLI (Bio-Layer Interferometry); AlF (Aluminum fluoride), Gαs(s) (the short isoform of Gαs), RA (Radioactive Assay); Mth (Methuselah); DOPC (1,2-dioleoyl-sn-glycero-3-phosphocholine); HCV (Hepatitis C Virus); KLH (Keyhole Limpet Hemocyanin)

Target	# of random residues	Library Diversity (#of unique sequences)	Affinity measurement method	Top Peptide Sequences	Affinity/IC_{50}/Kinetic Properties	Notes	Ref
boxBR RNA hairpin	2	150	FT	MDAQTRRRERRAEKQAQWKAANDYKDDDD KNSCA	K_D= 1.0±0.2 nM	GNRA: K_D= 9.0±0.7 nM P22: K_D= 41±3 nM	146
boxBR RNA hairpin	2	1600	FT	MDAQTRRRERRAEERVAQWKAANDYKDDD DKNSCA	K_D= 8.5±2 nM	GNRA: K_D= 800±150 nM P22: K_D= 580±20 nM	
Equimolar mixture of three hairpins: (i) boxBR RNA (*ii*) GNRA tetraloop and (*iii*) P22	10	~9 X 10^{12}	FT	MDAQTRRRERRALERTKLEKALQLRNNSCA	K_D= 3.4±0.1 nM	GNRA: K_D= 81±2 nM P22: K_D= 60±3 nM	
				MDAQTRRRERRAMERATLPQVLQLRNNSCA	K_D= 3.0±0.2 nM	GNRA: K_D= 288±7 nM P22: K_D= 246±7 nM	
				MDAQTRRRERRALQRSRARHALQLRNNSCA	K_D= 0.5±0.1 nM	GNRA: K_D= 6.5±0.7 nM P22: K_D= 8.4±0.8 nM	
				MDAQTRRRERRAALRNEKFWVVQLRNNSC A	K_D= 1.9±0.5 nM	GNRA: K_D= 93±9 nM P22: K_D= 140±10 nM	
				MDAQTRRRERRANMRMYRSLVIQLRNNSCA	K_D= 0.4±0.1 nM	GNRA: K_D= 9±2 nM P22: K_D= 14±1 nM	
Human PD-L1	17	>10^{12}	FP	MPIFLDHILNKFWILHYA	K_D= 67-119 nM	Selective binding for human PD-L1	
v-abl tyrosine kinase	10	~10^{12}-10^{13}		Consensus motif with fixed tyrosine: GCGGXXXXXYXXXXXGCG Consensus motif with upstream tyrosine: GCGGY_{1-5}YXXXXXGCG Consensus motif with downstream tyrosine: GCGGXXXXXYY$_{1-5}$GCG			172
Bovine trypsin	6	6.4 X 10^7	RA	PRILMR	K_D= 16±3.2 nM		166
				PRVLAL	K_D= 52±21.0 nM		
				PRLVQR	K_D= 53±9.0 nM		
				PRLLAP	K_D= 81±21.0 nM		
				PKLLAP	K_D= 21±2.4 nM		

Anti-c-myc antibody 9E10	27	2 X10^{13}	-	CASVISEREC EEYLVSEYVM RQYLISEYEH LQRLISEQMF IVRLLSEYHM EEYLLSEYVM MQNLISEHEL TMDLIPEHYM EQKLISEEDL DMMLISEKEL FQALIAEEEL QRVLISEFWL			
Human α-thrombin	15	1.2 X 10^{11}	SPR	ERNYNDFCDPGRVGL	K_D= 520±6 nM		187
				FFDRYDSARDPGRLL	K_D= 166±18 nM		
Giα1-GDP	6	6.4 X 10^{7}	SPR	MSQTKRLDDQLYWWEYL	K_D= 60 nM; IC_{50}~0.5uM		153
Anti-polyhistidine mAb	27	~10^{12}	SPR	DGHPERHDAGDHHHHHGVRQWRLISTG	K_D= 18 nM		168
				RHDAGDHHHHHGVRQ	K_D= 38 nM		
				ITNSPGRFRHHHVLARRHALYR	K_D= 15.5 nM		
				MKVRRDVMRWHHHHRMARRKANR	K_D= 7.6 nM		
Botulinum neurotoxin serotype A (light chain)	4		FT	MWMTSCRATKML	IC_{50}= 56.3 ± 2.9 uM K_i= 7.3 uM		188
Giα1 GDP-AlF	21	~2 X 10^{13}	SPR	DESDPEELMYWWEFLSEDPSS	K_D=10 nM		161
Mth ectodomain	27	~1.5 X 10^{13}	SPR	MRLVWIVRSRHFGPRLRMALLGSDRKMW	K_D= 4.1 nM IC_{50}=45±10 nM	N-stunted induced Mth signaling antagonist	162
				MAPRAVWIQRAIQAMFRLASRQESKAFN	K_D= 7.0 nM IC_{50}=115±25 nM	N-stunted induced Mth signaling antagonist	
				MNVSWGSFPSSWLQRYYLAKRREADVTL	K_D= 6.3 nM		
				MLKYPDTWLARSLSVFYLRKSARQGKSV	K_D= 9.5 nM		
				MVRIGYTSKPGGMNPGNSYTMSIIRMLI	K_D= 6.1 nM		
5' upstream binding site of Thymidylate Synthase mRNA	21	>10^{13}		HCYPLDESILRLVRGELGAVH YWFAWAKSWQLAKREGHMGFD NWSGFYNLKLNTLKSVRQVHY NWHHALLSDIVSALNKSSLWN NCGTEMFCMDKINEWREVYVD NWSLIHKKYLQQAKMKYARCH DWTLMKVHVKQCVRKLESFTN HCRFVRRVAGLMFRERLEDDH NWRLSHNAVLDDARVQYGVHH		The selected pool of peptides suppressed thymidylate synthase mRNA translation in a dose dependent manner	147
Gαs(s)	21	1.6 X 10^{13}	SPR	MAMSDRNKRLTVWEFLALPSST	K_D=100±15nM		160
	21	~2.5 X 10^{12}	SPR	MAMSDQNKRMTVREFLALPSSL	K_D=300 nM		
				MYTSDHNKLLTVREFLALPSST	K_D=130 nM		
Anti-human TP53	10	~10^{13}	SPR	TFSDLWKLLP	K_D= 6 nM		169
				LFSDLNKLKP	K_D= 11 nM		
				TDSDLHKLKS	K_D= 59 nM		
U87MG glioblastoma cell line	10	>10^{12}		NTCTWLKYHS			163, 164
Bcl-X_L	16		FP	FPRWKLLAHWADRWWF	IC_{50}= 0.9 uM		189
	11		FP	YQVARMLRRVADQMAS	IC_{50}=6.4 uM		
Bcl-X_L	20			MIETITIYNYKKAADHFSMSM	K_D= 23 pM		179
	20			MIEAISIYNYKKAADHYAMTK	K_D= 15 pM		
	20			MIDTNVILNYKKAADHFSITM	K_D= 2.4 pM		
Interleukin-6	11			INTLLSEINSILLDIISLL	IC_{50}= 2.8 uM		155
cetuximab	10			CLFSLSTRRLDC		The peptides did not show significant binding *in vitro* but showed binding after conjugation to keyhole limpet hemocyanin (KLH)	170
	20			MEGCLRTWSLFDRRLKCMVG			
	20			CYDVNGVWIRLRNPTHAGIRFC			
MDM2	12	5.1 X 10^{11}	SPR	PRFWEYWLRLME	K_D= 18.4 nM IC_{50} = 0.01 uM		154, 178
HEK293 cells	20	>10^{12}		MAMPGEPRRANVMAHKLEPASLQLRNSCA			165
HeLa cells	20	>10^{12}		MAPQRDTVGGRTTPPSWGPAKAQLRNSCA			165

Streptomyces mobaraensis Transglutaminase	10			RLQQP RTQPA			[173]
Hydroxyapatite (C face)	16		FT	NPPTRQTKPKRVANTN	Adsorption constant= 114 nm^2 mg^{-1}	Peptides selected were highly specific to the c face of hydroxyapatite rather than the unoriented surfaces	[185]
				SAANTTQLNTPTEDNEP	Adsorption constant= 70 nm^2 mg^{-1}		
				TTDPHRTDNNRTKYQT	Adsorption constant= 34 nm^2 mg^{-1}		
				TDPPSPKHHCLPTTAN	Adsorption constant= 23 nm^2 mg^{-1}		
				TKTSPTPENPTQQHRT	Adsorption constant= 14 nm^2 mg^{-1}		
HCV neutralizing mAb41	15 or 27		BLI	MMECEKGKYVQGWLCHLFWEDCQDRGWL EQLRNSCA	K_D= 16.7 nM		[167]
				MTMPTMVEHSEVAWLDRLVTPYEGWIECIQL RNSCA	K_D= 32.9 nM		
				MYMTSPMSQPCGWIEYLAHEDQPVP-WLDQLRNSCA	K_D= 69.7 nM		
				MQHWTQEYTTMWNEDTGWLDWLIEQDHCQ LRNSCA	K_D= 11.0 nM		
DOPC liposomes	30	6 X 10^{12}	BLI	RHSKSLPSRVIPRADPRTKTRRRRRRKRTL		The binding was not specific for this liposome	[186]
PEGylated pentafluoroarene	30	~5 X 10^{13}		MHQKYKMTKDCFFSFLAHHKKRKLYPMSGS GSLGHHHHHHRL	Rate constant: 0.28 $M^{-1}s^{-1}$		[181, 182]

7 Toward the Selection Of "Drug-Like" Peptides By mRNA Display

The development of peptide drugs has been limited in large part by poor stability in biological systems and poor cell permeability. Looking to nature, there are numerous examples of drug-like, bioactive peptides that are stable in biological systems, modulate protein-protein interactions, and are cell permeable (**Figure 10**). Many of these peptides are classified as NRSPs, and are assembled by large, multi-protein complexes found in prokaryotic and eukaryotic organisms.[190, 191] These peptides have several features in common. First, they contain a mixture of both natural and non-natural amino acids[191] (**Figure 10**), especially N-methylated amino acids. N-methyl amino acids are known to enhance cell permeability[192, 193] and impart resistance to proteolytic degradation.[50, 194] Secondly, a significant number of bioactive natural peptides are covalently cyclized (as opposed to cyclized by redox-labile disulfide bonds). Cyclization can enhance binding affinity by increasing conformational restraint and reducing the unfavorable loss of entropy upon target binding.[195] Cyclization has also been shown to enhance stability to proteolytic degradation and may enhance cell uptake.[196, 197]

In theory, introduction of unnatural amino acids or cyclization into a natural peptide might be achieved through systematic medicinal chemistry optimization without *in vitro* selection. However, introducing these modifications into a sequence is rarely straightforward. For example, starting with a

Gαi1-binding peptide, Fiacco and co-workers systematically substituted each position with its corresponding N-methyl amino acid analog followed by measuring binding for Gαi1.[50] Many N-methyl substitutions resulted in a significant increase in stability toward degradation by trypsin even when placed within two amino acids (either N- or C-terminal) of the scissile amide bond. However, while protease resistance was improved, almost all substitutions resulted in a reduction of binding affinity, apart from one position that showed a 2.5-fold increase in binding. More concerning, a single N-methyl amino acid substitution at one position in the peptide changed the binding specificity from Gαi1 towards a different family member, Gα12. While introduction of N-methylated amino acids can successfully increase the protease resistance of selected peptides, these modifications may also be accompanied by a reduction in affinity and/or selectivity.[50] This observation argues that a multi-parametric selection strategy that balances affinity, selectivity, stability, and potentially cell permeability is needed to generate drug-like peptides by mRNA display.

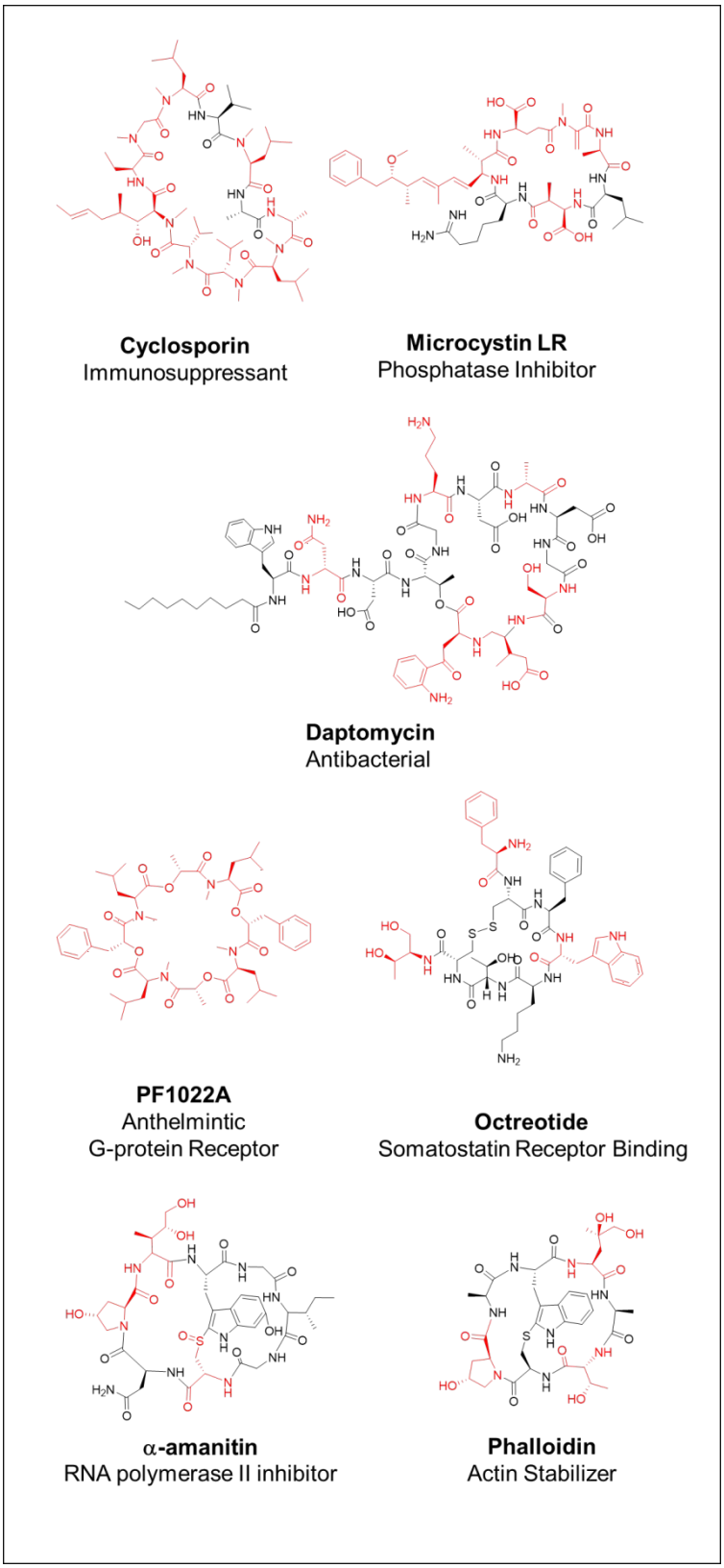

Figure 10. Examples of bioactive macrocyclic peptides. Non-natural amino acids are shown in red.

Directed evolution of mRNA display libraries containing unnatural amino acids and/or cyclization offers a potential solution. *In vitro* selection can simultaneously optimize multiple biochemical and physiochemical properties provided that appropriate selection pressures can be incorporated into the selection workflow. While the natural set of amino acids is sufficient for high affinity target binding, incorporation of non-natural modifications may facilitate the selection of more metabolically stable, cell-permeable peptides for *in vivo* applications. The challenge, however, is how best to efficiently incorporate these non-natural modifications into mRNA display libraries with high fidelity and minimal impact on the labile nucleic acid component. In the past twenty years, there have been significant efforts by multiple groups to **1)** incorporate non-natural amino acids and, **2)** incorporate covalent macrocyclization into mRNA display libraries for the purpose of selecting intrinsically "drug-like" peptides.

7.1 Addition of Non-Natural Amino Acids to mRNA Display Libraries

Incorporation of non-natural (non-proteogenic) amino acids in biological display systems via translation requires that the non-natural amino acid be coupled, or "charged" onto the 3' end of a tRNA molecule. This tRNA can recognize either a sense or nonsense codon and its aminoacylation can be accomplished in a variety of ways. In the chemoenzymatic approach (**Figure 11A**),[198, 199] an unnatural amino acid is chemically coupled to a dinucleotide, which is then ligated to tRNA. In the most widely adopted approach, the carboxylic acid is activated as a cyanomethyl ester following protection of the α-amino group. The activated amino acid is then coupled to phospho-deoxyC-riboA (pdCpA), a 5' phosphorylated dinucleotide. This "charged" dinucleotide is then enzymatically ligated to a tRNA lacking the last two nucleotides via T4 RNA Ligase to form an aminoacyl tRNA. Deprotection of the amino group is carried out immediately prior to translation.

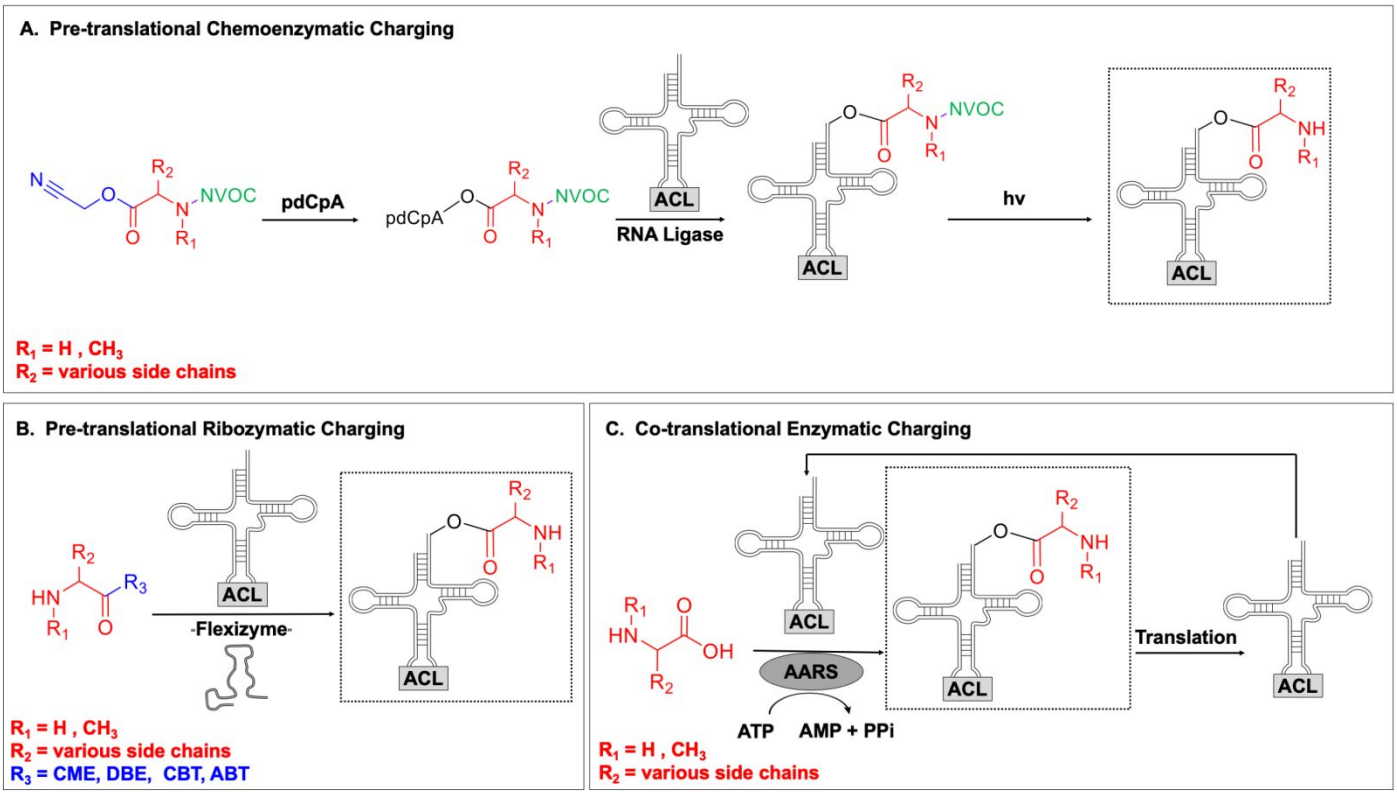

Figure 11: Methods for charging tRNA with non-natural amino acids for mRNA display selections. (A) In the chemoenzymatic method, the amino acid (R_1 = H, CH_3; R_2 = various side chains) is first protected at the α-amino group, typically with the photolabile NVOC group, and activated at the α-carboxylic acid as a cyanomethyl ester (CME). The resulting product is reacted with the 5' phosphorylated di-nucleotide pdCpA to form the aminoacylated product which is ligated to tRNA using T4 RNA ligase. The NVOC group is removed by photolysis (λ = 350 nm) immediately prior to translation. **(B)** In the ribozymatic method, the α-carboxylic acid is activated as an ester (CME = cyanomethyl ester, DBE = 3,5-dinitrobenzyl ester, CBT = 4-chlorobenzyl thioester, ABT = amino-modified benzyl thioester) which is then ligated to the 3' end of a tRNA by a small ribozyme ("flexizyme"). The aminoacylated tRNA is then added to the translation mixture. **(C)** Using a reconstituted translation system, non-natural amino acids are ligated to cognate tRNAs by aminoacyl tRNA synthetases (AARS) during the translation reaction. In this approach, a single tRNA molecule can undergo multiple rounds of charging and amide bond formation. ACL designates the anticodon loop of the tRNA.

This strategy was first applied in the context of mRNA display libraries in 2002 by Li and co-workers.[200] In this work, the non-natural amino acid biocytin (biotinyl-lysine) was protected with the photolabile NVOC protecting group and coupled to an amber suppressor tRNA derived from *Tetrahymena thermophilia* (THG73).[201] After removal of the NVOC group by UV photolysis, the charged tRNA was then added to an *in vitro* translation mixture containing an mRNA display library with a single randomized codon. After purification and selection for streptavidin binding, the selection resulted in near-total convergence to the UAG stop codon at the randomized position, indicating that the library

underwent selection for the non-natural biotin functionality. This work demonstrated that encoding of non-natural amino acids in mRNA display was efficient and that the addition of non-proteogenic chemical complexity provided a selective advantage in directed evolution experiments. A similar experiment was carried out by Sisido and co-workers which demonstrated that biocytin could be incorporated into mRNA display libraries by both nonsense suppression and four-base suppression and that selections against streptavidin resulted in enrichment of four-base or nonsense codons.[202]

While nonsense suppression of stop codons provides a facile way to incorporate non-natural chemical functionalities, it can only be used to incorporate a single non-natural amino acid (**Figure 12A**). While the use of the UAA and UGA stop codons is theoretically possible, release factors compete with these nonsense suppressors resulting in suboptimal suppression at these codons.[203] An alternative strategy of suppressing sense codons was first described by Frankel and co-workers in 2003,[204] where low-usage sense codons, particularly the valine codon GUA in the rabbit reticulocyte extract, were efficiently suppressed with chemoenzymatically acylated THG73 tRNA bearing a complementary UAC anticodon (**Figure 12B**). This approach enabled the production of mRNA-peptide fusions with up to 10 tandem N-methyl phenylalanine residues. These poly-N-methyl amino acid fusions were remarkably resistant to proteolytic degradation by Proteinase K, and this proteolytic resistance could be attenuated by replacement of even a single N-methyl phenylalanine with phenylalanine.

The chemoenzymatic approach for introducing non-natural amino acids is highly versatile virtually any non-proteogenic amino acid that is accepted by the translation system can be introduced into a peptide library. However, despite its flexibility, the chemoenzymatic approach requires multiple synthetic steps and a final deprotection step, which must be highly efficient and compatible with tRNA stability. To address this, Suga and co-workers developed a ribozyme-based ("ribozymatic") approach where amino acids are conjugated to tRNAs by engineered ribozymes ("Flexizymes")[205-207] prior to addition to a cell-free translation system **(Figure 11B)**. This technology is based on *in vitro* selected ribozymes that recognize and bind activated amino acids without recognition of specific R-groups. These flexizymes must also bind to the 3' end of tRNA, where the ribozyme catalyzes the aminoacylation of the terminal 3' hydroxyl group of the tRNA with concomitant release of the activating group. Although the first prototype ribozyme (Fx3)[206] only recognized and acetylated tRNAs with aromatic side chains, subsequent work resulted in the development of three additional flexizymes (dFx, eFx, and aFx)[205, 208, 209] that efficiently acylated tRNAs with a wide range of functionalities including amino acids with different R-groups, α-hydroxy acids, D-amino acids, N-methyl amino acids, and N-acyl amino acids.[208] By judiciously choosing the combination of activating group (CME (cyanomethyl ester); DBE (3, 5-dinitrobenzyl ester); CBT (4-chlorobenzyl thioester); or ABT (amino-modified benzyl

thioester)), amino acid side chain, and flexizyme, individual tRNAs can be charged with a wide range of non-proteogenic amino and hydroxy acids. Introduction of these ribozymatically charged tRNAs into a reconstituted cell-free expression system where corresponding aminoacyl tRNA synthetases (AARS) and sense tRNAs are omitted (the **F**lexible ***I****n vitro* **T**ranslation (FIT) system) allows for the reassignment of multiple sense codons and the expression of mRNA-peptide fusions with multiple non-natural amino acids.[210] While the ribozymatic approach supports robust peptide and protein translation *in vitro*, reassigned aminoacyl-tRNA species are still consumed stoichiometrically and cannot be regenerated during translation (**Figure 11C and Figure 12C**).

A third approach for incorporating non-natural amino acids involves using the natural substrate promiscuity of aminoacyl tRNA synthetases to recognize unnatural amino acid analogs and charge tRNAs with these amino acids. In 2001, Shimizu and co-workers developed a wholly reconstituted translation system based on purified recombinant components from *E. coli*.[211] This PURE system was later adapted for incorporation of multiple non-natural amino acids into a single peptide chain.[212-215] In 2012, Szostak and co-workers demonstrated the translation of mRNA display libraries in the PURE system with 12 codons reassigned to non-proteogenic amino acids.[216] Previously, the Szostak group had developed a method for screening non-natural amino acids that were able to be both activated and then charged onto tRNA by endogenous AARS,[217-219] including some N-methyl amino acids.[220] Using this knowledge, the PURE system could be simply supplied with non-natural amino acids, which would be faithfully incorporated via the natural translation machinery. One advantage of this co-translational charging strategy is that it is simpler to charge tRNAs with unnatural amino acids compared to the ribozyme or chemoenzymatic methods discussed above. Secondly, the system is more robust since aminoacyl tRNAs are constantly being replenished, resulting in high translational efficiency. Conversely, the disadvantage of this strategy is that the choice of non-natural amino acid is generally limited to those amino acids close in chemical space to their natural counterparts since they must be an efficient substrate for natural AARS enzymes. In the future, addition of engineered AARS enzymes[221] into the PURE system will likely further expand the non-natural amino acids that can be incorporated by this strategy.

7.2 Incorporation of Small Molecule "Warheads" And Branched Oligosaccharides In mRNA Display Libraries

The affinity and target selectivity of small molecule lead compounds are often suboptimal for *in vivo* applications. The affinity and/or specificity of a ligand can be dramatically enhanced by conjugating

the ligand to a peptide selected by mRNA display. Several strategies for conjugating a ligand to an mRNA display library include post-translational ligand conjugation or incorporation of the ligand into the library as a non-proteogenic amino acid.

In the first strategy, an mRNA display library is post-translationally conjugated with a small molecule through reactive moieties on amino acid side chains. Li and Roberts first demonstrated this strategy by conjugating 6-bromoacetyl penicillanate to a fixed cysteine residue within a randomized decapeptide library.[222] This library was used to target the *S. Aureus* penicillin-binding protein 2A (PBP2A), a major source of resistance against β-lactam antibiotics in Methicillin-Resistant *S. Aureus* (MRSA). After completion of the selection, the resulting penicillin-peptide conjugates were found to have a 100-fold greater inhibitory potency than the unconjugated penicillin alone.

A second strategy for addition of small molecule ligands uses the co-translational incorporation of a non-natural amino acid. One example of this strategy was described by Suga and co-workers where ε-N-trifluoroacetyl lysine (K^{Tfa}) was incorporated via a reassigned AUG codon/elongator tRNA-AA within the context of a randomized macrocyclic dodecapeptide library.[223] Selection against the human deacetylase SIRT2 resulted in the identification of a 3 nM inhibitor of SIRT2, approximately 3 orders of magnitude better than a control peptide where the K^{Tfa} residue was incorporated into an α-tubulin substrate motif.

A more recent study by Krauss and co-workers incorporated small molecules co-translationally by employing a reassigned AUG codon to direct the incorporation of homopropargylglycine (HPG) at either fixed or random positions within a randomized linear 27-mer mRNA display library.[224] Following translation in the presence of HPG, an azide-modified branched mannose oligosaccharide (Man_9-azide) was conjugated to HPG side chains via the copper-catalyzed azide-alkyne cycloaddition ("click chemistry"). This was one of the first studies to demonstrate the compatibility of click chemistry with mRNA display libraries and showed that the reaction does not affect mRNA integrity. The oligosaccharide libraries were then selected against the antibody 2G12, which recognizes a glycosylated epitope on the HIV envelope protein gp120. The resulting sequences showed a similar pattern of HPG incorporation with similar spacing between each site in both the fixed and random libraries. A consensus peptide sequence was observed in a fraction of the round 10 clones, although subsequent analysis showed very little correlation between binding affinity and the presence of the consensus sequence. The most promising variant, which incorporated HPG at five positions, was found to have a K_D of 1 nM against the 2G12 antibody, representing a >300,000-fold enhancement over a single Man_9 oligosaccharide. These results suggest that the mRNA display selection optimized the number and location of glycosylations within the peptide scaffold rather than the peptide sequence

itself. Lastly, although different strategies for addition of the ligand were used, all studies thus far incorporating small molecule ligands indicate that the selected peptide sequence is critical for increasing the affinity of the “warhead” for the target.

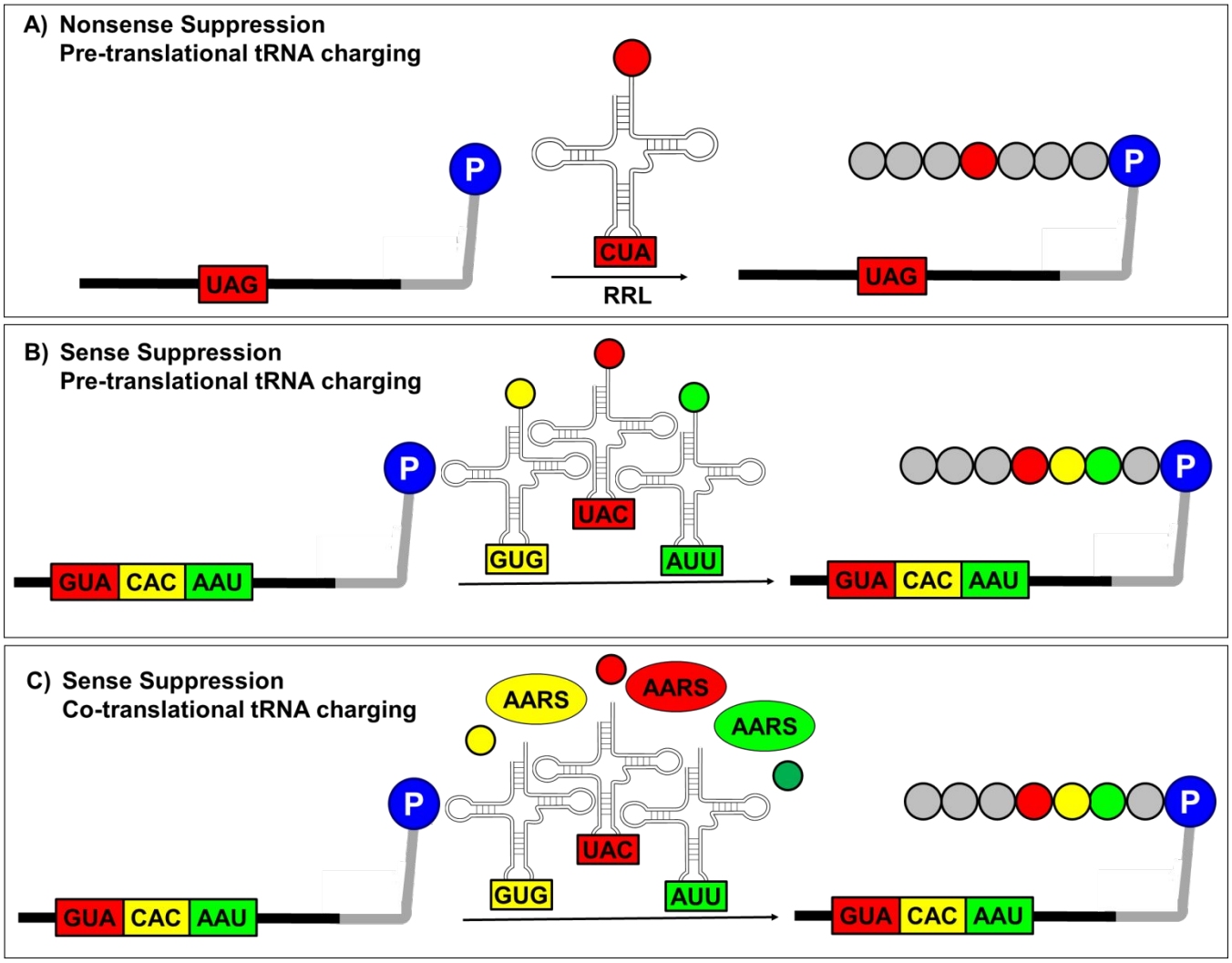

Figure 12. Strategies for non-natural amino acid incorporation into mRNA display libraries. (A) A single non-natural amino acid can be incorporated into mRNA-peptide fusions at UAG (amber) stop codons through the use of pre-charged nonsense suppressor tRNA. This strategy is typically used in non-reconstituted translation systems. **(B)** Multiple non-natural amino acids can be incorporated at sense codons by pre-charged aminoacyl sense tRNA. Although this strategy can be carried out in non-reconstituted translation systems such as RRL (rabbit reticulocyte lysate),[204] it is typically used in reconstituted systems where native AARS (aminoacyl tRNA synthetase) enzymes, tRNA, and amino acids are omitted. **(C)** In a fully reconstituted translation system, non-natural amino acids, tRNA, and AARS enzymes (native or re-engineered) can be selectively added to incorporate multiple non-natural amino acids at sense codons. In this strategy, AARS enzymes continuously recharge tRNAs with non-natural amino acids in the absence of their natural counterparts.

7.3 Macrocyclization

Several strategies have been used for macrocyclization in the context of mRNA display (**Figure 13**). Millward and co-workers were the first to demonstrate the cyclization of mRNA display libraries by post-translationally cross-linking the N-terminal amine and the ε-amino group of a fixed C-terminal lysine within a peptide using a bi-functional N-hydroxysuccinimide (NHS) ester, disuccinimidyl glutarate (DSG)[225] (**Figure 13A**). While disulfide bond-mediated cyclization has been described in PD methods for years,[226] disulfide bonds are not stable in reducing environments, thus this NHS crosslinking strategy is better suited for generating redox-insensitive binding peptides. While the efficiency of disulfide bond and other cyclization strategies in display techniques is rarely quantified, (i.e., the fraction of the library that is cyclized), in this study the efficiency of cyclization was determined by incorporation of an α-hydroxy amino acid that allowed specific and quantitative cleavage of the library. The authors reasoned that cyclization would result in retention of a radioactive label in the library after the α-hydroxy position was cleaved, whereas a linear peptide would lose the radioactive label, allowing a facile method to quantify cyclization efficiency. The cyclization efficiency was found to be dependent on the number of intervening residues between the amino groups, with the shortest libraries having the highest efficiency. Although this efficiency decreased as the chain length increased, 30% cyclization efficiency was still observed in libraries of ten random positions.

This strategy was later improved to allow DSG-mediated cyclization of mRNA-peptide libraries directly on oligo-deoxythymidine (dT)-cellulose. This resin is commonly used for purification of mRNA display libraries, although its commercial discontinuation has led to the development of alternate dT-modified resins[227, 228]. On-resin reaction with DSG increased the efficiency of cyclization and reduced the number of library manipulations required for each selection step.[229] In this study, the DSG-cyclized pentapeptide library was used to select cyclic peptides against the Fc region of human IgG for use in chromatographic purification of mAbs. The selection resulted in several peptides, one with a 7.6 μM K_D for human IgG at room temperature. This peptide was linked to a solid support and used for purification of mAbs from cell culture, facilitating antibody elution with less harsh conditions (pH 4) as compared with Protein A (pH 2.5). This on-resin DSG cyclization approach has recently been employed in the selection of peptide macrocycles targeting the WW domains of Yes-associated protein and the TOM22 mitochondrial import receptor[230] and to select for cyclic peptides that cross cell membranes.[231]

An alternative strategy for cyclizing mRNA-peptide fusions to generate redox-insensitive cycles was achieved by cross-linking cysteine residues with dibromo-*m*-xylene (DBX). This strategy was described by Timmerman *et al*.[232] and first used in mRNA display by Guillen Schlippe and co-workers

to select macrocyclic inhibitors of thrombin[216] (**Figure 13B**). In a recent study by Iqbal and Hartman, DBX crosslinking of *i* and *i*+4 α-methyl cysteine residues in an E2-binding peptide was found to result in a cyclized peptide with comparable affinity to a hydrocarbon stapled variant where crosslinking was carried out by olefin metathesis between similarly spaced (*S*)-2-(4-pentenyl)alanine residues.[233] The authors then demonstrated efficient incorporation of two α-methyl cysteine residues into an mRNA-peptide fusion through a combination of pre-charged tRNA and an editing-deficient AARS (ValRS T222P). These results suggest that DBX-mediated crosslinking of mRNA display libraries could be used as a nucleic acid-compatible alternative to hydrocarbon stapling by olefin metathesis.

Seebeck and co-workers described an alternative strategy where oxidative decomposition converts the non-natural amino acid 4-selenalysine into dehydroalanine (Dha),[234] which then undergoes a Michael addition with an intramolecular cysteine to form a thioether-linked macrocycle[235] (**Figure 13C**). While the latter method is highly selective, the chemistry of lanthionine bridge formation may limit the size of the macrocycle and therefore the chemical complexity of the constrained ring.

Suga and co-workers frequently employ the reaction between an N-terminal chloroacetyl group and a C-terminal cysteine to generate redox-stable thioether macrocycles (**Figure 13D**). The N-terminal chloroacetyl residue is charged onto an initiator tRNA using the flexizyme system and can have either L or D stereochemistry. Indeed, the choice of stereochemistry at this position can have significant effects on the sequence and affinity of the selected peptides.[236] mRNA display libraries cyclized in this manner have been employed in selections against a wide range of targets including SIRT2,[223] VEGFR2,[237] Akt2,[238] the Multidrug and Toxic Compound Extrusion (MATE) transporter[239], K-Ras,[240] and PlexinB1.[241] This cyclization strategy is highly selective and spontaneous allowing rapid and efficient macrocyclization of mRNA display libraries of various chain lengths. A recent study has expanded the repertoire of the N-terminal chloroacetyl-bearing amino acids to include cyclopropane-containing γ-amino acids which are proposed to provide additional constraint to selected macrocycles.[242]

The chloroacetyl-cyclization strategy was also used to discover cyclic peptides against the RBD of the SARS-CoV2 Spike protein.[243] Norman and co-workers used three libraries cyclized with an N-terminal N-chloroacetyl-Tyr, an N-chloroacetyl-D-Tyr, or with a Cys-Cys disulfide bond to develop cyclic peptides against the Spike RBD. All three libraries encoded 4-15 random positions and three selected sequences from each library were studied in more detail. Dissociation constants were obtained by SPR and were found to range from 15-550 nM. Interestingly, all three peptides from the disulfide cyclized library showed non-specific binding. Surprisingly, the highest affinity sequence did not compete with the ACE2/RBD interaction but could be used in an ELISA to detect Spike protein as low as 30 ng/mL.

A crystal structure of the peptide in complex with RBD showed that the cyclic peptide displaces a β-strand in the C-terminal region of RBD and shows some sequence homology to the primary sequence in this region of the spike protein.

Recently, chloroacetyl cyclization chemistry has been combined with native chemical ligation to generate head-to-tail peptide macrocycles in the context of mRNA-peptide fusions.[244] Indeed, all previously described methods for cyclizing mRNA display libraries employ N-terminal to side-chain crosslinking **(Figure 13A and Figure 13D)** or side-chain to side-chain crosslinking **(Figure 13B and Figure 13C)**. While these approaches have resulted in the selection of high affinity macrocycles, most bioactive peptides found in nature are cyclized by an N-terminus-to-C-terminus main chain linkage. Indeed, the fundamental mechanism of mRNA-peptide fusion formation (the covalent linkage between puromycin and the C-terminus of the peptide chain) precludes this macrocyclic structure. Suga and co-workers have described an intricate and elegant approach where mRNA-peptide fusions containing a backbone thioester linkage undergo thioester exchange with a C-terminal cysteine side chain **(Figure 13E)**. The resulting thiol group reacts with an N-terminal chloroacetyl side-chain to form the first cyclic intermediate. Reaction of an N-terminal thiazolidine capping group with $NaBH_3CN$ results in the formation of an N-terminal N-methyl cysteine which undergoes an intramolecular native chemical ligation reaction with the newly formed backbone thioether to afford a backbone cyclized peptide that retains the puromycin linkage with the encoding mRNA. In this manner, head-to-tail macrocycles can be selected for function by mRNA display.

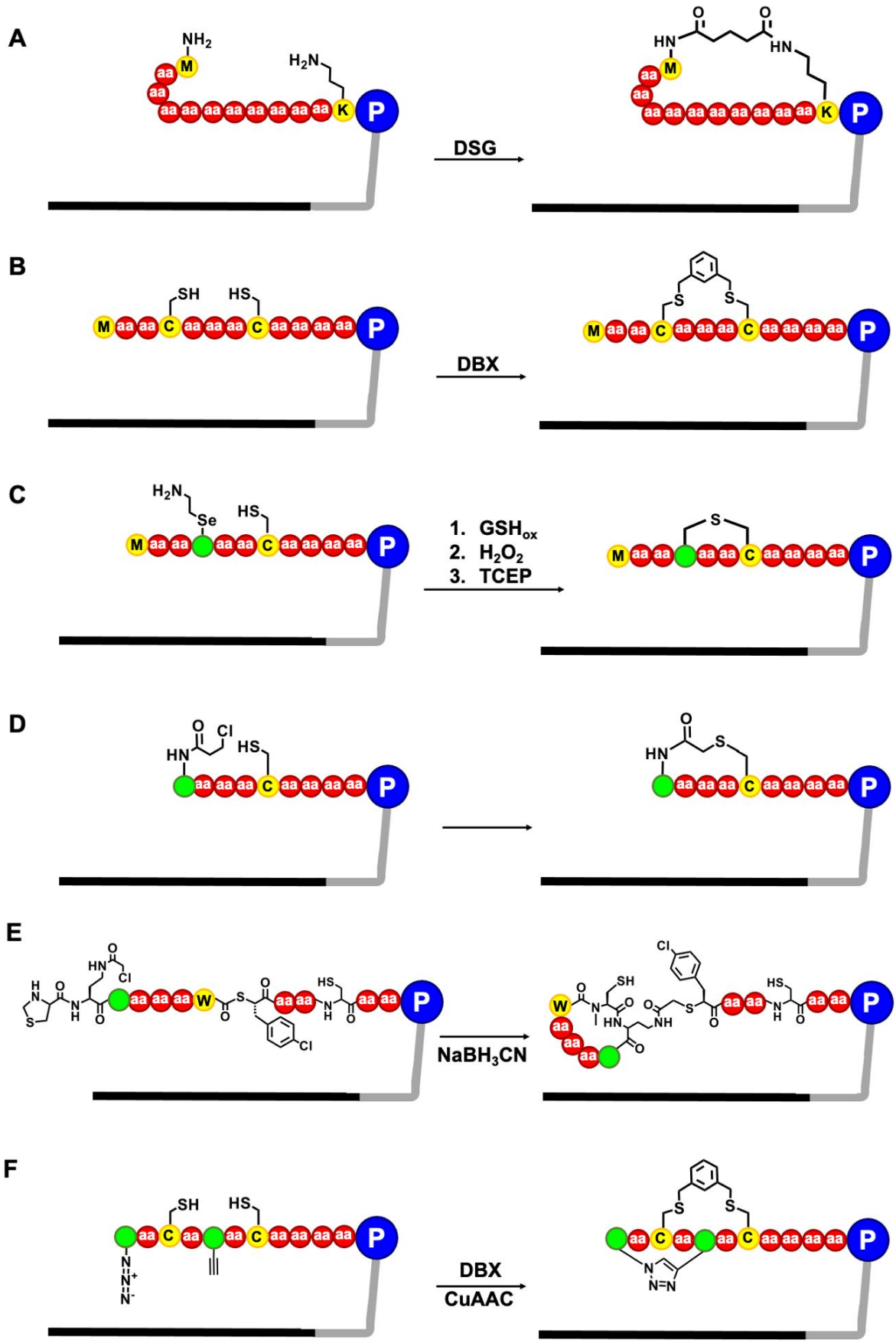
A
DSG
B
DBX
C
1. GSH$_{ox}$
2. H$_2$O$_2$
3. TCEP
D
E
NaBH$_3$CN
F
DBX
CuAAC

Figure 13. Strategies used for library macrocyclization in mRNA display. (A) Disuccinimidyl glutarate (DSG) mediated cyclization **(B)** Crosslinking cysteine residues with dibromo-m-xylene (DBX) **(C)** Oxidative conversion of 4-selenalysine (K') to dehydroalanine (Dha) using oxidized glutathione (GSHox) and hydrogen peroxide and subsequent intramolecular formation of a thioether linkage in the presence of tris(2-carboxyethyl)-phosphine (TCEP) **(D)** N-terminal chloroacetyl group crosslinking with cysteine residues **(E)** Spontaneous thioether exchange, formation of a thioether bond, deprotection and ring opening of an N-terminal thiazolidine, and finally native chemical ligation allow display of head-to-tail cyclized peptides as mRNA-peptide fusions. **(F)** Bicyclic peptide formation by a combination of cysteine residues crosslinking and copper mediated azide alkyne cycloaddition.

7.4 Bicyclic Peptides – If One Cycle Is Good, Why Not Two?

Extending the concept that macrocyclization can confer favorable properties on peptides, several groups have worked to create even more highly constrained peptides with more than one intramolecular bridge. Bicyclic peptides have been discovered with PD[245] using a trifunctional version of the bromoxylene chemistry described above, which in principle could be compatible with mRNA display. Choice of cyclization chemistry is important as it must not react with the mRNA portion of the fusions. The multiple crosslinking steps to form a multicyclic peptide also requires the cyclization chemistry to be efficient, as lower efficiency will reduce the fraction of the library that is correctly cyclized. Finally, the cyclization chemistry must be highly selective to avoid generation of multiple, topologically distinct molecules from the same sequence.

Toward this end, Hacker *et. al.* designed a library encoding bicyclic peptides using mRNA display technology to select for highly constrained peptide sequences formed through two orthogonal cyclization steps. This cyclization strategy results in the formation of theta (θ)-bridged bicyclic peptides consisting of three loops with different sizes (**Figure 13F**). Two chemistries were utilized for cyclization; the copper-mediated azide−alkyne cycloaddition (CuAAC; click chemistry) and DBX-mediated cysteine bisalkylation. To enable the CuAAC reaction, non-natural α-amino acids carrying azide and alkyne groups were incorporated into the sequence. The authors performed a model selection using a bicyclic peptide library and a monocyclic peptide library produced through cysteine bisalkylation to generate high-affinity streptavidin binders. Mid-nanomolar peptides were isolated using both libraries but, interestingly, addition of the second cyclization seemed to only result in a relatively modest 2-fold increase in affinity relative to clones isolated from the monocyclic library. Both monocyclized and bicyclized peptides showed an exceptional resistance to protease digestion with 57% of the monocyclic and 96% of the bicyclic peptide retaining binding to streptavidin after a 24 hour incubation with chymotrypsin.[246]

7.5 Integrating Non-Natural Amino Acids and Macrocyclization in mRNA Display Libraries

Millward and co-workers took the first step in integrating non-natural amino acid incorporation and macrocyclization by integrating nonsense suppression of the UAG stop codon with N-methyl phenylalanine and covalent macrocyclization to select cyclic peptides with antibody-like affinity for the Giα1 G-protein.[247] In this study, a randomized 10-mer peptide library was translated in the presence of THG73 amber suppressor tRNA charged with N-methyl phenylalanine, cyclized with DSG, and selected for binding to immobilized Giα1. After seven rounds of selection, the library converged on a (T/S)WYEF(V/L) consensus sequence, which was found to be highly conserved in a specific registry within the context of the macrocycle. The most promising sequence, cycGIBP, was found to have low single-digit nanomolar affinity for Gαi ($K_D \approx 2.1$ nM) and binding was highly dependent on macrocyclization. Surprisingly, no amber stop codons were present in any of the clones in the final pool suggesting that N-methyl Phe was lost either due to poor translation efficiency or the absence of a survival advantage in sequences that contained this residue.

Roberts and co-workers expanded on this work and attempted to answer the question of how much protease resistance could be achieved with only macrocyclization. They demonstrated that functional, protease-resistant Gαi1 binding cyclic peptides consisting of only natural amino acids could be obtained using a novel, dual challenge selection strategy.[52] In these experiments, a cyclic mRNA display library was first exposed to chymotrypsin digestion, followed by selection for binding to Gαi1. Thus, a sequence would need to both survive protease digestion with *and* bind to the target to survive and be amplified. Starting with Pool 7 of the previous Gαi1 selection above, three additional rounds of protease/binding selection were performed. Three cyclic protease resistant peptides (cycPRPs) were isolated with significant binding to Gαi1 along with a 100- to 400-fold increase in protease resistance relative to cycGIBP. The increased resistance was found to arise from a combination of reduced cleavage rate (k_{cat}) and a lower enzyme affinity (increased K_M). Although the cycPRPs were only exposed to chymotrypsin in this dual selection, the cycPRPs showed enhanced stability in human serum *ex vivo*, with one cycPRP showing a half-life in serum of up to 28 hours. Part of this stability may be attributable to cyclization which protects the peptide termini from aminopeptidases and carboxyesterases.[52] Although significant improvements in stability were obtained from selections with wholly natural peptide libraries, it was still unclear whether the inclusion of non-natural N-methyl amino acids could further enhance cyclic peptide stability in the context of selection.

7.5.1 SUPR Peptide mRNA Display

In 2016, a study by Roberts and co-workers shed additional light on this question.[51] A >10^6-member library based on cycGiBP was constructed so that each position in the sequence was randomized to code for a high fraction of wild type or UAG codons. This library was then translated in the presence of N-methyl alanine-charged amber suppressor tRNA to facilitate incorporation of N-methyl Ala at UAG stop codons. Using the strategy described above, the library was subjected to a cocktail of proteases prior to selection for target binding to enrich protease-resistant sequences. After five rounds of selection, the library converged to a macrocyclic peptide with the sequence MFY**A**YEY**A**QWSK where **A** represents the incorporation of N-methyl Ala **(1, Figure 14)**. This sequence, which differs significantly from the Gαi1 consensus sequence in the previous study, maintained high affinity and isoform selectivity for Gαi1 and showed dramatically enhanced stability towards *in vitro* proteolysis by chymotrypsin (~400-fold) and proteinase K (>5,000-fold) relative to cycGiBP. The selected peptide also showed reduced susceptibility to modification in human liver microsomes and reduced degradation in human serum *ex vivo*, even though the library had not been exposed to these metabolic processes during selection. Surprisingly, stability was profoundly cooperative as the protease resistance was dependent on the presence of *both* N-methyl Ala residues. Substitution of either N-methyl Ala with alanine resulted in complete abrogation of protease resistance. These highly stable non-natural macrocycles were named SUPR peptides (**S**canning **U**nnatural **P**rotease **R**esistant).

Although SUPR peptides showed dramatically enhanced hydrolytic stability relative to their linear and non-natural counterparts, it was unclear if this molecular architecture could support the selection of cell permeable peptide macrocycles. Although cell permeability is challenging to predict, even in the case of positively charged and/or highly N-methylated macrocyclic peptides,[197] the presence of an aliphatic crosslinker (DSG) and multiple N-methylated amino acids suggested that reasonable cell permeability was possible. Indeed, the hydrophobic DSG crosslinker is analogous to the hydrocarbon crosslinker employed in stapled peptides, many of which show excellent membrane permeability and cytosolic access.[248] A recent study by Gray and co-workers provided empirical evidence of SUPR peptide cell permeability and intracellular target engagement.[249] In this work, a SUPR peptide mRNA display library consisting of eight randomized positions within the macrocycle was translated in the presence of amber suppressor tRNA aminoacylated with N-methyl alanine, pre-selected for proteinase K resistance, and panned against the autophagy protein LC3. After seven rounds of selection, three peptide sequence families were found to be present. One of these families contained a F/Y-XXX-V motif in constant registration within the macrocycle which was analogous to the known LC3 interacting motif (F/Y/W-XX-V/L/I) albeit with an additional amino acid residue between the aromatic and aliphatic

positions. Almost all selected sequences contained an N-methyl alanine residue immediately adjacent to the invariant C-terminal lysine used for DSG cyclization. One of the most promising sequences in the round 7 pool (SUPR4B) showed mid-nanomolar affinity for LC3 which was enhanced by a factor of three by a single amino acid substitution (SUPR4B1W **2**, **Figure 14)**. Cyclization was found to enhance the binding affinity by a factor of 3 while substitution of the N-methyl alanine for alanine showed little effect on affinity. Conversely, cyclization only improved protease stability by a factor of two while the N-methyl alanine residue enhanced protease resistance by a factor of 18. Assessment of cell permeability and cytosolic access by the chloroalkane penetration assay[250] revealed a low micromolar CP_{50} for SUPR4B1W (1.3 μM) which was increased by a factor of 7 following linearization and a factor of nearly 3 when the N-methyl alanine residue was replaced with alanine. These results indicated that cyclization and N-methylation played key roles in driving affinity, stability, and cell permeability of the selected SUPR peptide. SUPR4B1W inhibited autophagy in cell culture models and, in combination with carboplatin, almost completely eliminated intraperitoneal tumor burden in an orthotopic mouse model of ovarian cancer. These results indicate that the SUPR peptide architecture supports the selection of cell permeable cyclic peptides for the disruption of intracellular protein-protein interactions *in vitro* and *in vivo*.

7.5.2 Integration of unnatural amino acids and cyclization in mRNA Display Libraries

In 2012 Szostak and co-workers reported a selection against thrombin using an mRNA display library where 12 sense codons were reprogrammed with non-natural amino acids in a reconstituted translation system (co-translational enzymatic charging).[216] Cyclization of the resulting libraries using dibromo-*m*-xylene and selection for thrombin binding resulted in 13-membered macrocycles with 0-80% of the randomized positions within the macrocycle occupied by non-natural amino acids. Functional analysis of two non-natural variants and one selected from a wholly natural library showed that all three sequences bound to thrombin with low nanomolar affinities. Replacement of natural amino acids in the non-natural variants or linearization (all variants) resulted in significant attenuation of affinity. Interestingly, a natural variant showed the highest affinity and inhibitory potency and was the least dependent on cyclization. The structure of the most potent non-natural variant **(3)** is shown in **Figure 14.** This suggests that selection of non-natural amino acids is dependent on conformation and that merely increasing the content of non-natural amino acids within the macrocycle does not necessarily result in increased function.

In 2011, Suga and co-workers combined ribozymatic tRNA charging, thiol-chloroacetyl cyclization, and a reconstituted translation system to select numerous drug-like peptides (the **Ra**ndom non-standard **P**eptide **I**ntegrated **D**iscovery (RaPID) system). This methodology was employed to select macrocyclic peptides that bound with sub-nanomolar affinity to the E6AP HECT domain.[194] The most promising peptides from this selection contained up to four N-methyl amino acids within the context of the macrocycle (>33% of the randomized positions). Similar selections against VEGFR2 have also been carried out using a combination of N-methyl, D-, and α,α-dimethyl amino acids.[237]

Recently, mRNA display selections using the RaPID system have yielded several high affinity macrocyclic peptides where unnatural amino acids have been selected within the randomized region. Nitsche and co-workers have described the identification of a potent inhibitor of the Zika virus protease from a library of libraries with 8-10 randomized positions within the macrocyclic scaffold **(4, Figure 14)**.[251] In this selection, six N-methyl amino acids were included in the genetic code and the most promising selected peptide contained three unique N-methyl amino acids in the randomized region (N-methyl serine, N-methyl phenylalanine, and N-methyl-4-*O*-methyl-tyrosine). This peptide bound the Zika virus protease with a K_D of 9 nM and showed sub-micromolar inhibitory potency in *in vitro* assays of protease activity. The effect of cyclization and N-methyl amino acid incorporation on the affinity, selectivity, and stability of the selected compounds was not addressed in this study.

Johansen-Leete and co-workers recently described the selection of macrocyclic inhibitors of the chemokine CCL11. In this selection, a library of libraries with 4-15 randomized positions within the macrocycle was translated in the presence of tRNA charged with the unnatural amino acids sulfotyrosine (sY) and the sulfonate mimic of sY, Phe(*p*-$CH_2SO_3^-$).[252] sY is frequently found on chemokine receptors and chemokine-binding proteins and therefore represents a potentially useful chemical functionality to enhance the affinity of selected CCL11-binding macrocyclic peptides. Indeed, the selection resulted in the identification of a 17-mer peptide containing an internal four residue macrocycle. Three Phe(*p*-$CH_2SO_3^-$) residues were present in the peptide with two located in the macrocyclic portion. A variant of the selected peptide, where all three Phe(*p*-$CH_2$2SO_3^-) residues were replaced with sY bound to CCL11 with a K_D of 10.4 nM and inhibited CCL11 signaling in HEK cells with an IC_{50} of 160 nM. Replacing the sY residues with tyrosine residues resulted in almost complete abrogation of binding while replacement with Phe(*p*-$CH_2SO_3^-$) resulted in a more modest (2- to 4-fold) reduction in affinity. This study illustrates the critical role of unnatural amino acids in selections where these residues are specifically chosen for their favorable interaction with the biological target.

In a recent elegant study by Katoh and co-workers, thiol-chloroacetyl cyclized mRNA display libraries were translated in the presence of three cyclic β-amino acids and selected for binding to the

human factor XIIa (hXIIa).[253] The library was sequenced after four rounds of selection and each of most abundant clones contained at least one β-amino acid and each bound to hXIIa with low nanomolar affinity. Replacement of the two selected β-amino acids with alanine in the highest affinity sequence resulted in undetectable target binding by SPR. Similarly, substitution of selected β-amino acids with alanine in the highest affinity sequence **(5, Figure 14)** resulted in >20-fold reduction in serum stability. These results indicate **1)** β-amino acids with five- and six-membered rings can be efficiently incorporated into mRNA display libraries through the translation machinery and **2)** these residues can make substantial contributions to both target affinity and serum stability.

The first clinical-stage peptide resulting from mRNA display Zilucoplan (RA101495) is currently in Phase III trials for treatment of Myasthenia Gravis. This cyclic peptide prevents the cleavage of the complement component, C5, by binding to the C5b domain and blocking binding to complement component C6.[254] While literature is scarce on the exact development path of Zilucoplan, mRNA display using the co-translational enzymatic charging method resulted in several peptides binding C5, containing a mixture of natural, non-natural, and N-methyl amino acids.[255] Many peptides were tested for their ability to inhibit red blood cell hemolysis, with some peptides showing IC_{50} constants in the single-digit nM range. One sequence was also shown to have >1,440 min half-life in human plasma. A synthesis of Zilucoplan has been published.[256]

A comprehensive list of mRNA display selections for drug-like peptides is shown in **Table 3**.

Table 3. mRNA Display Selections for Macrocyclic Peptides with And Without the Incorporation of Non-Natural Amino Acids. Residues shown in bold indicate points of macrocyclization. [1]Refers to the stated complexity of the library in the original reference. N/S is used if this value is not provided. [2]Refers to the total number of non-natural amino acids present during translation including those that were held constant in the library. The number in parentheses indicates the number of non-natural amino acids that were not held constant during the selection. [3]Refers to the unnatural amino acids obtained in the selected peptide which were not held constant in the library. [4]IC_{50} value. [5]K_i value.

Target	# random positions	Library Diversity[1]	# non-natural Monomers[2]	Selected non-natural amino acids[3]	K_D (nM)	Affinity Measurement Method	Affinity Fold-increase from cyclization	$t_{1/2}$ Fold-increase (protease) from cyclization	Peptide Sequence	Ref
Gαi1	10	$1.7X10^{12}$	1(1)	0	2.1	Radioligand Displacement	15	2.6 (chymotrypsin)	**M**ITWYEFVAGT**K**	247
E6AP	8-15	$>10^{12}$	5(4)	mS, mF, mG	0.6	SPR	300	N/S	**ClAc-w**CDV-mS-GR-mF-mG-Y-mF-P**C**G	194
Akt2	4-12	$>10^{12}$	1(0)	-	110[4]	Enzyme Inhibition	N/S	N/S	**ClAc-Y**ILVRNRLLRVD**C**G	238
SIRT2	7-11	$>10^{12}$	2(0)	-	3.7	SPR	2.7	N/S	**ClAc-y**HDYRI-K^{Tfa}-RYHTYP**C**	223
					3.8		3.4		**ClAc-Y**SNFRI-K^{Tfa}-RYSNSS**C**	
Thrombin	10	$2.3X10^{13}$	12(5)	M_a, L_a, Y_a, T_a, K_a	4.5	Equilibrium Ultrafiltration	78	N/S	M_a-**C**-L_a-QNS-Y_a-IA-T_a-K_a-G**C**	216
		$1.9X10^{13}$	0(0)	-	1.5		11		M**C**IIKKSRDPGR**C**	
Sortase A	9	$5X10^{11}$	1(0)	-	3000	FP	>133-fold	N/S	MRGLWY-K^{Se}-LS-**C**-WGRIGRR	235
Fc	5	N/S	0(0)	-	7600	Solid-phase adsorption	N/S	N/S	**M**WFRHY**K**	229
Human Serum Albumin	8-12	$10^{12} – 10^{13}$	1(0)	-	41	FP	N/S	N/S	**ClAB-F**TYNERLFW**C**	15
VEGFR2	8-15	$\leq 10^{13}$	1(0)	-	94	BLI	N/S	N/S	**ClAc-F**VVVSTDPWVNGLYID**C**	237
			1(0)	-	8				**ClAB-F**IGHYRVKVHPISLER**C**	
			1(0)	-	2				**ClAB-f**KPDWWTYYDLRHP**C**	
			5(4)	D-Tyr	33				**ClAB-f**DCGLWRRNIPSN**C**	
MATE transporter	7-15	$\geq 10^{12}$	1(0)	-	>10000[4]	Enzyme Inhibition in cells	N/S	N/S	**ClAc-ClAcf**SVA**C**SAFVRIAHHASC	239, 257

Gαi1	10	N/S	0(0)	-	9	Radioligand Displacement	N/S	133 (serum) 0.72 (Chymotrypsin)	**M**TWFEFLSSTS**K**	[52]
c-Met	4-15	>1X10^{12}	1(0)	-	2.3	SPR	83	N/S	**ClAc-y**WYYAWDQTYKAFP**C**	[236] [258]
EpCAM	4-12	10^{14}	1(0)	-	1.7	SPR	N/S (strongly dependent)	N/S	**Ac-w**RPTRYRLLPWWI**C**	[259]
Gαi1	10	4X10^{6}	1(1)	mA	60	Radioligand Displacement	N/S	19 (chymotrypsin) 1.9 (proteinase K) 570 (serum)	**M**FY-mA-YEY-mA-QWS**K**	[51]
Her2	8	1.6X10^{7}	1(1)	mnV	76	ELISA	N/S	N/S	**M**VC-mnV-mnV-LYDD**K**	
Plexin B1	10-15	>10^{12}	1(0)	-	3.5	SPR	N/S	N/S	**ClAc-w**RPRVARWTGQIIY**C**	[260]
Streptavidin	8	2.6X10^{10}	2(0)	-	361 (monocyclic) 593 (bicyclic)	Radioligand binding	N/S	~ 200 (monocyclic) ~350 (bicyclic)	**AzHA**-TDPN**C-yneF**-GNP**C** (monocyclic**)** **AzHA**-HPQN**C**-**yneF**-HVFS**C** (bicyclic)	[246]
α-amylase	6-15	>10^{12}	2(1)	-	1^{5}	Enzyme Inhibition	N/S	N/S	**ClAc-y**PYS**C**WARHVRIREN	[261]
KDM4A	8-10	6.8X10^{12}	1(0)	-	6^{4}	Enzyme Inhibition	N/S	N/S	**ClAc-y**TRFRRSGIVFYY**C**	[262]
NS2B-NS3 protease	8-10	>5X10^{13}	7(6)	mYm, mF, mS	9	SPR	N/S	N/S	**ClAc-Y-**mYm-K-mF-K-mS-mYm-K-mYm-mYm-K**C**	[251]
CCL11	4-15	>10^{12}	2(1)	sY	10.4	FP	N/S	N/S	**ClAc-y**-sY-sY-**C**VDWGL-sY-RPIET-sY-S	[252]
K-Ras (G12D)	8-12	>10^{12}	1(0)	-	9000	ITC	N/S	N/S	**ClAc-y**-FVNFRNFRTFR**C**	[240]
WW-YAP	5, 7, or 10	10^{12}	0(0)	-	36,000	Solid phase adsorption	0.14	N/S	**M-**AFRLC-**K**	[230]
CeiPGM	6-12	>10^{12}	1(0)	-	0.3	SPR	N/S	N/S	**ClAc-Cp-F**-FSISGIEWN	[242]

								GPEI-**C**	
hFXIIa	6-15	NS	5(3)	2ACHC	0.98	SPR	N/S	N/S	**ClAc-y**-FAYDRR-2ACHC-LSNN-2ACHC-RNY-**c**G	[253]
IFNGR1	6-15	NS	5(3)	RR2ACPC, SS2ACPC	1.87	SPR	N/S	N/S	**ClAc-y-**FGV-SS2ACPC-RRACPC-FYNRT-**c**G	[253]
Ubiquitin tetramer	6-12	>10^{12}	7(6)	Aoc, mA, mG	9	SPR	N/S	N/S	**ClAc-f-**QYW-Aoc-Y-mA-T-mG-V**C**G	[263]
Plexin B1	13	~10^{11}	1(0)	-	0.28	SPR	N/S	N/S	**ClAc-w**-RPYIERWTG RLIV-**C**G	[241]
LC3A	8	NS	1(1)	mA	120	FP	3.1	1.9 (proteinase K)	**M**-WPHRVTA-mA-**K**	[249]

7.6 Cyclic Unnatural mRNA Display Libraries – What Have We Learned?

The past 15 years have shown considerable advances in the selection of drug-like peptides from mRNA display libraries. However, given the technical challenges and time cost of unnatural amino acid incorporation, post-translational chemical modification, and macrocyclization, it is vital to consider their actual contribution to the drug-like properties of selected lead compounds. Put another way, how do these design elements enhance binding affinity, specificity, resistance to protease, and cell permeability?

In the case of macrocyclization, in almost all selections where cyclization was enforced, it was found to be essential for affinity as evidenced by the loss of activity versus the linear versions of the peptides. In some cases the effect was modest (3-fold)[223] and in some cases it was quite dramatic (1,000-fold) **(Table 3)**.[194] Furthermore, although consensus motifs in linear peptides can be found in various registers within the peptide sequence, they are typically found to be conserved in a single register within the macrocycle. This suggests that the position within the macrocyclic architecture plays a role in the optimal configuration of the molecule and that binding motifs may only be compatible with specific 3D conformations.[52, 194, 216, 247]

These observations suggest that the benefits of macrocyclization will be highly context-dependent. Indeed, a recent study provided direct experimental evidence to address the contribution

of cyclization to peptide fitness.[264] In this work, mixed libraries containing linear, cyclic, and bicyclic peptides were panned against streptavidin to identify the relative representation of each topology in the final pool. Surprisingly, sequencing of the late round pools revealed that all the top 100 sequences were linear as evidenced by the absence of residues required for cyclization. When the selection was repeated with a protease pre-selection step, eight of the 10 most highly enriched peptides contained the residues required for cyclization. This indicates that cyclization is not absolutely required for high affinity, but when other selection pressures are present (e.g., protease challenge), cyclic peptides may emerge as a preferred topology.

The case for non-natural amino acids is more complex. In cases where the non-natural functionality is explicitly[200, 202, 252] or implicitly[51, 249] selected for, non-natural amino acids are typically well-represented in the final pool and are essential for the function of the resulting peptides. However, when there is no explicit selection pressure, the results are somewhat mixed. In selections against thrombin[216] and Akt2,[238] libraries containing only natural amino acids produced the most highly functional sequences as measured by affinity and inhibitory potency. In the aforementioned selection against the E6AP domain,[194] replacement of the selected N-methyl amino acids with their natural counterparts resulted in complete abrogation of target binding, although some individual N-methyl amino acids could be replaced with natural residues with only minimal effect on peptide function. In a recent report describing the optimization of a macrocyclic peptide obtained from a selection against proprotein convertase subtilisin/kexin type 9 (PCSK9), two fluorinated tryptophan residues and a fluorinated N-methyl phenylalanine residue were found in one of the most promising selected peptides.[265] Elimination of the fluorinated N-methyl phenylalanine decreased the IC_{50} of the selected peptide by more than an order or magnitude while

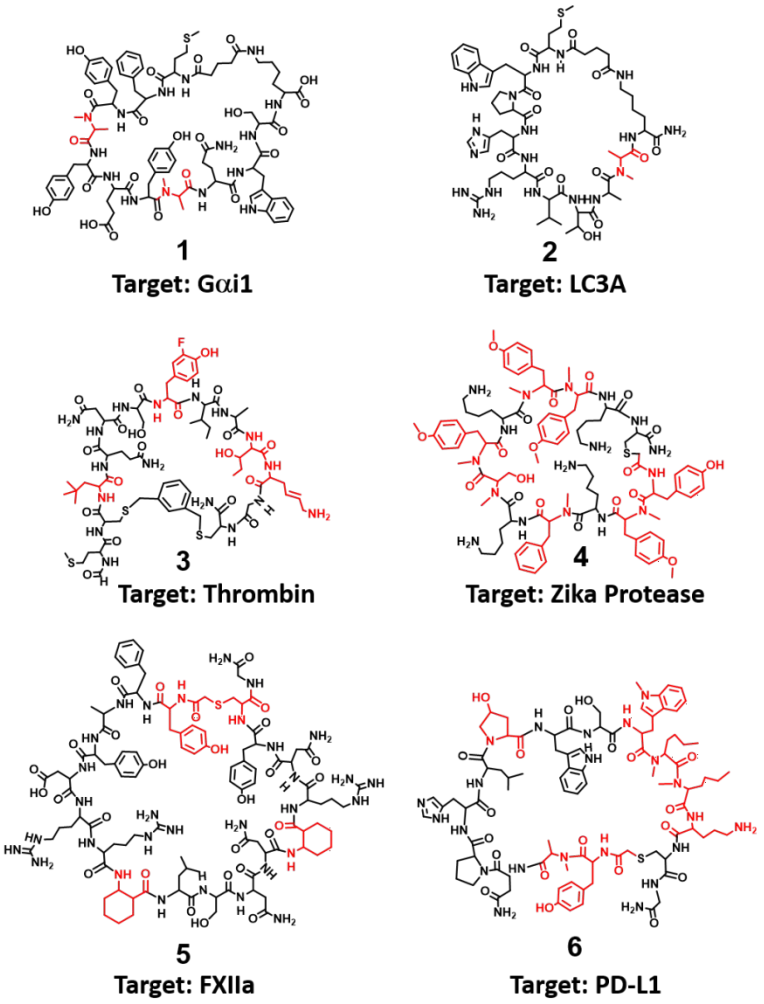

Figure 14: Cyclic Unnatural Peptides Identified by mRNA Display. Unnatural amino acids are shown in red. For clarity, stereochemistry is not shown.

substitution of the fluorinated tryptophan at position 3 with tryptophan only increased the IC_{50} by a factor of 2. In contrast, replacement of the fluorinated tryptophan at position 4 with tryptophan increased the IC_{50} by >20-fold. In initial cyclic selections against Gαi1, no non-natural N-methyl Phe was found in the final pool despite being available throughout the selection. In all five cases, no explicit or implicit selection pressure was placed on the library to enforce non-natural amino acid incorporation. While unnatural amino acids are often found to drive peptide affinity and/or stability[249, 253], their presence in selected sequences is not guaranteed nor are they certain to enhance peptide function.

In selections that include a protease challenge prior to target binding, N-methyl amino acid incorporation was strongly enforced and was essential for peptide function.[51, 249] N-methyl amino acids increase protease resistance of peptides,[204, 266, 267] and the presence of the non-natural amino acid has a significant positive effect on the overall fitness of a selected peptide. From this, albeit limited data set, we could draw the provisional conclusion that in the absence of explicit selection pressure for non-natural function there is no guarantee that including unnatural amino acids in the library will confer additional fitness to selected sequences relative to the set of 20 natural amino acids. Indeed, protease resistance and serum stability can be obtained in mRNA display selections with only the natural set of amino acids provided that a protease pre-selection is included.[52]

7.7 Evolving Drug-like peptides for molecular imaging

Real-time imaging of cancer biomarkers by molecular imaging can inform diagnosis and monitor the progress of treatment. Increasingly, macrocyclic peptide scaffolds are being exploited as targeting agents for molecular imaging applications. mRNA display is well-positioned to create metabolically stable peptides that combine rapid peptide pharmacokinetics with the high target affinities characteristic of mAbs. While antibodies generally have excellent target affinities (nanomolar or below), they suffer from slow tumor uptake and blood pool clearance, requiring the use of long half-life radionuclides (e.g., Zr-89).[268] In contrast, metabolically stable macrocyclic peptides can persist in circulation long enough to be taken up into the tumor, but are cleared rapidly enough for same-day imaging. Antibodies often suffer from high liver uptake making them poor contrast agents for the detection of primary tumors and lesions in the abdominal cavity.[269]

mRNA display targeting of the immune checkpoint programmed death ligand-1 (PD-L1) resulted in the identification of highly potent macrocyclic peptides for non-invasive imaging of this critical immune checkpoint receptor.[270-272] Recently, Bristol Myers Squibb (BMS) disclosed patents describing mRNA display-generated macrocyclic peptides that bind PD-L1, which are described in a patent review by Shaabani et al.[273] Independent characterization confirmed that a subset of these peptides bound to a

site on PD-L1 that abrogated the engagement with PD-1.[274] One of the macrocyclic peptides, termed WL12 **(6, Figure 14)**, was investigated as a PET imaging probe using murine subcutaneous xenograft tumor models.[272] DOTA was conjugated to WL-12 via an ornithine side chain for stable chelation of ^{64}Cu. This study found that PD-L1 expressing CHO xenograft tumors showed significantly higher uptake of [^{64}Cu]-WL12 relative to control tumors (14.9% ID/g versus 4.0% ID/g).

To help mitigate trans-chelation of ^{64}Cu in the liver,[272] ^{68}Ga was investigated as an alternative radiometal.[270] The 67.6 min half-life of ^{68}Ga is also predicted to result in improved dosimetry (lower total dose to patients) and is well-matched to the biological half-life of WL-12. [^{68}Ga]-WL12 showed significantly decreased liver uptake relative to [^{64}Cu]-WL12, but maintained its affinity for PD-L1 in the same xenograft subcutaneous models (11.56 ± 3.18 %ID/g for PD-L1 tumors versus 1.33 ± 0.21 %ID/g for negative controls).[270] [^{64}Cu]-WL12 uptake was also shown to be useful in informing anti-PD-L1 antibody dosing and efficacy[271] as reduction of WL12 uptake was correlated to increased target engagement by anti-PD-L1 antibodies. By employing mathematical models of WL12 biodistribution, the authors could predict the optimal antibody dose required to saturate systemic PD-L1[271] which may allow real-time optimization of immune checkpoint blockade therapy.

The Her2 binding peptide, SUPR4,[51] was used as a model system for developing ^{18}F-based peptide radiolabeling strategies and SUPR peptide-based PET imaging. In a recent study, SUPR4 was radiolabeled via click chemistry-mediated conjugation of 2-[^{18}F]-fluoroethylazide (FEA) to a C-terminal alkyne on an automated radiochemical synthetic platform.[275] This methodology also introduced a novel azide-linked resin to scavenge unreacted alkyne in the precursor peptide which eliminated the need for high performance liquid chromatography (HPLC) purification and resulted in tracers with high specific activity (>200 GBq/μmol). [^{18}F]-SUPR4 showed Her2-selective tumor uptake and rapid renal clearance.[275] As expected, the probe was not degraded or modified *in vivo* prior to imaging and showed no appreciable liver uptake suggesting that SUPR peptides are attractive scaffolds for the development of molecular imaging probes.

8 mRNA Display Technology Development

As library design becomes more robust, it is worth turning our attention to technologies that increase the rate and throughput of selection rounds. As the number of validated targets for drug development increases, these technologies will increasingly become part of the mRNA design toolbox as they enable a more rapid progression from library to lead. Indeed, given the technical challenges inherent in the mRNA display platform, reducing the number of steps in a selection, or increasing the

rate of each step vastly simplifies the directed evolution process and makes this technology accessible to non-expert users.

Several detailed protocols for performing mRNA display experiments have been published.[276-280] Improvements in mRNA display methods have been made across all steps in the mRNA display cycle. In some cases, improvements have been out of necessity as key reagents are not commercially available. For example, two groups describe the production of dT beads used for mRNA-protein purification since dT-cellulose typically used for purification after translation is no longer commercially available.[227, 228] Other improvements have focused on the production of mRNA display libraries, the production of target, increasing the selection speed, or integrating high-throughput sequencing into selection analysis.

8.1 mRNA display Library Production

Construction of long random protein libraries (e.g., > 100 amino acids) introduces a number of challenges including the presence of stop codons, frameshifts introduced by insertions or deletions during DNA synthesis, and the inherently low synthetic yields associated with long DNA oligos. Cho *et al*., described strategies to construct long randomized reading frames by systematically addressing these challenges. First, to reduce stop codons and frameshifts, a pre-selection for full-length translation products was performed, where random libraries were translated with N-terminal and C-terminal tags (e.g., FLAG or His) and affinity purified to select for full-length open reading frames. Next, these pre-selected fragments were assembled into longer open reading frames using Type IIS restriction enzymes followed by ligation of the restriction fragments. This strategy resulted in an increase in full-length ORFs in the library by up to 84-fold.

Open reading frame assembly was also achieved by incorporating deoxyinosine (I) into DNA primers followed by endonuclease V digestion.[281] Endonuclease V specifically cleaves at I bases and proper placement of I into PCR primers allows for generation of sticky ends, allowing multiple DNA fragments to be ligated. Using this strategy, a single domain (nanobody) library was constructed.

8.2 Target Production

Target production is one of the most important steps for an mRNA display selection but is often overlooked. Often, proteins are produced with a biotin tag[153] (e.g., the Avitag) that allows immobilization of the target on Neutravidin or Streptavidin beads. For bacterial systems, expression and biotinylation is straightforward,[282] however many human proteins are unsuitable for bacterial expression. While mammalian expression systems can often produce these proteins, biotinylation of these targets must

be done *in vitro* using purified enzyme. To address this, Grindel and co-workers developed a mammalian co-expression system that resulted in production of both target protein and BirA protein (responsible for biotinylating the Avitag) in a transient transfection system.[283] Using this *in situ* biotinylation system, milligram quantities of >90% pure biotinylated proteins could be produced and used as targets for mRNA display selections.

While purified proteins are often used as targets for mRNA display selections, some proteins – such as membrane proteins – are challenging or even impossible to purify. To address this, selections have been performed on cells expressing the protein target on the cell surface. However, one disadvantage with this strategy is that a random selection may not result in ligands against the target of interest but instead against other cell surface proteins. Fiacco *et al*. designed a doped library based on a known Her2-binding peptide to direct the library to bind to Her2 on a Her2-overexpressing cell line.[51] In another study, the Yes-Associated Protein 1 (YAP) was expressed on the surface of yeast cells and a counter selection against cells expressing an unrelated protein were used as a negative selection to remove non-YAP binding sequences.[230]

8.3 Increasing mRNA Display Selection Speed

Decreasing the time required to perform mRNA display selections is an attractive goal since it narrows the gap between selection and lead and allows more selections to be attempted in a given time. These speed improvements can either be focused on decreasing the time to perform a selection round or decreasing the number of selection cycles that are needed to find a functional sequence.

A microfluidics selection strategy called **C**ontinuous **F**low **M**agnetic **S**eparation (CFMS) was implemented to increase the speed of mRNA display selections. In CFMS, biotinylated antigens are first immobilized on neutravidin-coated superparamagnetic beads and incubated with an mRNA display library. The mixture is then flowed through a microfluidic system where the magnetic beads are trapped by a series of rare-earth NdFeB magnets. Using the CFMS system, enrichment efficiency is improved by >1,000-fold versus traditional mRNA display methods, resulting in a selection that converges in 3-4 rounds versus 6-10 rounds for typical agarose-based mRNA display selections.[115] The CFMS system also allows off-rate selections to be performed easily.[284] The magnetic beads containing the target-bound fusions are eluted directly into PCR buffer for amplification and sequencing. Using a fibronectin library, the CFMS system was used to successfully identify a fibronectin ligand against Interleukin-6 that bound with a 21 nM K_D and an off-rate of 8.8×10^{-4} s^{-1} after only four rounds of selection.[115]

In a follow-up study, the CFMS system was used in the first mRNA display selection to combine high-throughput selection with high-throughput sequencing (HTS).[116] By pairing the high levels of

enrichment achieved via the CFMS system with the millions of sequence reads achieved via high-throughput sequencing, the authors were able to engineer functional fibronectin ligands with only a single round of mRNA display. A two loop ^{10}Fn3 library (**Figure 9C**) was used to target maltose binding protein (MBP) and human Fc (from IgG) and the CFMS system was used to carry out one round of selection. The target-bound fusions were eluted, PCR amplified, and sequenced on an Illumina GAIIx. Clones were ranked by copy number and clones with high copy numbers were selected for further study. Sequences present in both libraries were omitted from further analysis, as they were hypothesized to be artifacts or non-target binding sequences (e.g., matrix-binding sequences). High copy number, target-unique clones were expressed and analyzed for target binding. Interestingly, almost all target-unique clones tested showed binding to their respective target, with the most promising ligands showing a K_D value of ~28 nM vs. IgG and 129-282 nM towards MBP.[116] With current HTS instruments capable of providing billions of sequence reads, novel selection platforms such as CFMS/HTS have extraordinary potential to improve the current selections by reducing the time needed to generate lead clones for further characterization and affinity maturation.

An alternative approach to microfluidic selection was developed using a 3D printed microfluidic device.[285] A **M**icro**F**luidic **E**nrichment **D**evice (MFED) was assembled using 3D printed parts and a frit and was designed to capture the beads from an mRNA display selection, allow highly controlled washing. Similar to the CFMS system above, the MFED allows off-rate selections to be performed easily, without the need to add competitor target. Using this device, a >2-fold increase in the enrichment of functional sequences was observed compared with manual washing methods.

These technologies enable parallel selections, selections against multiple targets, selections under different binding conditions, and selections with different libraries. The ability to perform multiple selections in parallel allows different experimental conditions to be tested and provides a greater chance of success by reducing the risks of selection failure present in with manual, single target selections. As microfluidic devices and 3D printing become cheaper and more accessible to non-expert users, we expect these technologies to make rapid, high-throughput selection experiments routine.

8.4 Post Selection Analysis of mRNA Display Libraries

After an mRNA display selection, peptide sequences in the final pool are determined using DNA sequencing. In the age of Sanger Sequencing, practical and economic considerations typically limited this analysis to several hundred DNA sequences.[146] With the advent of next-generation sequencing technologies, millions to billions of DNA sequences in the final library can now be analyzed. It is clear from these experiments that, typically, there are tens of thousands of putative functional sequences in

these final, “converged” libraries. An emerging question is thus how to best use these data to determine which sequences should be selected for further study.

To a first approximation, a sequence’s functionality correlates with the number of times it appears in the final pool.[116] However, more recent experiments have shown that abundance does not always correlate with affinity.[179] This could be due to various non-binding selective pressures that are exerted on the pool during the selection cycle (i.e., PCR, transcription, translation, efficiency of fusion formation, etc.). Thus, rank order might not always correlate with affinity if these other steps affect overall fitness of a sequence in the context of the entire selection cycle. As more sequence information is obtained from mRNA display selections by high throughput sequencing, the cost and time of traditional lead validation precludes the synthesis of all high-frequency sequences that appear in the final pool. These constraints provide the impetus to develop new methods that enable rapid, high throughput, high-quality synthesis and purification of proteins and peptides. Similarly, there is also a need to be able to test these sequences quickly, giving quantitative data about binding affinity, binding specificity, protease resistance, cell permeability, and serum stability.

One strategy for high throughput synthesis and purification of peptides is to use mRNA display technology to test individual sequence clones. This strategy is attractive since DNA sequences can easily and cheaply be ordered, synthesized, and quickly converted into purified mRNA-peptide fusions. Using the ribosome to translate a peptide allows for high quality peptide synthesis (as opposed to chemical peptide synthesis that often requires HPLC purification) and easy purification by oligo-dT chromatography. Translating putative sequences as mRNA-peptide fusions is a relatively straightforward method to making high-quality peptides for further testing.

Jalali-Yazdi *et al*. used this strategy to quantitatively characterize the binding of several *in vitro* translated peptides using an acoustic sensing device.[286] In this method, a peptide ligand of interest is translated *in vitro* with a C-terminal HA-tag. After purification by oligo-dT chromatography, the mRNA-peptide fusions are incubated with magnetic beads that contain the target of interest, in this case, Bcl-x_L. The sample is then added to an acoustic sensor surface that contains an anti-HA antibody, which binds to the HA-tag on the mRNA-peptide fusion. If the peptide binds the target, a sandwich is created between the magnetic bead and acoustic sensor, generating a binding signal. The authors tested a number of *in vitro* translated HA-tagged peptides that have affinity toward Bcl-x_L and showed that they could measure dose-dependent binding.

However, to rank order the affinities of different sequences, this assay would need to also determine relative binding affinities. Different sequences are translated with different efficiencies, resulting in unequal peptide concentrations and the need to correct for peptide expression in order to

determine relative binding affinities. The authors used a second competition assay where a synthetic peptide doubly labeled with an HA-tag and fluorescein was used to create a sandwich between magnetic beads and an anti-HA antibody on an acoustic sensor, similar to the assay described above. This signal was then decreased by addition of the same *in vitro* translated HA-tagged peptides or proteins, which compete with the synthetic peptide for binding to anti-HA beads. However, since these translated peptides lack fluorescein, their binding to the anti-HA antibody results in a decreased signal, allowing the concentration of the translated peptide to be determined. With both concentration and binding of each peptide, the relative affinity of the peptides could be determined, and the sequences ranked by affinity for the target. Compared to ELISA, this method provides the same quantitation range but is more automated, sensitive, and requires less antibody and target protein.[286]

In an alternate method to rank *in vitro* translated peptides based on their binding affinity, Larsen *et al*. designed a membrane-based 96-well dot blot apparatus that allows the partitioning of peptide-protein complexes and unbound peptides.[287] In this method, the peptides are translated *in vitro* and are incubated with their cognate protein target until equilibrium is reached. The reaction is then passed through a double filter system consisting of a cellulose top membrane, that can bind the protein-peptide complexes, and a nylon bottom membrane that retains unbound peptides that pass through the first filter. The K_D can be determined by quantifying the complexed and unbound populations over a range of concentrations using phosphor imaging. Using this method, the binding affinity was investigated for peptides ranging from 22 to 74 residues and with K_D values ranging from 1 to 500 nM. The authors were able to analyze 22 new peptides from a previous mRNA display selection targeting human α-thrombin, where two peptides had been previously tested and characterized for binding.[187] The double-filter method identified five new peptides that bound α-thrombin with equal or superior binding affinity compared to previously characterized peptides. The K_D values of these peptides were then determined using the same assay and were found to be consistent with K_D values measured by microscale thermophoresis.[287] Overall, the double filter method shows promise for screening different clones as well as generating accurate equilibrium binding constants.

Arrays of proteins or peptides offer an even higher-throughput method of testing thousands or more compounds simultaneously to determine binding affinity, selectivity, and epitope mapping. The ability to test many interactions in parallel on a protein chip would be an immensely powerful technique for screening potential ligands or for understanding off-target binding of a lead compound However, the challenges of generating a protein chip can easily hamper such experiments. For example, in typical protein arrays, each protein must be expressed, purified, spotted, and immobilized on a surface. Conjugation of the protein to the surface must not lead to protein unfolding.[288]

mRNA-protein fusions offer an elegant solution to the construction of peptide and protein chips. In a pioneering study, Weng *et al*. used mRNA display to make a self-assembling protein microarray.[289] In this study, the authors first synthesized a chip with DNA capture probes that were specific for mRNA coding for a unique epitope (Myc, FLAG, or HA11). When mRNA-protein fusions were incubated with this chip, the DNA capture probes specifically hybridized to their corresponding mRNA-protein fusions, resulting in self-assembly of the protein chip. These immobilized mRNA-protein fusions were then specifically recognized by their corresponding antibody, demonstrating that they retained functionality when immobilized on the chip surface. If this approach can be extended to cover a significant fraction of the proteome, it may provide a rapid and inexpensive route to a comprehensive protein microarray.

8.5 Integration of mRNA display with Next Generation Sequencing

The impact of Next Generation Sequencing technologies on mRNA display has been discussed above. Next Generation sequencing has enabled unparalleled analysis of the sequences obtained during mRNA display selections and has facilitated a dramatic acceleration of the mRNA display process. As described in Section 8.4, the emerging challenge in post-mRNA display analysis is choosing, synthesizing, and characterizing lead sequences in a rapid and cost-effective manner. Combining next generation sequencing with chip-based analysis to characterize millions of peptides or proteins represents another potential solution to this problem. In such a system, an mRNA displayed peptide or protein can either be hybridized to the DNA on a next generation sequencing chip or generated in situ by performing translation and mRNA display on the surface of the chip. In theory, this would allow a DNA sequence to be obtained and binding characterization to be performed on the peptide or protein coded by that DNA sequence.

A next generation sequencing analysis platform was developed by Swenson *et al*. to perform high-throughput characterization of the binding affinities of peptides displayed on the surface of an Illumina flow-cell. In a typical Illumina sequencing experiment, millions of monoclonal clusters of DNA strands are generated in the form of bound oligos on the solid surface of the flow-cell chip through a bridge amplification process.[290] These DNA clusters, called “polonies,” are then sequenced to determine the DNA sequence of that cluster. In order to adapt this process to an mRNA display format, the DNA clusters not only needed to be transcribed into mRNA that could be translated on the chip, but also requires the mRNA remains covalently attached to the surface near its corresponding cluster. A covalent linkage in this system is important to ensure the fidelity of information so that a DNA sequence corresponds to its encoded peptide and the binding information for that peptide. To solve this problem, the authors identified a primer-dependent RNA polymerase, poliovirus polymerase $3D^{Pol}$, which can utilize DNA or RNA templates *in vitro*, but also transcribes the mRNA strand so that it remains covalently

attached to the initiating primer. A second challenge was that $3D^{Pol}$ requires an RNA primer for initiation, but a typical Illumina workflow uses DNA primers. To solve this issue, the authors used terminal transferase (TdT) to add several guanosine ribonucleotides to the 3' end of the flow-cell bound DNA primers, generating hybrid DNA-RNA primers. The authors further confirmed that the mRNA strands synthesized by $3D^{Pol}$ were full-length and the synthesis using this approach was very efficient. mRNA protein fusions were then formed by hybridizing a puromycin-containing oligo to the 3' end of the mRNA, in a manner analogous to TRAP display.[15] To demonstrate functionality in this system, the authors used templates encoding Myc and FLAG peptides. Anti-FLAG and anti-Myc antibodies were then incubated with the immobilized mRNA- peptide fusions and showed specific binding to their cognate sequences. While only two peptides were displayed in the system and no sequencing of the DNA was performed, the core elements of this system show potential for a high throughput sequencing and characterization platform.[291]

A study using **H**igh-**T**hroughput **S**equencing **K**inetics (HTSK) of mRNA display libraries was used to obtain the association and dissociation rate constants of thousands of peptides simultaneously.[179] To do this, the authors collected fractions of an mRNA display pool of Bcl-x_L binding peptides at different time points during the association or the dissociation phase of target binding. The cDNA from the mRNA-peptide fusions at each time point was amplified and subjected to high-throughput sequencing, which provided the normalized frequency of each peptide sequence at that time point. By fitting the rate of increase of each peptide sequence, a kinetic association rate constant could be determined for each peptide sequence that appeared in the pool. Likewise, fitting the rate of decrease of each peptide sequence during the dissociation phase yielded kinetic dissociation rate constants. Using both rate constants together, the K_D for each sequence could then be determined. The authors demonstrated strong correlation between rate constants determined using this method and those measured using radioactive assays. Further, using this method, rare sequences with lower frequency rank but higher binding affinities were found, demonstrating that the abundance of a sequence in the final mRNA display pool does not always correlate with binding affinity. While this method might be best suited for very strong affinity pools (i.e., it could not be used on pools with too fast on- or off-rates), it is a powerful method for analysis and characterization of multiple individual sequence in mRNA display pools.

Lastly, Illumina sequencing of mRNA display libraries is challenging because processing of the sequencing data does not fit well with standard genomic workflows. Although some specialized tools exist for processing of selection sequencing data, Blanco *et al*. developed a set of user-friendly scripts called EasyDIVER for specifically processing high throughput sequence data for mRNA display.[292] Using EasyDIVER, the DNA sequence data is extracted, trimmed to remove primers and Illumina

adapters, translated into peptide sequences if necessary, and the counts of individual sequences are determined. Such scripts will help to make the use of high-throughput sequencing data for mRNA display selections more accessible to a wider array of researchers.

9 Conclusions and Outlook

mRNA display is a powerful technique for performing directed evolution of proteins and peptides. The linkage of protein to mRNA via puromycin allows the amplification of minute quantities of functional proteins and the facile identification of these proteins via DNA sequencing. As a wholly *in vitro* technique, the minimalist architecture of mRNA display libraries to provides significant advantages over other display platforms which include **1)** reduction in library bias and access to a wide range of selection conditions, **2)** the ability to search large libraries (over a quadrillion sequences) for function and **3)** access to unnatural amino acids and non-proteogenic chemical functionalities.

Over the past 15 years, mRNA display selections have yielded many novel functional proteins and peptides. mRNA display libraries of antibody and antibody-mimetic proteins have resulted in new molecules that have found use as tools for chemical biology, *in vivo* imaging, and therapeutic development. mRNA display selections have also yielded natural, linear peptides as well as unnatural, cyclic, NRSP-like peptides with high target affinity, superior metabolic stability, and in some cases, high cell permeability. These selections have set the stage for the use of mRNA display to evolve potent lead compounds for drug development, and potentially, for the direct selection of translation-ready therapeutics. As the list of targets generated from genomic and proteomic analyses increases in size, mRNA display is well-positioned to play a critical role in identifying new ligands to modulate these targets *in* vivo.

Despite its potential as a directed evolution platform, mRNA display is often seen as technically challenging and time-intensive which may have prevented its adoption by non-experts. However, we believe that this is likely to change in the next twenty years for a variety of reasons. First, the synthesis of high-quality DNA libraries has been simplified by the dramatically lower costs of synthetic DNA in conjunction with the commensurate increase in the quality of commercial oligos. Wholly reconstituted *in vitro* translation systems are now commercially available which provides a facile path for the incorporation of non-natural amino acids into mRNA display libraries. Protein expression has been greatly simplified and accelerated by the advent of synthetic DNA technologies (e.g., the rapid and inexpensive synthesis of entire genes) and can be readily integrated with *in situ* biotinylation to generate multi-milligram quantities of target protein for directional immobilization on solid phase.[283] The rapidly

diminishing cost of next generation sequencing, one of the few techniques in biology to roughly follow Moore's Law, allows deep analysis of selection results and may facilitate hit identification in early rounds. Finally, automated selection technologies offer the prospect of high throughput, massively parallel selections with minimal consumption of library and target. We believe that these enabling technologies, in conjunction with advances in library design and selection workflow, will lead to the wide adoption of mRNA display as a design tool to meet the challenges of drug discovery in the post-genomic world.

List of Acronyms and Abbreviations

2ACHC: (1S, 2S)-2-aminocyclohexanecarboxyllic acid
^{10}Fn3: 10th subunit of Fibronectin type III
AARS: Aminoacyl tRNA synthetase
ABT: amino-modified benzyl thioester
ACL: Anti Codon Loop
ADCC: Antibody-dependent cell-mediated toxicity
AIF: Aluminum fluoride
Aoc: L-2-aminooctanoic acid
AzHA: β-azidohomoalanine
Bcl-x_L: B-cell lymphoma-extra large
BLI: Bio-Layer Interferometry
CaMKIIα: Ca^{2+}/calmodulin-dependent protein kinase II α
CAR: Chimeric antigen receptor
CBT: 4-chlorobenzyl thioester
CCR1: CC Chemokine Receptor-1
CDRs: Complementarity determining regions
CFMS: Continuous flow magnetic separation
CH: Constant heavy chain; **CL**: Constant light chain
ClAB-f: N-[3-2-chloroacetamido)benzoyl]-D-phenylalanine
ClAB-F: N-[3-2-chloroacetamido)benzoyl]-L-phenylalanine
ClAB-Y: N-[3-2-chloroacetamido)benzoyl]-L-tyrosine
ClAc-F: a-N-(2-chloroacetyl)-L-phenylalanine
ClAc-w: a-N-(2-chloroacetyl)-D-tryptophan
ClAc-y: a-N-(2-chloroacetyl)-D-tyrosine
ClAc-Y: a-N-(2-chloroacetyl)-L-tyrosine
CME: Cyanomethyl ester
CPG: Controlled pore glass
^{CNV}K: 3-cyanovinylcarbazole nucleoside
CuAAC: Copper-mediated azide−alkyne cycloaddition
cycPRPs: Cyclic protease resistant peptides
DBCO: dibenzocyclooctyne
DBE: 3,5-dinitrobenzyl ester
DBX: dibromo-*m*-xylene
DC-SIGN: Dendritic cell-specific ICAM3-grabbing non-integrin receptor
DHFR: Dihydrofolate reductase
Dha: dehydroalanine
DIVERSE: Directed In Vitro Evolution of Reactive peptide tags via Sequential Enrichment
DOPC: 1,2-dioleoyl-sn-glycero-3-phosphocholine
DSG: disuccinimidyl glutarate
ED: *E. coli* display
EETI-II: Ecballium elaterium trypsin inhibitor two
EGFR: Epidermal growth factor receptor
ELISA: enzyme-linked immunosorbent assay
Fab: Fragment antigen binding
FANGs: Fibronectin Antibody-mimetic Nicotinic acetylcholine receptor Generated ligands
Fc: Fragment crystallizable
FEA: 2-[^{18}F]-fluoroethylazide
FingRs: Fibronectin intrabodies generated with mRNA display
FIT: Flexible *in vitro* Translation
Fn3: Fibronectin type III
FP: Fluorescence polarization
FRET: Fluorescence resonance energy transfer
FT: Fluorescence Titration
Fv: Immunoglobulin variable domains
GFP: Green fluorescent protein
GIRK: G-protein activated inwardly rectifying potassium channels
GPCRs: G-Protein Coupled Receptors
GPR: G-protein regulatory motif
GSHox: Oxidized glutathione
Gαs(s): The short isoform of Gαs
HCV: Hepatitis C Virus
HA-tag: Hemagglutinin tag
HIV: human immunodeficiency virus
HPLC: high performance liquid chromatography

HPG: homopropargylglycine
HTS: High throughput sequencing
HTSK: High-Throughput Sequencing Kinetics
ID: injected dose
IGF-1R: Insulin-like growth factor-I receptor
IL: interleukin
IVV: *in vitro* virus
K_a: Trans-4,5-dehydro-DL-lysine
K^{Se}: 4-selenalysine
K_D: Dissociation constant
KDR: Kinase insert domain receptor
KLH: Keyhole Limpet Hemocyanin
K^{Tfa}: ε-N-trifluoroacetyl lysine
L_a: β-t-butyl-DL-alanine
M_a: DL-2-amino-hex-5-ynoic acid
mA: N-methyl-L-alanine
mAbs: Monoclonal antibodies
MATE: Multidrug and Toxic Compound Extrusion
MBP: Maltose binding protein
MDM2: Mouse Double Minute 2 homolog
MFED: MicroFluidic Enrichment Device
mF: N-methyl-L-phenylalanine
mG: N-methyl glycine
MIP: MDM2 Inhibitory Peptide
mnV: N-methyl-L-norvaline
MRSA: Methicillin-Resistant *S. Aureus*
mS: N-methyl-L-serine
Mth: Methuselah
mYm: N-methyl-4-*O*-methyl-tyrosine
NHS: N-hydroxysuccinimide
NRPS: Non-ribosomal peptide synthetase
OBOC: One-bead-one-compound
ORF: Open reading frame
PBP2A: penicillin-binding protein 2A
p-ClBz: p-(chloromethyl)benzamide
PCR: Polymerase chain reaction
PCSK9: subtilisin/kexin type 9
PD: Phage display
pdCpA: phospho-deoxyC-riboA
PD-L1: Programmed death ligand 1
PET: Positron emission tomography
pI: isoelectric point
PEG: polyethylene glycol
PKS: Polyketide synthetase
PSD-95: Post Synaptic Density-95
PSD: Post Synaptic Density
PURE: Protein Synthesis from Recombinant Elements
PXR: human pregnane x receptor
RA: Radioactive Assay
RANK: Receptor Activator of Nuclear Factor κB
RaPID: Random non-standard Peptide Integrated Discovery
RasIn: Ras Intrabody
Cp-puromycin: Ribocytidyl-puromycin
RBD: Receptor binding domain
RiPP: Ribosomally synthesized and post-translationally modified peptide
RR2ACPC: (1R, 2R)-2-aminocyclopentanecarboxyllic acid
RRL: Rabbit reticulocyte lysate
SARS-CoV-2: severe acute respiratory syndrome (SARS) Coronavirus-2
SARS-N: Severe acute respiratory syndrome nucleocapsid protein
scFv: Single chain fragment variable
SPAM: Signal Peptide-based Affinity Maturated ligand
SPR: Surface Plasmon Resonance
SRC-1: steroid receptor co-activator-1
SS2ACPC: (1S, 2S)-2-aminopentanecarboxyllic acid
STG: Streptomyces mobaraensis transglutaminase
SUPR: Scanning Unnatural Protease Resistant

sY: sulfotyrosine
$t_{1/2}$: Half-life
T_a: DL-hydroxy-norvaline
TCEP: Tris(2-carboxyethyl)-phosphine
TdT: Terminal transferase
TNFR: Tumor Necrosis Factor α Receptor
TNFα: Tumor Necrosis Factor α
TRAP: Transcription−Translation coupled with Association of Puromycin linker
UTR: Untranslated region
VEGFR-2: Vascular endothelial growth factor receptor-2
V_H: Variable heavy chain
V_L: Variable light chains
y: D-tyrosine
Y_a: 3-fluoro-L-tyrosine
YAP: Yes-Associated Protein 1
YD: Yeast display
yneF: p-ethynyl phenylalanine
ZF: zinc-finger

Conflicts of Interest

There are no conflicts of interest to declare

Acknowledgments

This work was supported by UT MDACC Startup Funds (SWM), a Cancer Prevention and Research Institute of Texas (CPRIT) Individual Investigator Award (RP200166-IIRA, SWM), a University of Texas MD Anderson Cancer Center Institutional Research Grant, the National Institutes of Health R44CA206771 (SWM), R01CA170820 (R.W.R., T.T.T.), and R01CA231509 (SWM). We also acknowledge support from the Glioblastoma Research Foundation (The Lee Project), a G.E. In-kind Multi-Investigator Imaging (MI2) Research Award (SWM, RWR, TTT), the Department of Defense/CDMRP CA140291 (TTT), the Ming Hsieh Institute for Research on Engineering-Medicine for Cancer (R.W.R., TTT) as well as T32A196561 (BJG).

References

1. Huang, P. S.; Boyken, S. E.; Baker, D., The coming of age of de novo protein design. *Nature* **2016,** *537* (7620), 320-7.
2. Smith, G. P., Filamentous fusion phage: novel expression vectors that display cloned antigens on the virion surface. *Science* **1985,** *228* (4705), 1315-1317.
3. Smith, G. P.; Petrenko, V. A., Phage display. *Chemical reviews* **1997,** *97* (2), 391-410.
4. Roberts, R. W.; Szostak, J. W., RNA-peptide fusions for the in vitro selection of peptides and proteins. *Proceedings of the National Academy of Sciences of the United States of America* **1997,** *94* (23), 12297-302.
5. Hanes, J.; Pluckthun, A., In vitro selection and evolution of functional proteins by using ribosome display. *Proceedings of the National Academy of Sciences of the United States of America* **1997,** *94* (10), 4937-42.
6. Cull, M. G.; Miller, J. F.; Schatz, P. J., Screening for receptor ligands using large libraries of peptides linked to the C terminus of the lac repressor. *Proceedings of the National Academy of Sciences of the United States of America* **1992,** *89* (5), 1865-9.
7. Odegrip, R.; Coomber, D.; Eldridge, B.; Hederer, R.; Kuhlman, P. A.; Ullman, C.; FitzGerald, K.; McGregor, D., CIS display: In vitro selection of peptides from libraries of protein-DNA complexes. *Proceedings of the National Academy of Sciences of the United States of America* **2004,** *101* (9), 2806-10.
8. Winter, G.; Griffiths, A. D.; Hawkins, R. E.; Hoogenboom, H. R., Making antibodies by phage display technology. *Annual review of immunology* **1994,** *12* (1), 433-455.
9. Sergeeva, A.; Kolonin, M. G.; Molldrem, J. J.; Pasqualini, R.; Arap, W., Display technologies: application for the discovery of drug and gene delivery agents. *Advanced drug delivery reviews* **2006,** *58* (15), 1622-1654.
10. Galán, A.; Comor, L.; Horvatić, A.; Kuleš, J.; Guillemin, N.; Mrljak, V.; Bhide, M., Library-based display technologies: where do we stand? *Molecular BioSystems* **2016,** *12* (8), 2342-2358.
11. Tizei, P. A.; Csibra, E.; Torres, L.; Pinheiro, V. B., Selection platforms for directed evolution in synthetic biology. *Biochemical Society Transactions* **2016,** *44* (4), 1165-1175.
12. Colas, P., Combinatorial protein reagents to manipulate protein function. *Current opinion in chemical biology* **2000,** *4* (1), 54-59.
13. Liu, R.; Barrick, J. E.; Szostak, J. W.; Roberts, R. W., Optimized synthesis of RNA-protein fusions for in vitro protein selection. *Methods Enzymol* **2000,** *318*, 268-93.
14. Starck, S. R.; Roberts, R. W., Puromycin oligonucleotides reveal steric restrictions for ribosome entry and multiple modes of translation inhibition. *RNA* **2002,** *8* (7), 890-903.
15. Ishizawa, T.; Kawakami, T.; Reid, P. C.; Murakami, H., TRAP display: a high-speed selection method for the generation of functional polypeptides. *J Am Chem Soc* **2013,** *135* (14), 5433-40.
16. Kreider, B. L., PROfusion: genetically tagged proteins for functional proteomics and beyond. *Med Res Rev* **2000,** *20* (3), 212-5.
17. Nemoto, N.; Miyamoto-Sato, E.; Husimi, Y.; Yanagawa, H., In vitro virus: bonding of mRNA bearing puromycin at the 3'-terminal end to the C-terminal end of its encoded protein on the ribosome in vitro. *FEBS Lett* **1997,** *414* (2), 405-8.
18. Yamaguchi, J.; Naimuddin, M.; Biyani, M.; Sasaki, T.; Machida, M.; Kubo, T.; Funatsu, T.; Husimi, Y.; Nemoto, N., cDNA display: a novel screening method for functional disulfide-rich peptides by solid-phase synthesis and stabilization of mRNA-protein fusions. *Nucleic acids research* **2009,** *37* (16), e108.
19. Moore, M. J.; Sharp, P. A., Site-specific modification of pre-mRNA: the 2'-hydroxyl groups at the splice sites. *Science* **1992,** *256* (5059), 992-7.
20. Kurz, M.; Gu, K.; Al-Gawari, A.; Lohse, P. A., cDNA–protein fusions: covalent protein–gene conjugates for the in vitro selection of peptides and proteins. *Chembiochem* **2001,** *2* (9), 666-672.
21. Kurz, M.; Gu, K.; Lohse, P. A., Psoralen photo-crosslinked mRNA-puromycin conjugates: a novel template for the rapid and facile preparation of mRNA-protein fusions. *Nucleic acids research* **2000,** *28* (18), E83.
22. Mochizuki, Y.; Suzuki, T.; Fujimoto, K.; Nemoto, N., A versatile puromycin-linker using cnvK for high-throughput in vitro selection by cDNA display. *J Biotechnol* **2015,** *212*, 174-80.

23. Barrick, J. E.; Takahashi, T. T.; Balakin, A.; Roberts, R. W., Selection of RNA-binding peptides using mRNA-peptide fusions. *Methods* **2001,** *23* (3), 287-293.
24. Tabuchi, I.; Soramoto, S.; Nemoto, N.; Husimi, Y., An in vitro DNA virus for in vitro protein evolution. *FEBS Lett* **2001,** *508* (3), 309-12.
25. Nishigaki, K.; Taguchi, K.; Kinoshita, Y.; Aita, T.; Husimi, Y., Y-ligation: an efficient method for ligating single-stranded DNAs and RNAs with T4 RNA ligase. *Mol Divers* **1998,** *4* (3), 187-90.
26. Tabuchi, I.; Soramoto, S.; Suzuki, M.; Nishigaki, K.; Nemoto, N.; Husimi, Y., An Efficient Ligation Method in the Making of an in vitro Virus for in vitro Protein Evolution. *Biol Proced Online* **2002,** *4*, 49-54.
27. Biyani, M.; Husimi, Y.; Nemoto, N., Solid-phase translation and RNA-protein fusion: a novel approach for folding quality control and direct immobilization of proteins using anchored mRNA. *Nucleic acids research* **2006,** *34* (20), e140.
28. Naimuddin, M.; Kubo, T., A High Performance Platform Based on cDNA Display for Efficient Synthesis of Protein Fusions and Accelerated Directed Evolution. *ACS Comb Sci* **2016,** *18* (2), 117-29.
29. Reyes, S. G.; Kuruma, Y.; Fujimi, M.; Yamazaki, M.; Eto, S.; Nishikawa, S.; Tamaki, S.; Kobayashi, A.; Mizuuchi, R.; Rothschild, L.; Ditzler, M.; Fujishima, K., PURE mRNA display and cDNA display provide rapid detection of core epitope motif via high-throughput sequencing. *Biotechnol Bioeng* **2021,** *118* (4), 1736-1749.
30. Hanes, J.; Plückthun, A., In vitro selection and evolution of functional proteins by using ribosome display. *Proceedings of the National Academy of Sciences* **1997,** *94* (10), 4937-4942.
31. Lam, K. S.; Lebl, M.; Krchnak, V., The "One-Bead-One-Compound" Combinatorial Library Method. *Chem Rev* **1997,** *97* (2), 411-448.
32. Wong, F. T.; Khosla, C., Combinatorial biosynthesis of polyketides—a perspective. *Current opinion in chemical biology* **2012,** *16* (1-2), 117-123.
33. Walsh, C. T., Polyketide and nonribosomal peptide antibiotics: modularity and versatility. *Science* **2004,** *303* (5665), 1805-1810.
34. Lancet, D.; Sadovsky, E.; Seidemann, E., Probability model for molecular recognition in biological receptor repertoires: significance to the olfactory system. *Proceedings of the National Academy of Sciences* **1993,** *90* (8), 3715-3719.
35. Vaughan, T. J.; Williams, A. J.; Pritchard, K.; Osbourn, J. K.; Pope, A. R.; Earnshaw, J. C.; McCafferty, J.; Hodits, R. A.; Wilton, J.; Johnson, K. S., Human Antibodies with Sub-nanomolar Affinities Isolated from a Large Non-immunized Phage Display Library. *Nat Biotech* **1996,** *14* (3), 309-314.
36. Rosenwald, S.; Kafri, R. A. N.; Lancet, D., Test of a Statistical Model for Molecular Recognition in Biological Repertoires. *Journal of Theoretical Biology* **2002,** *216* (3), 327-336.
37. Wilson, D. S.; Keefe, A. D.; Szostak, J. W., The use of mRNA display to select high-affinity protein-binding peptides. *Proceedings of the National Academy of Sciences* **2001,** *98* (7), 3750-3755.
38. Voss, S.; Skerra, A., Mutagenesis of a flexible loop in streptavidin leads to higher affinity for the Strep-tag II peptide and improved performance in recombinant protein purification. *Protein engineering* **1997,** *10* (8), 975-982.
39. Schmidt, T. G.; Skerra, A., The random peptide library-assisted engineering of a C-terminal affinity peptide, useful for the detection and purification of a functional Ig Fv fragment. *Protein Engineering, Design and Selection* **1993,** *6* (1), 109-122.
40. Knight, R.; Yarus, M., Analyzing partially randomized nucleic acid pools: straight dope on doping. *Nucleic acids research* **2003,** *31* (6), e30.
41. Brule, C. E.; Grayhack, E. J., Synonymous codons: choose wisely for expression. *Trends in Genetics* **2017,** *33* (4), 283-297.
42. Hall, M. N.; Gabay, J.; Débarbouillé, M.; Schwartz, M., A role for mRNA secondary structure in the control of translation initiation. *Nature* **1982,** *295* (5850), 616-618.
43. Gold, L., mRNA display: diversity matters during in vitro selection. *Proceedings of the National Academy of Sciences of the United States of America* **2001,** *98* (9), 4825-6.
44. Sha, F.; Salzman, G.; Gupta, A.; Koide, S., Monobodies and other synthetic binding proteins for expanding protein science. *Protein Sci* **2017,** *26* (5), 910-924.
45. Shi, L.; Wheeler, J. C.; Sweet, R. W.; Lu, J.; Luo, J.; Tornetta, M.; Whitaker, B.; Reddy, R.; Brittingham, R.; Borozdina, L., De novo selection of high-affinity antibodies from synthetic fab libraries displayed on phage as pIX fusion proteins. *Journal of molecular biology* **2010,** *397* (2), 385-396.

46. Cwirla, S. E.; Peters, E. A.; Barrett, R. W.; Dower, W. J., Peptides on phage: a vast library of peptides for identifying ligands. *Proceedings of the National Academy of Sciences of the United States of America* **1990,** *87* (16), 6378-82.
47. Zade, H. M.; Keshavarz, R.; Shekarabi, H. S. Z.; Bakhshinejad, B., Biased selection of propagation-related TUPs from phage display peptide libraries. *Amino acids* **2017,** *49* (8), 1293-1308.
48. Krumpe, L. R.; Atkinson, A. J.; Smythers, G. W.; Kandel, A.; Schumacher, K. M.; McMahon, J. B.; Makowski, L.; Mori, T., T7 lytic phage-displayed peptide libraries exhibit less sequence bias than M13 filamentous phage-displayed peptide libraries. *Proteomics* **2006,** *6* (15), 4210-4222.
49. Yamane, K.; Mizushima, S., Introduction of basic amino acid residues after the signal peptide inhibits protein translocation across the cytoplasmic membrane of Escherichia coli. Relation to the orientation of membrane proteins. *Journal of Biological Chemistry* **1988,** *263* (36), 19690-19696.
50. Fiacco, S. V.; Roberts, R. W., N-Methyl Scanning Mutagenesis Generates Protease-Resistant G Protein Ligands with Improved Affinity and Selectivity. *ChemBioChem* **2008,** *9* (14), 2200-2203.
51. Fiacco, S. V.; Kelderhouse, L. E.; Hardy, A.; Peleg, Y.; Hu, B.; Ornelas, A.; Yang, P.; Gammon, S. T.; Howell, S. M.; Wang, P.; Takahashi, T. T.; Millward, S. W.; Roberts, R. W., Directed Evolution of Scanning Unnatural-Protease-Resistant (SUPR) Peptides for in Vivo Applications. *Chembiochem* **2016,** *17* (17), 1643-51.
52. Howell, S. M.; Fiacco, S. V.; Takahashi, T. T.; Jalali-Yazdi, F.; Millward, S. W.; Hu, B.; Wang, P.; Roberts, R. W., Serum stable natural peptides designed by mRNA display. *Scientific reports* **2014,** *4*, 6008.
53. Nichols, A. L.; Noridomi, K.; Hughes, C. R.; Jalali-Yazdi, F.; Eaton, J. B.; Lai, L. H.; Advani, G.; Lukas, R. J.; Lester, H. A.; Chen, L.; Roberts, R. W., alpha1-FANGs: Protein Ligands Selective for the alpha-Bungarotoxin Site of the alpha1-Nicotinic Acetylcholine Receptor. *ACS Chem Biol* **2018,** *13* (9), 2568-2576.
54. Cotten, S. W.; Zou, J.; Valencia, C. A.; Liu, R., Selection of proteins with desired properties from natural proteome libraries using mRNA display. *Nat Protoc* **2011,** *6* (8), 1163-82.
55. Wang, H.; Liu, R., Advantages of mRNA display selections over other selection techniques for investigation of protein-protein interactions. *Expert Rev Proteomics* **2011,** *8* (3), 335-46.
56. Kintzing, J. R.; Filsinger Interrante, M. V.; Cochran, J. R., Emerging Strategies for Developing Next-Generation Protein Therapeutics for Cancer Treatment. *Trends Pharmacol Sci* **2016,** *37* (12), 993-1008.
57. Freise, A. C.; Wu, A. M., In vivo imaging with antibodies and engineered fragments. *Mol Immunol* **2015,** *67* (2 Pt A), 142-52.
58. Gebauer, M.; Skerra, A., Engineered protein scaffolds as next-generation antibody therapeutics. *Curr Opin Chem Biol* **2009,** *13* (3), 245-55.
59. Rossmann, M.; S, J. G.; Moschetti, T.; Dinan, M.; Hyvonen, M., Development of a multipurpose scaffold for the display of peptide loops. *Protein Eng Des Sel* **2017,** *30* (6), 419-430.
60. Hosse, R. J.; Rothe, A.; Power, B. E., A new generation of protein display scaffolds for molecular recognition. *Protein Sci* **2006,** *15* (1), 14-27.
61. Zoller, F.; Haberkorn, U.; Mier, W., Miniproteins as phage display-scaffolds for clinical applications. *Molecules* **2011,** *16* (3), 2467-85.
62. Koide, A.; Bailey, C. W.; Huang, X.; Koide, S., The fibronectin type III domain as a scaffold for novel binding proteins1. *Journal of molecular biology* **1998,** *284* (4), 1141-1151.
63. Forrer, P.; Jung, S.; Pluckthun, A., Beyond binding: using phage display to select for structure, folding and enzymatic activity in proteins. *Curr Opin Struct Biol* **1999,** *9* (4), 514-20.
64. Takahashi, T. T.; Austin, R. J.; Roberts, R. W., mRNA display: ligand discovery, interaction analysis and beyond. *Trends in biochemical sciences* **2003,** *28* (3), 159-165.
65. Keefe, A. D.; Szostak, J. W., Functional proteins from a random-sequence library. *Nature* **2001,** *410* (6829), 715-8.
66. Cho, G.; Keefe, A. D.; Liu, R.; Wilson, D. S.; Szostak, J. W., Constructing high complexity synthetic libraries of long ORFs using in vitro selection. *J Mol Biol* **2000,** *297* (2), 309-19.
67. Schmidt, M. M.; Wittrup, K. D., A modeling analysis of the effects of molecular size and binding affinity on tumor targeting. *Molecular cancer therapeutics* **2009,** *8* (10), 2861-71.
68. Doshi, R.; Chen, B. R.; Vibat, C. R.; Huang, N.; Lee, C. W.; Chang, G., In vitro nanobody discovery for integral membrane protein targets. *Scientific reports* **2014,** *4*, 6760.
69. Tanaka, J.; Yanagawa, H.; Doi, N., Comparison of the frequency of functional SH3 domains with different limited sets of amino acids using mRNA display. *PLoS One* **2011,** *6* (3), e18034.

70. Sumida, T.; Yanagawa, H.; Doi, N., In vitro selection of fab fragments by mRNA display and gene-linking emulsion PCR. *J Nucleic Acids* **2012,** *2012*, 371379.
71. Xu, L.; Aha, P.; Gu, K.; Kuimelis, R. G.; Kurz, M.; Lam, T.; Lim, A. C.; Liu, H.; Lohse, P. A.; Sun, L., Directed evolution of high-affinity antibody mimics using mRNA display. *Chemistry & biology* **2002,** *9* (8), 933-942.
72. Emanuel, S. L.; Engle, L. J.; Chao, G.; Zhu, R.-R.; Cao, C.; Lin, Z.; Yamniuk, A. P.; Hosbach, J.; Brown, J.; Fitzpatrick, E. In *A fibronectin scaffold approach to bispecific inhibitors of epidermal growth factor receptor and insulin-like growth factor-I receptor*, MAbs, Taylor & Francis: 2011; pp 38-48.
73. Getmanova, E. V.; Chen, Y.; Bloom, L.; Gokemeijer, J.; Shamah, S.; Warikoo, V.; Wang, J.; Ling, V.; Sun, L., Antagonists to human and mouse vascular endothelial growth factor receptor 2 generated by directed protein evolution in vitro. *Chemistry & biology* **2006,** *13* (5), 549-556.
74. Grilo, A. L.; Mantalaris, A., The Increasingly Human and Profitable Monoclonal Antibody Market. *Trends Biotechnol* **2019,** *37* (1), 9-16.
75. Kohler, G.; Milstein, C., Continuous cultures of fused cells secreting antibody of predefined specificity. *Nature* **1975,** *256* (5517), 495-7.
76. Geyer, C. R.; McCafferty, J.; Dubel, S.; Bradbury, A. R.; Sidhu, S. S., Recombinant antibodies and in vitro selection technologies. *Methods Mol Biol* **2012,** *901*, 11-32.
77. Kipriyanov, S. M.; Le Gall, F., Generation and production of engineered antibodies. *Mol Biotechnol* **2004,** *26* (1), 39-60.
78. Liu, H.; May, K., Disulfide bond structures of IgG molecules: structural variations, chemical modifications and possible impacts to stability and biological function. *MAbs* **2012,** *4* (1), 17-23.
79. Hsieh, C. M.; Kutskova, Y. A.; Memmott, J. E. Methods of RNA Display. US8916504, December 23, 2014.
80. Nagumo, Y.; Fujiwara, K.; Horisawa, K.; Yanagawa, H.; Doi, N., PURE mRNA display for in vitro selection of single-chain antibodies. *J Biochem* **2016,** *159* (5), 519-26.
81. Chen, L.; Kutskova, Y. A.; Hong, F.; Memmott, J. E.; Zhong, S.; Jenkinson, M. D.; Hsieh, C. M., Preferential germline usage and VH/VL pairing observed in human antibodies selected by mRNA display. *Protein Eng Des Sel* **2015,** *28* (10), 427-35.
82. Tabata, N.; Sakuma, Y.; Honda, Y.; Doi, N.; Takashima, H.; Miyamoto-Sato, E.; Yanagawa, H., Rapid antibody selection by mRNA display on a microfluidic chip. *Nucleic acids research* **2009,** *37* (8), e64.
83. Shibui, T.; Kobayashi, T.; Kanatani, K., A completely in vitro system for obtaining scFv using mRNA display, PCR, direct sequencing, and wheat embryo cell-free translation. *Biotechnol Lett* **2009,** *31* (7), 1103-10.
84. Fukuda, I.; Kojoh, K.; Tabata, N.; Doi, N.; Takashima, H.; Miyamoto-Sato, E.; Yanagawa, H., In vitro evolution of single-chain antibodies using mRNA display. *Nucleic acids research* **2006,** *34* (19), e127.
85. Shibui, T.; Kobayashi, T.; Kanatani, K.; Koga, H.; Misawa, S.; Isomura, T.; Sasaki, T., In vitro selection of scFv and its production: an application of mRNA display and wheat embryo cell-free and E. coli cell production system. *Appl Microbiol Biotechnol* **2009,** *84* (4), 725-32.
86. Ducancel, F.; Muller, B. H., Molecular engineering of antibodies for therapeutic and diagnostic purposes. *MAbs* **2012,** *4* (4), 445-57.
87. Chan, C. E.; Chan, A. H.; Lim, A. P.; Hanson, B. J., Comparison of the efficiency of antibody selection from semi-synthetic scFv and non-immune Fab phage display libraries against protein targets for rapid development of diagnostic immunoassays. *Journal of immunological methods* **2011,** *373* (1-2), 79-88.
88. Steinwand, M.; Droste, P.; Frenzel, A.; Hust, M.; Dübel, S.; Schirrmann, T. In *The influence of antibody fragment format on phage display based affinity maturation of IgG*, MAbs, Taylor & Francis: 2014; pp 204-218.
89. Gebauer, M.; Skerra, A., Engineered Protein Scaffolds as Next-Generation Therapeutics. *Annu Rev Pharmacol Toxicol* **2020,** *60*, 391-415.
90. 16 - Development issues: antibody stability, developability, immunogenicity, and comparability. In *Therapeutic Antibody Engineering*, Strohl, W. R.; Strohl, L. M., Eds. Woodhead Publishing: 2012; pp 377-595.
91. Chung, W. K.; Russell, B.; Yang, Y.; Handlogten, M.; Hudak, S.; Cao, M.; Wang, J.; Robbins, D.; Ahuja, S.; Zhu, M., Effects of antibody disulfide bond reduction on purification process performance and final drug substance stability. *Biotechnol Bioeng* **2017,** *114* (6), 1264-1274.
92. Zollinger, A. J.; Smith, M. L., Fibronectin, the extracellular glue. *Matrix Biol* **2017,** *60-61*, 27-37.

93. Koide, S.; Koide, A.; Lipovšek, D., Target-binding proteins based on the 10th human fibronectin type III domain (10Fn3). In *Methods in enzymology*, Elsevier: 2012; Vol. 503, pp 135-156.
94. Olson, C. A.; Roberts, R. W., Design, expression, and stability of a diverse protein library based on the human fibronectin type III domain. *Protein science* **2007,** *16* (3), 476-484.
95. Bannas, P.; Hambach, J.; Koch-Nolte, F., Nanobodies and nanobody-based human heavy chain antibodies as antitumor therapeutics. *Frontiers in immunology* **2017,** *8*, 1603.
96. Ramamurthy, V.; Krystek, S. R., Jr.; Bush, A.; Wei, A.; Emanuel, S. L.; Das Gupta, R.; Janjua, A.; Cheng, L.; Murdock, M.; Abramczyk, B.; Cohen, D.; Lin, Z.; Morin, P.; Davis, J. H.; Dabritz, M.; McLaughlin, D. C.; Russo, K. A.; Chao, G.; Wright, M. C.; Jenny, V. A.; Engle, L. J.; Furfine, E.; Sheriff, S., Structures of adnectin/protein complexes reveal an expanded binding footprint. *Structure* **2012,** *20* (2), 259-69.
97. Khan, J. A.; Camac, D. M.; Low, S.; Tebben, A. J.; Wensel, D. L.; Wright, M. C.; Su, J.; Jenny, V.; Gupta, R. D.; Ruzanov, M.; Russo, K. A.; Bell, A.; An, Y.; Bryson, J. W.; Gao, M.; Gambhire, P.; Baldwin, E. T.; Gardner, D.; Cavallaro, C. L.; Duncia, J. V.; Hynes, J., Jr., Developing Adnectins that target SRC co-activator binding to PXR: a structural approach toward understanding promiscuity of PXR. *J Mol Biol* **2015,** *427* (4), 924-42.
98. Han, X.; Cinay, G. E.; Zhao, Y.; Guo, Y.; Zhang, X.; Wang, P., Adnectin-Based Design of Chimeric Antigen Receptor for T Cell Engineering. *Mol Ther* **2017,** *25* (11), 2466-2476.
99. Donnelly, D. J.; Smith, R. A.; Morin, P.; Lipovsek, D.; Gokemeijer, J.; Cohen, D.; Lafont, V.; Tran, T.; Cole, E. L.; Wright, M.; Kim, J.; Pena, A.; Kukral, D.; Dischino, D. D.; Chow, P.; Gan, J.; Adelakun, O.; Wang, X. T.; Cao, K.; Leung, D.; Bonacorsi, S. J., Jr.; Hayes, W., Synthesis and Biologic Evaluation of a Novel (18)F-Labeled Adnectin as a PET Radioligand for Imaging PD-L1 Expression. *J Nucl Med* **2018,** *59* (3), 529-535.
100. Waldo, G. S.; Standish, B. M.; Berendzen, J.; Terwilliger, T. C., Rapid protein-folding assay using green fluorescent protein. *Nat Biotechnol* **1999,** *17* (7), 691-5.
101. Lipovsek, D., Adnectins: engineered target-binding protein therapeutics. *Protein Eng Des Sel* **2011,** *24* (1-2), 3-9.
102. Xiao, L.; Hung, K. C.; Takahashi, T. T.; Joo, K. I.; Lim, M.; Roberts, R. W.; Wang, P., Antibody-mimetic ligand selected by mRNA display targets DC-SIGN for dendritic cell-directed antigen delivery. *ACS Chem Biol* **2013,** *8* (5), 967-77.
103. Mangan, P. R.; Su, L. J.; Jenny, V.; Tatum, A. L.; Picarillo, C.; Skala, S.; Ditto, N.; Lin, Z.; Yang, X.; Cotter, P. Z.; Shuster, D. J.; Song, Y.; Borowski, V.; Thomas, R. L.; Heimrich, E. M.; Devaux, B.; Das Gupta, R.; Carvajal, I.; McIntyre, K. W.; Xie, J.; Zhao, Q.; Struthers, M.; Salter-Cid, L. M., Dual Inhibition of Interleukin-23 and Interleukin-17 Offers Superior Efficacy in Mouse Models of Autoimmunity. *J Pharmacol Exp Ther* **2015,** *354* (2), 152-65.
104. Stutvoet, T. S.; van der Veen, E. L.; Kol, A.; Antunes, I. F.; de Vries, E. F.; Hospers, G. A.; de Vries, E. G.; de Jong, S.; Lub-de Hooge, M. N., Molecular imaging of PD-L1 expression and dynamics with the adnectin-based PET tracer 18F-BMS-986192. *Journal of Nuclear Medicine* **2020,** *61* (12), 1839-1844.
105. Huisman, M. C.; Niemeijer, A.-L. N.; Windhorst, A. D.; Schuit, R. C.; Leung, D.; Hayes, W.; Poot, A.; Bahce, I.; Radonic, T.; Oprea-Lager, D. E., Quantification of PD-L1 Expression with 18F-BMS-986192 PET/CT in Patients with Advanced-Stage Non–Small Cell Lung Cancer. *Journal of Nuclear Medicine* **2020,** *61* (10), 1455-1460.
106. Robu, S.; Richter, A.; Gosmann, D.; Seidl, C.; Leung, D.; Hayes, W.; Cohen, D.; Morin, P.; Donnelly, D. J.; Lipovšek, D., Synthesis and Preclinical Evaluation of 68Ga-labeled Adnectin, 68Ga-BMS-986192 as a PET Agent for Imaging PD-L1 Expression. *Journal of Nuclear Medicine* **2021**.
107. Wensel, D.; Sun, Y.; Li, Z.; Zhang, S.; Picarillo, C.; McDonagh, T.; Fabrizio, D.; Cockett, M.; Krystal, M.; Davis, J., Discovery and Characterization of a Novel CD4-Binding Adnectin with Potent Anti-HIV Activity. *Antimicrob Agents Chemother* **2017,** *61* (8).
108. Wensel, D.; Sun, Y.; Davis, J.; Li, Z.; Zhang, S.; McDonagh, T.; Fabrizio, D.; Cockett, M.; Krystal, M., A Novel gp41-Binding Adnectin with Potent Anti-HIV Activity Is Highly Synergistic when Linked to a CD4-Binding Adnectin. *J Virol* **2018,** *92* (14).
109. Wensel, D.; Sun, Y.; Davis, J.; Li, Z.; Zhang, S.; McDonagh, T.; Langley, D.; Mitchell, T.; Tabruyn, S.; Nef, P., GSK3732394: a Multi-specific Inhibitor of HIV Entry. *Journal of virology* **2019,** *93* (20).
110. Lipovsek, D.; Carvajal, I.; Allentoff, A. J.; Barros, A., Jr.; Brailsford, J.; Cong, Q.; Cotter, P.; Gangwar, S.; Hollander, C.; Lafont, V.; Lau, W. L.; Li, W.; Moreta, M.; O'Neil, S.; Pinckney, J.; Smith, M. J.; Su, J.; Terragni, C.; Wallace, M. A.; Wang, L.; Wright, M.; Marsh, H. N.; Bryson, J. W., Adnectin-drug conjugates for Glypican-3-specific delivery of a cytotoxic payload to tumors. *Protein Eng Des Sel* **2018,** *31* (5), 159-171.

111. Kondo, T.; Iwatani, Y.; Matsuoka, K.; Fujino, T.; Umemoto, S.; Yokomaku, Y.; Ishizaki, K.; Kito, S.; Sezaki, T.; Hayashi, G., Antibody-like proteins that capture and neutralize SARS-CoV-2. *Science advances* **2020,** *6* (42), eabd3916.
112. Parker, M.; Chen, Y.; Danehy, F.; Dufu, K.; Ekstrom, J.; Getmanova, E.; Gokemeijer, J.; Xu, L.; Lipovsek, D., Antibody mimics based on human fibronectin type three domain engineered for thermostability and high-affinity binding to vascular endothelial growth factor receptor two. *Protein Engineering Design and Selection* **2005,** *18* (9), 435-444.
113. Olson, C. A.; Liao, H.-I.; Sun, R.; Roberts, R. W., mRNA display selection of a high-affinity, modification-specific phospho-IκBα-binding fibronectin. *ACS chemical biology* **2008,** *3* (8), 480-485.
114. Liao, H. I.; Olson, C. A.; Hwang, S.; Deng, H.; Wong, E.; Baric, R. S.; Roberts, R. W.; Sun, R., mRNA display design of fibronectin-based intrabodies that detect and inhibit severe acute respiratory syndrome coronavirus nucleocapsid protein. *The Journal of biological chemistry* **2009,** *284* (26), 17512-20.
115. Olson, C. A.; Adams, J. D.; Takahashi, T. T.; Qi, H.; Howell, S. M.; Wu, T. T.; Roberts, R. W.; Sun, R.; Soh, H. T., Rapid mRNA-Display Selection of an IL-6 Inhibitor Using Continuous-Flow Magnetic Separation. *Angewandte Chemie International Edition* **2011,** *50* (36), 8295-8298.
116. Olson, C. A.; Nie, J.; Diep, J.; Al-Shyoukh, I.; Takahashi, T. T.; Al-Mawsawi, L. Q.; Bolin, J. M.; Elwell, A. L.; Swanson, S.; Stewart, R.; Thomson, J. A.; Soh, H. T.; Roberts, R. W.; Sun, R., Single-round, multiplexed antibody mimetic design through mRNA display. *Angew Chem Int Ed Engl* **2012,** *51* (50), 12449-53.
117. Gross, G. G.; Junge, J. A.; Mora, R. J.; Kwon, H.-B.; Olson, C. A.; Takahashi, T. T.; Liman, E. R.; Ellis-Davies, G. C.; McGee, A. W.; Sabatini, B. L., Recombinant probes for visualizing endogenous synaptic proteins in living neurons. *Neuron* **2013,** *78* (6), 971-985.
118. Mora, R. J.; Roberts, R. W.; Arnold, D. B., Recombinant probes reveal dynamic localization of CaMKIIalpha within somata of cortical neurons. *J Neurosci* **2013,** *33* (36), 14579-90.
119. Cetin, M.; Evenson, W. E.; Gross, G. G.; Jalali-Yazdi, F.; Krieger, D.; Arnold, D.; Takahashi, T. T.; Roberts, R. W., RasIns: genetically encoded intrabodies of activated Ras proteins. *Journal of molecular biology* **2017,** *429* (4), 562-573.
120. Dineen, S. P.; Sullivan, L. A.; Beck, A. W.; Miller, A. F.; Carbon, J. G.; Mamluk, R.; Wong, H.; Brekken, R. A., The Adnectin CT-322 is a novel VEGF receptor 2 inhibitor that decreases tumor burden in an orthotopic mouse model of pancreatic cancer. *BMC cancer* **2008,** *8* (1), 352.
121. Mamluk, R.; Carvajal, I. M.; Morse, B. A.; Wong, H. K.; Abramowitz, J.; Aslanian, S.; Lim, A.-C.; Gokemeijer, J.; Storek, M. J.; Lee, J. In *Anti-tumor effect of CT-322 as an adnectin inhibitor of vascular endothelial growth factor receptor-2*, MAbs, Taylor & Francis: 2010; pp 199-208.
122. Bloom, L.; Calabro, V., FN3: a new protein scaffold reaches the clinic. *Drug discovery today* **2009,** *14* (19-20), 949-955.
123. Tolcher, A. W.; Sweeney, C. J.; Papadopoulos, K.; Patnaik, A.; Chiorean, E. G.; Mita, A. C.; Sankhala, K.; Furfine, E.; Gokemeijer, J.; Iacono, L., Phase I and pharmacokinetic study of CT-322 (BMS-844203), a targeted Adnectin inhibitor of VEGFR-2 based on a domain of human fibronectin. *Clinical Cancer Research* **2011**.
124. Evans, J. B.; Syed, B. A., Next-generation antibodies. Nature Publishing Group: 2014.
125. Schiff, D.; Kesari, S.; de Groot, J.; Mikkelsen, T.; Drappatz, J.; Coyle, T.; Fichtel, L.; Silver, B.; Walters, I.; Reardon, D., Phase 2 study of CT-322, a targeted biologic inhibitor of VEGFR-2 based on a domain of human fibronectin, in recurrent glioblastoma. *Invest New Drugs* **2015,** *33* (1), 247-53.
126. El-Husseini, A. E.; Schnell, E.; Chetkovich, D. M.; Nicoll, R. A.; Bredt, D. S., PSD-95 involvement in maturation of excitatory synapses. *Science* **2000,** *290* (5495), 1364-8.
127. Proba, K.; Worn, A.; Honegger, A.; Pluckthun, A., Antibody scFv fragments without disulfide bonds made by molecular evolution. *J Mol Biol* **1998,** *275* (2), 245-53.
128. Ishikawa, F. N.; Chang, H. K.; Curreli, M.; Liao, H. I.; Olson, C. A.; Chen, P. C.; Zhang, R.; Roberts, R. W.; Sun, R.; Cote, R. J.; Thompson, M. E.; Zhou, C., Label-free, electrical detection of the SARS virus N-protein with nanowire biosensors utilizing antibody mimics as capture probes. *ACS Nano* **2009,** *3* (5), 1219-24.
129. Yushen, D.; Tian-hao, Z.; Xiangzhi, M.; Yuan, S.; Menglong, H.; Shuofeng, Y.; Chit Ying, L.; Shu-xing, L.; Siwei, L.; Jiayan, L.; Haigen, H.; Hong, J.; Dongdong, C.; Li, S.; Mengying, H.; Anders, O.; Hsiang, I. L.; Xiaojiang, C.; Xinmin, L.; Gexin, Z.; Richard, W. R.; Jasper, F. W. C.; Dong-Yan, J.; Irvin, S. Y. C.; Honglin, C.; Kwok-Yung, Y.; Quan, H.; Ren, S., Development of high affinity monobodies recognizing SARS-CoV-2 antigen. *Research Square* **2021**.
130. Koide, S., Engineering of recombinant crystallization chaperones. *Curr Opin Struct Biol* **2009,** *19* (4), 449-57.

131. Son, J. H.; Keefe, M. D.; Stevenson, T. J.; Barrios, J. P.; Anjewierden, S.; Newton, J. B.; Douglass, A. D.; Bonkowsky, J. L., Transgenic FingRs for Live Mapping of Synaptic Dynamics in Genetically-Defined Neurons. *Scientific reports* **2016,** *6*, 18734.
132. Bensussen, S.; Shankar, S.; Ching, K. H.; Zemel, D.; Ta, T. L.; Mount, R. A.; Shroff, S. N.; Gritton, H. J.; Fabris, P.; Vanbenschoten, H.; Beck, C.; Man, H. Y.; Han, X., A Viral Toolbox of Genetically Encoded Fluorescent Synaptic Tags. *iScience* **2020,** *23* (7), 101330.
133. Li, Y.; Junge, J. A.; Arnesano, C.; Gross, G. G.; Miner, J. H.; Moats, R.; Roberts, R. W.; Arnold, D. B.; Fraser, S. E., Discs large 1 controls daughter-cell polarity after cytokinesis in vertebrate morphogenesis. *Proceedings of the National Academy of Sciences of the United States of America* **2018,** *115* (46), E10859-E10868.
134. Fosgerau, K.; Hoffmann, T., Peptide therapeutics: current status and future directions. *Drug discovery today* **2015,** *20* (1), 122-128.
135. Arkin, M. R.; Randal, M.; DeLano, W. L.; Hyde, J.; Luong, T. N.; Oslob, J. D.; Raphael, D. R.; Taylor, L.; Wang, J.; McDowell, R. S., Binding of small molecules to an adaptive protein–protein interface. *Proceedings of the National Academy of Sciences* **2003,** *100* (4), 1603-1608.
136. Conte, L. L.; Chothia, C.; Janin, J., The atomic structure of protein-protein recognition sites. *Journal of molecular biology* **1999,** *285* (5), 2177-2198.
137. Stites, W. E., Protein− protein interactions: interface structure, binding thermodynamics, and mutational analysis. *Chemical reviews* **1997,** *97* (5), 1233-1250.
138. Manning, M. C.; Chou, D. K.; Murphy, B. M.; Payne, R. W.; Katayama, D. S., Stability of protein pharmaceuticals: an update. *Pharmaceutical research* **2010,** *27* (4), 544-575.
139. Larsen, B. D., Pharmacologically active peptide conjugates having a reduced tendency towards enzymatic hydrolysis. Google Patents: 2008.
140. Timmerman, P.; Puijk, W.; Boshuizen, R.; Dijken, P. V.; Slootstra, J.; Beurskens, F.; Parren, P.; Huber, A.; Bachmann, M.; Meloen, R., Functional reconstruction of structurally complex epitopes using CLIPS™ Technology. *The Open Vaccine Journal* **2009,** *2* (1).
141. Sim, S.; Kim, Y.; Kim, T.; Lim, S.; Lee, M., Directional assembly of α-helical peptides induced by cyclization. *Journal of the American Chemical Society* **2012,** *134* (50), 20270-20272.
142. Thurber, G. M.; Schmidt, M. M.; Wittrup, K. D., Antibody tumor penetration: transport opposed by systemic and antigen-mediated clearance. *Advanced drug delivery reviews* **2008,** *60* (12), 1421-34.
143. Ladner, R. C.; Sato, A. K.; Gorzelany, J.; de Souza, M., Phage display-derived peptides as therapeutic alternatives to antibodies. *Drug discovery today* **2004,** *9* (12), 525-529.
144. Li, Z. J.; Cho, C. H. In *Peptides as targeting probes against tumor vasculature for diagnosis and drug delivery*, Journal of translational medicine, BioMed Central: 2012; p S1.
145. Ruoslahti, E., Peptides as targeting elements and tissue penetration devices for nanoparticles. *Advanced Materials* **2012,** *24* (28), 3747-3756.
146. Barrick, J. E.; Takahashi, T. T.; Ren, J.; Xia, T.; Roberts, R. W., Large libraries reveal diverse solutions to an RNA recognition problem. *Proceedings of the National Academy of Sciences* **2001,** *98* (22), 12374-12378.
147. Yan, S.; Niu, R.; Wang, Z.; Lin, X., In vitro selected peptides bind with thymidylate synthase mRNA and inhibit its translation. *Science in China Series C: Life Sciences* **2007,** *50* (5), 630-636.
148. Barrick, J. E.; Roberts, R. W., Sequence analysis of an artificial family of RNA-binding peptides. *Protein Science* **2002,** *11* (11), 2688-2696.
149. Austin, R. J.; Xia, T.; Ren, J.; Takahashi, T. T.; Roberts, R. W., Differential modes of recognition in N peptide− BoxB complexes. *Biochemistry* **2003,** *42* (50), 14957-14967.
150. Austin, R. J.; Xia, T.; Ren, J.; Takahashi, T. T.; Roberts, R. W., Designed arginine-rich RNA-binding peptides with picomolar affinity. *Journal of the American Chemical Society* **2002,** *124* (37), 10966-10967.
151. Kinch, M. S.; Hoyer, D.; Patridge, E.; Plummer, M., Target selection for FDA-approved medicines. *Drug discovery today* **2015,** *20* (7), 784-789.
152. Hauser, A. S.; Attwood, M. M.; Rask-Andersen, M.; Schiöth, H. B.; Gloriam, D. E., Trends in GPCR drug discovery: new agents, targets and indications. *Nature reviews Drug discovery* **2017,** *16* (12), 829.
153. Ja, W. W.; Roberts, R. W., In vitro selection of state-specific peptide modulators of G protein signaling using mRNA display. *Biochemistry* **2004,** *43* (28), 9265-9275.

154. Shiheido, H.; Takashima, H.; Doi, N.; Yanagawa, H., mRNA display selection of an optimized MDM2-binding peptide that potently inhibits MDM2-p53 interaction. *PLoS One* **2011,** *6* (3), e17898.
155. Kobayashi, T.; Kakui, M.; Shibui, T.; Kitano, Y., In vitro selection of a peptide inhibitor of human IL-6 using mRNA display. *Molecular biotechnology* **2011,** *48* (2), 147-155.
156. Flock, T.; Hauser, A. S.; Lund, N.; Gloriam, D. E.; Balaji, S.; Babu, M. M., Selectivity determinants of GPCR–G-protein binding. *Nature* **2017,** *545* (7654), 317-322.
157. Goricanec, D.; Stehle, R.; Egloff, P.; Grigoriu, S.; Plückthun, A.; Wagner, G.; Hagn, F., Conformational dynamics of a G-protein α subunit is tightly regulated by nucleotide binding. *Proceedings of the National Academy of Sciences* **2016,** *113* (26), E3629-E3638.
158. William, W. J.; Roberts, R. W., G-protein-directed ligand discovery with peptide combinatorial libraries. *Trends in biochemical sciences* **2005,** *30* (6), 318-324.
159. William, W. J.; Adhikari, A.; Austin, R. J.; Sprang, S. R.; Roberts, R. W., A peptide core motif for binding to heterotrimeric G protein α subunits. *Journal of Biological Chemistry* **2005,** *280* (37), 32057-32060.
160. Austin, R. J.; William, W. J.; Roberts, R. W., Evolution of class-specific peptides targeting a hot spot of the Gαs subunit. *Journal of molecular biology* **2008,** *377* (5), 1406-1418.
161. Ja, W. W.; Wiser, O.; Austin, R. J.; Jan, L. Y.; Roberts, R. W., Turning G proteins on and off using peptide ligands. *ACS chemical biology* **2006,** *1* (9), 570-574.
162. William, W. J.; West Jr, A. P.; Delker, S. L.; Bjorkman, P. J.; Benzer, S.; Roberts, R. W., Extension of Drosophila melanogaster life span with a GPCR peptide inhibitor. *Nature chemical biology* **2007,** *3* (7), 415.
163. Kamide, K.; Nakakubo, H.; Uno, S.; Fukamizu, A., Isolation of novel cell-penetrating peptides from a random peptide library using in vitro virus and their modifications. *International journal of molecular medicine* **2010,** *25* (1), 41-51.
164. Higa, M.; Katagiri, C.; Shimizu-Okabe, C.; Tsumuraya, T.; Sunagawa, M.; Nakamura, M.; Ishiuchi, S.; Takayama, C.; Kondo, E.; Matsushita, M., Identification of a novel cell-penetrating peptide targeting human glioblastoma cell lines as a cancer-homing transporter. *Biochemical and biophysical research communications* **2015,** *457* (2), 206-212.
165. Lee, J. H.; Song, H. S.; Lee, S. G.; Park, T. H.; Kim, B. G., Screening of cell-penetrating peptides using mRNA display. *Biotechnology journal* **2012,** *7* (3), 387-396.
166. Baggio, R.; Burgstaller, P.; Hale, S. P.; Putney, A. R.; Lane, M.; Lipovsek, D.; Wright, M. C.; Roberts, R. W.; Liu, R.; Szostak, J. W., Identification of epitope-like consensus motifs using mRNA display. *Journal of Molecular Recognition* **2002,** *15* (3), 126-134.
167. Guo, N.; Duan, H.; Kachko, A.; Krause, B. W.; Major, M. E.; Krause, P. R., Reverse Engineering of Vaccine Antigens Using High Throughput Sequencing-enhanced mRNA Display. *EBioMedicine* **2015,** *2* (8), 859-867.
168. Ja, W. W.; Olsen, B. N.; Roberts, R. W., Epitope mapping using mRNA display and a unidirectional nested deletion library. *Protein Engineering Design and Selection* **2005,** *18* (7), 309-319.
169. Shiratori, M.; Kobayashi, T.; Shibui, T., Identification of amino acids essential for antibody binding by mRNA-display using a random peptide library: an anti-human tumor protein p53 antibody as a model. *Molecular biotechnology* **2009,** *41* (2), 99-105.
170. Shibui, T.; Kobayashi, T., Mimotopes to Cetuximab Isolated by mRNA-Display using Random Peptide Libraries and their Characteristics. *International Journal of Peptide Research and Therapeutics* **2011,** *17* (1), 69-74.
171. Duan, H.; Kachko, A.; Zhong, L.; Struble, E.; Pandey, S.; Yan, H.; Harman, C.; Virata-Theimer, M. L.; Deng, L.; Zhao, Z.; Major, M.; Feinstone, S.; Zhang, P., Amino acid residue-specific neutralization and nonneutralization of hepatitis C virus by monoclonal antibodies to the E2 protein. *J Virol* **2012,** *86* (23), 12686-94.
172. Cujec, T. P.; Medeiros, P. F.; Hammond, P.; Rise, C.; Kreider, B. L., Selection of v-abl tyrosine kinase substrate sequences from randomized peptide and cellular proteomic libraries using mRNA display. *Chemistry & biology* **2002,** *9* (2), 253-264.
173. Lee, J. H.; Song, C.; Kim, D. H.; Park, I. H.; Lee, S. G.; Lee, Y. S.; Kim, B. G., Glutamine (Q)-peptide screening for transglutaminase reaction using mRNA display. *Biotechnology and bioengineering* **2013,** *110* (2), 353-362.
174. Fleming, S. R.; Himes, P. M.; Ghodge, S. V.; Goto, Y.; Suga, H.; Bowers, A. A., Exploring the Post-translational Enzymology of PaaA by mRNA Display. *J Am Chem Soc* **2020,** *142* (11), 5024-5028.
175. Vinogradov, A. A.; Nagai, E.; Chang, J. S.; Narumi, K.; Onaka, H.; Goto, Y.; Suga, H., Accurate Broadcasting of Substrate Fitness for Lactazole Biosynthetic Pathway from Reactivity-Profiling mRNA Display. *J Am Chem Soc* **2020**.
176. Hanahan, D.; Weinberg, R. A., Hallmarks of cancer: the next generation. *Cell* **2011,** *144* (5), 646-74.

177. Kamalinia, G.; Engel, B. J.; Srinivasamani, A.; Grindel, B. J.; Ong, J. N.; Curran, M. A.; Takahashi, T. T.; Millward, S. W.; Roberts, R. W., mRNA Display Discovery of a Novel Programmed Death Ligand 1 (PD-L1) Binding Peptide (a Peptide Ligand for PD-L1). *ACS Chem Biol* **2020,** *15* (6), 1630-1641.
178. Nagata, T.; Shirakawa, K.; Kobayashi, N.; Shiheido, H.; Tabata, N.; Sakuma-Yonemura, Y.; Horisawa, K.; Katahira, M.; Doi, N.; Yanagawa, H., Structural basis for inhibition of the MDM2: p53 interaction by an optimized MDM2-binding peptide selected with mRNA display. *PloS one* **2014,** *9* (10), e109163.
179. Jalali-Yazdi, F.; Lai, L. H.; Takahashi, T. T.; Roberts, R. W., High-Throughput Measurement of Binding Kinetics by mRNA Display and Next-Generation Sequencing. *Angew Chem Int Ed Engl* **2016,** *55* (12), 4007-10.
180. Kawakami, T.; Ogawa, K.; Goshima, N.; Natsume, T., DIVERSE System: De Novo Creation of Peptide Tags for Non-enzymatic Covalent Labeling by In Vitro Evolution for Protein Imaging Inside Living Cells. *Chem Biol* **2015,** *22* (12), 1671-9.
181. Evans, E. D.; Pentelute, B. L., Discovery of a 29-Amino-Acid Reactive Abiotic Peptide for Selective Cysteine Arylation. *ACS Chem Biol* **2018,** *13* (3), 527-532.
182. Evans, E. D.; Pentelute, B. L., Studies on a landscape of perfluoroaromatic-reactive peptides. *Organic & biomolecular chemistry* **2019,** *17* (7), 1862-1868.
183. Ando, T.; Takamori, Y.; Yokoyama, T.; Yamamoto, M.; Kawakami, T., Directed evolution of dibenzocyclooctyne-reactive peptide tags for protein labeling. *Biochem Biophys Res Commun* **2021,** *534*, 27-33.
184. Terai, T.; Anzai, H.; Nemoto, N., Selection of Peptides that Associate with Dye-Conjugated Solid Surfaces in a pH-Dependent Manner Using cDNA Display. *ACS Omega* **2019,** *4* (4), 7378-7384.
185. Ono, S.; Tsuji, T.; Oaki, Y.; Imai, H., Artificial peptides binding to the c face of hydroxyapatite obtained by molecular display technology. *RSC Advances* **2013,** *3* (6), 1885-1889.
186. Kobayashi, S.; Terai, T.; Yoshikawa, Y.; Ohkawa, R.; Ebihara, M.; Hayashi, M.; Takiguchi, K.; Nemoto, N., In vitro selection of random peptides against artificial lipid bilayers: A potential tool to immobilize molecules on membranes. *Chemical Communications* **2017,** *53* (24), 3458-3461.
187. Raffler, N. A.; Schneider-Mergener, J.; Famulok, M., A novel class of small functional peptides that bind and inhibit human α-thrombin isolated by mRNA display. *Chemistry & biology* **2003,** *10* (1), 69-79.
188. Yiadom, K. P.; Muhie, S.; Yang, D. C., Peptide inhibitors of botulinum neurotoxin by mRNA display. *Biochemical and biophysical research communications* **2005,** *335* (4), 1247-1253.
189. Matsumura, N.; Tsuji, T.; Sumida, T.; Kokubo, M.; Onimaru, M.; Doi, N.; Takashima, H.; Miyamoto-Sato, E.; Yanagawa, H., mRNA display selection of a high-affinity, Bcl-XL-specific binding peptide. *The FASEB Journal* **2010,** *24* (7), 2201-2210.
190. Thell, K.; Hellinger, R.; Schabbauer, G.; Gruber, C. W., Immunosuppressive peptides and their therapeutic applications. *Drug discovery today* **2014,** *19* (5), 645-653.
191. Hancock, R. E.; Chapple, D. S., Peptide antibiotics. *Antimicrobial agents and chemotherapy* **1999,** *43* (6), 1317-1323.
192. Chatterjee, J.; Laufer, B.; Kessler, H., Synthesis of N-methylated cyclic peptides. *Nature protocols* **2012,** *7* (3), 432.
193. Ovadia, O.; Greenberg, S.; Chatterjee, J.; Laufer, B.; Opperer, F.; Kessler, H.; Gilon, C.; Hoffman, A., The effect of multiple N-methylation on intestinal permeability of cyclic hexapeptides. *Molecular pharmaceutics* **2011,** *8* (2), 479-487.
194. Yamagishi, Y.; Shoji, I.; Miyagawa, S.; Kawakami, T.; Katoh, T.; Goto, Y.; Suga, H., Natural product-like macrocyclic N-methyl-peptide inhibitors against a ubiquitin ligase uncovered from a ribosome-expressed de novo library. *Chemistry & biology* **2011,** *18* (12), 1562-1570.
195. Khan, A. R.; Parrish, J. C.; Fraser, M. E.; Smith, W. W.; Bartlett, P. A.; James, M. N. G., Lowering the Entropic Barrier for Binding Conformationally Flexible Inhibitors to Enzymes. *Biochemistry* **1998,** *37* (48), 16839-16845.
196. Josephson, K.; Ricardo, A.; Szostak, J. W., mRNA display: from basic principles to macrocycle drug discovery. *Drug Discovery Today* **2014,** *19* (4), 388-399.
197. Dougherty, P. G.; Sahni, A.; Pei, D., Understanding Cell Penetration of Cyclic Peptides. *Chem Rev* **2019,** *119* (17), 10241-10287.
198. Heckler, T. G.; Chang, L. H.; Zama, Y.; Naka, T.; Chorghade, M. S.; Hecht, S. M., T4 RNA ligase mediated preparation of novel "chemically misacylated" tRNAPheS. *Biochemistry* **1984,** *23* (7), 1468-73.
199. Noren, C.; Anthony-Cahill, S.; Griffith, M.; Schultz, P., A general method for site-specific incorporation of unnatural amino acids into proteins. *Science* **1989,** *244* (4901), 182-188.

200. Li, S.; Millward, S.; Roberts, R., In vitro selection of mRNA display libraries containing an unnatural amino acid. *J Am Chem Soc* **2002,** *124* (34), 9972-3.
201. Saks, M. E.; Sampson, J. R.; Nowak, M. W.; Kearney, P. C.; Du, F.; Abelson, J. N.; Lester, H. A.; Dougherty, D. A., An engineered Tetrahymena tRNAGln for in vivo incorporation of unnatural amino acids into proteins by nonsense suppression. *The Journal of biological chemistry* **1996,** *271* (38), 23169-75.
202. Muranaka, N.; Hohsaka, T.; Sisido, M., Four-base codon mediated mRNA display to construct peptide libraries that contain multiple nonnatural amino acids. *Nucleic acids research* **2006,** *34* (1), e7.
203. Johnson, D. B.; Xu, J.; Shen, Z.; Takimoto, J. K.; Schultz, M. D.; Schmitz, R. J.; Xiang, Z.; Ecker, J. R.; Briggs, S. P.; Wang, L., RF1 knockout allows ribosomal incorporation of unnatural amino acids at multiple sites. *Nature chemical biology* **2011,** *7* (11), 779-786.
204. Frankel, A.; Millward, S. W.; Roberts, R. W., Encodamers: unnatural peptide oligomers encoded in RNA. *Chem Biol* **2003,** *10* (11), 1043-50.
205. Murakami, H.; Ohta, A.; Ashigai, H.; Suga, H., A highly flexible tRNA acylation method for non-natural polypeptide synthesis. *Nat Methods* **2006,** *3* (5), 357-9.
206. Murakami, H.; Saito, H.; Suga, H., A versatile tRNA aminoacylation catalyst based on RNA. *Chem Biol* **2003,** *10* (7), 655-62.
207. Ohuchi, M.; Murakami, H.; Suga, H., The flexizyme system: a highly flexible tRNA aminoacylation tool for the translation apparatus. *Curr Opin Chem Biol* **2007,** *11* (5), 537-42.
208. Goto, Y.; Katoh, T.; Suga, H., Flexizymes for genetic code reprogramming. *Nat Protoc* **2011,** *6* (6), 779-90.
209. Niwa, N.; Yamagishi, Y.; Murakami, H.; Suga, H., A flexizyme that selectively charges amino acids activated by a water-friendly leaving group. *Bioorg Med Chem Lett* **2009,** *19* (14), 3892-4.
210. Hipolito, C. J.; Suga, H., Ribosomal production and in vitro selection of natural product-like peptidomimetics: the FIT and RaPID systems. *Curr Opin Chem Biol* **2012,** *16* (1-2), 196-203.
211. Shimizu, Y.; Inoue, A.; Tomari, Y.; Suzuki, T.; Yokogawa, T.; Nishikawa, K.; Ueda, T., Cell-free translation reconstituted with purified components. *Nat Biotech* **2001,** *19* (8), 751-755.
212. Forster, A. C.; Cornish, V. W.; Blacklow, S. C., Pure translation display. *Analytical biochemistry* **2004,** *333* (2), 358-364.
213. Tan, Z.; Blacklow, S. C.; Cornish, V. W.; Forster, A. C., De novo genetic codes and pure translation display. *Methods* **2005,** *36* (3), 279-290.
214. Forster, A. C.; Tan, Z.; Nalam, M. N.; Lin, H.; Qu, H.; Cornish, V. W.; Blacklow, S. C., Programming peptidomimetic syntheses by translating genetic codes designed de novo. *Proceedings of the National Academy of Sciences* **2003,** *100* (11), 6353-6357.
215. Zhang, B.; Tan, Z.; Dickson, L. G.; Nalam, M. N.; Cornish, V. W.; Forster, A. C., Specificity of translation for N-alkyl amino acids. *Journal of the American Chemical Society* **2007,** *129* (37), 11316-11317.
216. Guillen Schlippe, Y. V.; Hartman, M. C. T.; Josephson, K.; Szostak, J. W., In Vitro Selection of Highly Modified Cyclic Peptides That Act as Tight Binding Inhibitors. *Journal of the American Chemical Society* **2012,** *134* (25), 10469-10477.
217. Hartman, M. C.; Josephson, K.; Szostak, J. W., Enzymatic aminoacylation of tRNA with unnatural amino acids. *Proceedings of the National Academy of Sciences of the United States of America* **2006,** *103* (12), 4356-61.
218. Josephson, K.; Hartman, M. C.; Szostak, J. W., Ribosomal synthesis of unnatural peptides. *J Am Chem Soc* **2005,** *127* (33), 11727-35.
219. Hartman, M. C.; Josephson, K.; Lin, C. W.; Szostak, J. W., An expanded set of amino acid analogs for the ribosomal translation of unnatural peptides. *PLoS One* **2007,** *2* (10), e972.
220. Subtelny, A. O.; Hartman, M. C.; Szostak, J. W., Ribosomal synthesis of N-methyl peptides. *J Am Chem Soc* **2008,** *130* (19), 6131-6.
221. Liu, C. C.; Schultz, P. G., Adding new chemistries to the genetic code. *Annu Rev Biochem* **2010,** *79*, 413-44.
222. Li, S.; Roberts, R. W., A Novel Strategy for In Vitro Selection of Peptide-Drug Conjugates. *Chemistry & biology* **2003,** *10* (3), 233-239.
223. Morimoto, J.; Hayashi, Y.; Suga, H., Discovery of Macrocyclic Peptides Armed with a Mechanism-Based Warhead: Isoform-Selective Inhibition of Human Deacetylase SIRT2. *Angewandte Chemie International Edition* **2012,** *51* (14), 3423-3427.

224. Horiya, S.; Bailey, J. K.; Temme, J. S.; Guillen Schlippe, Y. V.; Krauss, I. J., Directed evolution of multivalent glycopeptides tightly recognized by HIV antibody 2G12. *J Am Chem Soc* **2014,** *136* (14), 5407-15.
225. Millward, S. W.; Takahashi, T. T.; Roberts, R. W., A general route for post-translational cyclization of mRNA display libraries. *J Am Chem Soc* **2005,** *127* (41), 14142-3.
226. O'Neil, K. T.; Hoess, R. H.; Jackson, S. A.; Ramachandran, N. S.; Mousa, S. A.; DeGrado, W. F., Identification of novel peptide antagonists for GPIIb/IIIa from a conformationally constrained phage peptide library. *Proteins* **1992,** *14* (4), 509-15.
227. Engel, B. J.; Grindel, B. J.; Gray, J. P.; Millward, S. W., Purification of poly-dA oligonucleotides and mRNA-protein fusions with dT25-OAS resin. *Bioorg Med Chem Lett* **2020,** *30* (4), 126934.
228. Sau, S. P.; Larsen, A. C.; Chaput, J. C., Automated solid-phase synthesis of high capacity oligo-dT cellulose for affinity purification of poly-A tagged biomolecules. *Bioorg Med Chem Lett* **2014,** *24* (24), 5692-5694.
229. Menegatti, S.; Hussain, M.; Naik, A. D.; Carbonell, R. G.; Rao, B. M., mRNA display selection and solid-phase synthesis of Fc-binding cyclic peptide affinity ligands. *Biotechnol Bioeng* **2013,** *110* (3), 857-70.
230. Bacon, K.; Bowen, J.; Reese, H.; Rao, B. M.; Menegatti, S., Use of Target-Displaying Magnetized Yeast in Screening mRNA-Display Peptide Libraries to Identify Ligands. *ACS Comb Sci* **2020,** *22* (12), 738-744.
231. Bowen, J.; Schloop, A. E.; Reeves, G. T.; Menegatti, S.; Rao, B. M., Discovery of Membrane-Permeating Cyclic Peptides via mRNA Display. *Bioconjugate chemistry* **2020,** *31* (10), 2325-2338.
232. Timmerman, P.; Beld, J.; Puijk, W. C.; Meloen, R. H., Rapid and quantitative cyclization of multiple peptide loops onto synthetic scaffolds for structural mimicry of protein surfaces. *Chembiochem* **2005,** *6* (5), 821-4.
233. Iqbal, E. S.; Richardson, S. L.; Abrigo, N. A.; Dods, K. K.; Osorio Franco, H. E.; Gerrish, H. S.; Kotapati, H. K.; Morgan, I. M.; Masterson, D. S.; Hartman, M. C. T., A new strategy for the in vitro selection of stapled peptide inhibitors by mRNA display. *Chem Commun (Camb)* **2019,** *55* (61), 8959-8962.
234. Seebeck, F. P.; Szostak, J. W., Ribosomal synthesis of dehydroalanine-containing peptides. *J Am Chem Soc* **2006,** *128* (22), 7150-1.
235. Hofmann, F. T.; Szostak, J. W.; Seebeck, F. P., In vitro selection of functional lantipeptides. *J Am Chem Soc* **2012,** *134* (19), 8038-41.
236. Ito, K.; Sakai, K.; Suzuki, Y.; Ozawa, N.; Hatta, T.; Natsume, T.; Matsumoto, K.; Suga, H., Artificial human Met agonists based on macrocycle scaffolds. *Nature communications* **2015,** *6* (1), 1-12.
237. Kawakami, T.; Ishizawa, T.; Fujino, T.; Reid, P. C.; Suga, H.; Murakami, H., In Vitro Selection of Multiple Libraries Created by Genetic Code Reprogramming To Discover Macrocyclic Peptides That Antagonize VEGFR2 Activity in Living Cells. *ACS Chemical Biology* **2013,** *8* (6), 1205-1214.
238. Hayashi, Y.; Morimoto, J.; Suga, H., In Vitro Selection of Anti-Akt2 Thioether-Macrocyclic Peptides Leading to Isoform-Selective Inhibitors. *ACS Chemical Biology* **2012,** *7* (3), 607-613.
239. Hipolito, C.; Tanaka, Y.; Katoh, T.; Nureki, O.; Suga, H., A Macrocyclic Peptide that Serves as a Cocrystallization Ligand and Inhibits the Function of a MATE Family Transporter. *Molecules* **2013,** *18* (9), 10514.
240. Zhang, Z.; Gao, R.; Hu, Q.; Peacock, H.; Peacock, D. M.; Dai, S.; Shokat, K. M.; Suga, H., GTP-State-Selective Cyclic Peptide Ligands of K-Ras(G12D) Block Its Interaction with Raf. *ACS Cent Sci* **2020,** *6* (10), 1753-1761.
241. Bashiruddin, N. K.; Hayashi, M.; Nagano, M.; Wu, Y.; Matsunaga, Y.; Takagi, J.; Nakashima, T.; Suga, H., Development of cyclic peptides with potent in vivo osteogenic activity through RaPID-based affinity maturation. *Proceedings of the National Academy of Sciences of the United States of America* **2020,** *117* (49), 31070-31077.
242. Okuma, R.; Kuwahara, T.; Yoshikane, T.; Watanabe, M.; Dranchak, P.; Inglese, J.; Shuto, S.; Goto, Y.; Suga, H., A Macrocyclic Peptide Library with a Structurally Constrained Cyclopropane-containing Building Block Leads to Thiol-independent Inhibitors of Phosphoglycerate Mutase. *Chem Asian J* **2020,** *15* (17), 2631-2636.
243. Norman, A.; Franck, C.; Christie, M.; Hawkins, P. M. E.; Patel, K.; Ashhurst, A. S.; Aggarwal, A.; Low, J. K. K.; Siddiquee, R.; Ashley, C. L.; Steain, M.; Triccas, J. A.; Turville, S.; Mackay, J. P.; Passioura, T.; Payne, R. J., Discovery of Cyclic Peptide Ligands to the SARS-CoV-2 Spike Protein using mRNA Display. *bioRxiv* **2020**, 2020.12.22.424069.
244. Takatsuji, R.; Shinbara, K.; Katoh, T.; Goto, Y.; Passioura, T.; Yajima, R.; Komatsu, Y.; Suga, H., Ribosomal Synthesis of Backbone-Cyclic Peptides Compatible with In Vitro Display. *J Am Chem Soc* **2019,** *141* (6), 2279-2287.
245. Heinis, C.; Rutherford, T.; Freund, S.; Winter, G., Phage-encoded combinatorial chemical libraries based on bicyclic peptides. *Nat Chem Biol* **2009,** *5* (7), 502-7.

246. Hacker, D. E.; Hoinka, J.; Iqbal, E. S.; Przytycka, T. M.; Hartman, M. C., Highly constrained bicyclic scaffolds for the discovery of protease-stable peptides via mRNA display. *ACS chemical biology* **2017,** *12* (3), 795-804.
247. Millward, S. W.; Fiacco, S.; Austin, R. J.; Roberts, R. W., Design of cyclic peptides that bind protein surfaces with antibody-like affinity. *ACS Chem Biol* **2007,** *2* (9), 625-34.
248. Chu, Q.; Moellering, R. E.; Hilinski, G. J.; Kim, Y.-W.; Grossmann, T. N.; Yeh, J. T. H.; Verdine, G. L., Towards understanding cell penetration by stapled peptides. *MedChemComm* **2015,** *6* (1), 111-119.
249. Gray, J. P.; Uddin, M. N.; Chaudhari, R.; Sutton, M. N.; Yang, H.; Rask, P.; Locke, H.; Engel, B. J.; Batistatou, N.; Wang, J.; Grindel, B. J.; Bhattacharya, P.; Gammon, S. T.; Zhang, S.; Piwnica-Worms, D.; Kritzer, J. A.; Lu, Z.; Bast, R. C.; Millward, S. W., Directed evolution of cyclic peptides for inhibition of autophagy. *Chemical Science* **2021,** *12* (10), 3526-3543.
250. Peraro, L.; Deprey, K. L.; Moser, M. K.; Zou, Z.; Ball, H. L.; Levine, B.; Kritzer, J. A., Cell Penetration Profiling Using the Chloroalkane Penetration Assay. *J Am Chem Soc* **2018,** *140* (36), 11360-11369.
251. Nitsche, C.; Passioura, T.; Varava, P.; Mahawaththa, M. C.; Leuthold, M. M.; Klein, C. D.; Suga, H.; Otting, G., De Novo Discovery of Nonstandard Macrocyclic Peptides as Noncompetitive Inhibitors of the Zika Virus NS2B-NS3 Protease. *ACS Med Chem Lett* **2019,** *10* (2), 168-174.
252. Johansen-Leete, J.; Passioura, T.; Foster, S. R.; Bhusal, R. P.; Ford, D. J.; Liu, M.; Jongkees, S. A. K.; Suga, H.; Stone, M. J.; Payne, R. J., Discovery of Potent Cyclic Sulfopeptide Chemokine Inhibitors via Reprogrammed Genetic Code mRNA Display. *J Am Chem Soc* **2020,** *142* (20), 9141-9146.
253. Katoh, T.; Sengoku, T.; Hirata, K.; Ogata, K.; Suga, H., Ribosomal synthesis and de novo discovery of bioactive foldamer peptides containing cyclic beta-amino acids. *Nat Chem* **2020,** *12* (11), 1081-1088.
254. Howard, J. F., Jr.; Nowak, R. J.; Wolfe, G. I.; Freimer, M. L.; Vu, T. H.; Hinton, J. L.; Benatar, M.; Duda, P. W.; MacDougall, J. E.; Farzaneh-Far, R.; Kaminski, H. J.; Zilucoplan, M. G. S. G.; Barohn, R.; Dimachkie, M.; Pasnoor, M.; Farmakidis, C.; Liu, T.; Colgan, S.; Benatar, M. G.; Bertorini, T.; Pillai, R.; Henegar, R.; Bromberg, M.; Gibson, S.; Janecki, T.; Freimer, M.; Elsheikh, B.; Matisak, P.; Genge, A.; Guidon, A.; David, W.; Habib, A. A.; Mathew, V.; Mozaffar, T.; Hinton, J. L.; Hewitt, W.; Barnett, D.; Sullivan, P.; Ho, D.; Howard, J. F., Jr.; Traub, R. E.; Chopra, M.; Kaminski, H. J.; Aly, R.; Bayat, E.; Abu-Rub, M.; Khan, S.; Lange, D.; Holzberg, S.; Khatri, B.; Lindman, E.; Olapo, T.; Sershon, L. M.; Lisak, R. P.; Bernitsas, E.; Jia, K.; Malik, R.; Lewis-Collins, T. D.; Nicolle, M.; Nowak, R. J.; Sharma, A.; Roy, B.; Nye, J.; Pulley, M.; Berger, A.; Shabbir, Y.; Sachdev, A.; Patterson, K.; Siddiqi, Z.; Sivak, M.; Bratton, J.; Small, G.; Kohli, A.; Fetter, M.; Vu, T.; Lam, L.; Harvey, B.; Wolfe, G. I.; Silvestri, N.; Patrick, K.; Zakalik, K.; Duda, P. W.; MacDougall, J.; Farzaneh-Far, R.; Pontius, A.; Hoarty, M., Clinical Effects of the Self-administered Subcutaneous Complement Inhibitor Zilucoplan in Patients With Moderate to Severe Generalized Myasthenia Gravis: Results of a Phase 2 Randomized, Double-Blind, Placebo-Controlled, Multicenter Clinical Trial. *JAMA Neurol* **2020,** *77* (5), 582-592.
255. Modulation of complement activity.
256. Gorman, D. M.; Lee, J.; Payne, C. D.; Woodruff, T. M.; Clark, R. J., Chemical synthesis and characterisation of the complement C5 inhibitory peptide zilucoplan. *Amino Acids* **2021,** *53* (1), 143-147.
257. Tanaka, Y.; Hipolito, C. J.; Maturana, A. D.; Ito, K.; Kuroda, T.; Higuchi, T.; Katoh, T.; Kato, H. E.; Hattori, M.; Kumazaki, K., Structural basis for the drug extrusion mechanism by a MATE multidrug transporter. *Nature* **2013,** *496* (7444), 247-251.
258. Bahng, N.; Ito, K.; Ha, S.; Kim, M. Y.; Lee, E.; Suga, H.; Lee, D. S., In vivo targeting of c-Met using a non-standard macrocyclic peptide in gastric carcinoma. *Cancer letters* **2017,** *385*, 144-149.
259. Iwasaki, K.; Goto, Y.; Katoh, T.; Yamashita, T.; Kaneko, S.; Suga, H., A fluorescent imaging probe based on a macrocyclic scaffold that binds to cellular EpCAM. *Journal of molecular evolution* **2015,** *81* (5-6), 210-217.
260. Matsunaga, Y.; Bashiruddin, N. K.; Kitago, Y.; Takagi, J.; Suga, H., Allosteric inhibition of a semaphorin 4D receptor plexin B1 by a high-affinity macrocyclic peptide. *Cell chemical biology* **2016,** *23* (11), 1341-1350.
261. Jongkees, S. A.; Caner, S.; Tysoe, C.; Brayer, G. D.; Withers, S. G.; Suga, H., Rapid discovery of potent and selective glycosidase-inhibiting de novo peptides. *Cell chemical biology* **2017,** *24* (3), 381-390.
262. Passioura, T.; Bhushan, B.; Tumber, A.; Kawamura, A.; Suga, H., Structure-activity studies of a macrocyclic peptide inhibitor of histone lysine demethylase 4A. *Bioorganic & medicinal chemistry* **2018,** *26* (6), 1225-1231.
263. Rogers, J. M.; Nawatha, M.; Lemma, B.; Vamisetti, G. B.; Livneh, I.; Barash, U.; Vlodavsky, I.; Ciechanover, A.; Fushman, D.; Suga, H.; Brik, A., In vivo modulation of ubiquitin chains by N-methylated non-proteinogenic cyclic peptides. *RSC Chemical Biology* **2021**.

264. Hacker, D. E.; Abrigo, N. A.; Hoinka, J.; Richardson, S. L.; Przytycka, T. M.; Hartman, M. C. T., Direct, Competitive Comparison of Linear, Monocyclic, and Bicyclic Libraries Using mRNA Display. *ACS Comb Sci* **2020,** *22* (6), 306-310.
265. Alleyne, C.; Amin, R. P.; Bhatt, B.; Bianchi, E.; Blain, J. C.; Boyer, N.; Branca, D.; Embrey, M. W.; Ha, S. N.; Jette, K.; Johns, D. G.; Kerekes, A. D.; Koeplinger, K. A.; LaPlaca, D.; Li, N.; Murphy, B.; Orth, P.; Ricardo, A.; Salowe, S.; Seyb, K.; Shahripour, A.; Stringer, J. R.; Sun, Y.; Tracy, R.; Wu, C.; Xiong, Y.; Youm, H.; Zokian, H. J.; Tucker, T. J., Series of Novel and Highly Potent Cyclic Peptide PCSK9 Inhibitors Derived from an mRNA Display Screen and Optimized via Structure-Based Design. *J Med Chem* **2020,** *63* (22), 13796-13824.
266. Haviv, F.; Fitzpatrick, T. D.; Swenson, R. E.; Nichols, C. J.; Mort, N. A.; Bush, E. N.; Diaz, G.; Bammert, G.; Nguyen, A.; Rhutasel, N. S.; et al., Effect of N-methyl substitution of the peptide bonds in luteinizing hormone-releasing hormone agonists. *J Med Chem* **1993,** *36* (3), 363-9.
267. Ostresh, J. M.; Husar, G. M.; Blondelle, S. E.; Dorner, B.; Weber, P. A.; Houghten, R. A., "Libraries from libraries": chemical transformation of combinatorial libraries to extend the range and repertoire of chemical diversity. *Proceedings of the National Academy of Sciences of the United States of America* **1994,** *91* (23), 11138-42.
268. van de Watering, F. C.; Rijpkema, M.; Perk, L.; Brinkmann, U.; Oyen, W. J.; Boerman, O. C., Zirconium-89 labeled antibodies: a new tool for molecular imaging in cancer patients. *Biomed Res Int* **2014,** *2014*, 203601.
269. Vaickus, L.; Foon, K. A., Biotechnology Update: Overview of Monoclonal Antibodies in the Diagnosis and Therapy of Cancer. *Cancer investigation* **1991,** *9* (2), 195-209.
270. De Silva, R. A.; Kumar, D.; Lisok, A.; Chatterjee, S.; Wharram, B.; Venkateswara Rao, K.; Mease, R.; Dannals, R. F.; Pomper, M. G.; Nimmagadda, S., Peptide-Based (68)Ga-PET Radiotracer for Imaging PD-L1 Expression in Cancer. *Mol Pharm* **2018,** *15* (9), 3946-3952.
271. Kumar, D.; Lisok, A.; Dahmane, E.; McCoy, M.; Shelake, S.; Chatterjee, S.; Allaj, V.; Sysa-Shah, P.; Wharram, B.; Lesniak, W. G.; Tully, E.; Gabrielson, E.; Jaffee, E. M.; Poirier, J. T.; Rudin, C. M.; Gobburu, J. V.; Pomper, M. G.; Nimmagadda, S., Peptide-based PET quantifies target engagement of PD-L1 therapeutics. *J Clin Invest* **2019,** *129* (2), 616-630.
272. Chatterjee, S.; Lesniak, W. G.; Miller, M. S.; Lisok, A.; Sikorska, E.; Wharram, B.; Kumar, D.; Gabrielson, M.; Pomper, M. G.; Gabelli, S. B.; Nimmagadda, S., Rapid PD-L1 detection in tumors with PET using a highly specific peptide. *Biochem Biophys Res Commun* **2017,** *483* (1), 258-263.
273. Shaabani, S.; Huizinga, H. P. S.; Butera, R.; Kouchi, A.; Guzik, K.; Magiera-Mularz, K.; Holak, T. A.; Domling, A., A patent review on PD-1/PD-L1 antagonists: small molecules, peptides, and macrocycles (2015-2018). *Expert Opin Ther Pat* **2018,** *28* (9), 665-678.
274. Magiera-Mularz, K.; Skalniak, L.; Zak, K. M.; Musielak, B.; Rudzinska-Szostak, E.; Berlicki, L.; Kocik, J.; Grudnik, P.; Sala, D.; Zarganes-Tzitzikas, T.; Shaabani, S.; Domling, A.; Dubin, G.; Holak, T. A., Bioactive Macrocyclic Inhibitors of the PD-1/PD-L1 Immune Checkpoint. *Angew Chem Int Ed Engl* **2017,** *56* (44), 13732-13735.
275. Pisaneschi, F.; Kelderhouse, L. E.; Hardy, A.; Engel, B. J.; Mukhopadhyay, U.; Gonzalez-Lepera, C.; Gray, J. P.; Ornelas, A.; Takahashi, T. T.; Roberts, R. W.; Fiacco, S. V.; Piwnica-Worms, D.; Millward, S. W., Automated, Resin-Based Method to Enhance the Specific Activity of Fluorine-18 Clicked PET Radiotracers. *Bioconjugate chemistry* **2017,** *28* (2), 583-589.
276. Takahashi, T. T.; Roberts, R. W., In vitro selection of protein and peptide libraries using mRNA display. In *Nucleic Acid and Peptide Aptamers*, Springer: 2009; pp 293-314.
277. Seelig, B., mRNA display for the selection and evolution of enzymes from in vitro-translated protein libraries. *Nat Protoc* **2011,** *6* (4), 540-52.
278. Barendt, P. A.; Ng, D. T.; McQuade, C. N.; Sarkar, C. A., Streamlined protocol for mRNA display. *ACS Comb Sci* **2013,** *15* (2), 77-81.
279. Arai, H.; Kumachi, S.; Nemoto, N., cDNA Display: A Stable and Simple Genotype-Phenotype Coupling Using a Cell-Free Translation System. *Methods Mol Biol* **2020,** *2070*, 43-56.
280. Nemoto, N.; Kumachi, S.; Arai, H., In Vitro Selection of Single-Domain Antibody (VHH) Using cDNA Display. *Methods Mol Biol* **2018,** *1827*, 269-285.
281. Yamamoto, Y.; Terai, T.; Kumachi, S.; Nemoto, N., In Vitro Construction of Large-scale DNA Libraries from Fragments Containing Random Regions using Deoxyinosine-containing Oligonucleotides and Endonuclease V. *ACS Comb Sci* **2020,** *22* (4), 165-171.

282. Tsao, K. L.; DeBarbieri, B.; Michel, H.; Waugh, D. S., A versatile plasmid expression vector for the production of biotinylated proteins by site-specific, enzymatic modification in Escherichia coli. *Gene* **1996,** *169* (1), 59-64.
283. Grindel, B. J.; Engel, B. J.; Hall, C. G.; Kelderhouse, L. E.; Lucci, A.; Zacharias, N. M.; Takahashi, T. T.; Millward, S. W., Mammalian Expression and In Situ Biotinylation of Extracellular Protein Targets for Directed Evolution. *ACS Omega* **2020,** *5* (39), 25440-25455.
284. Boder, E. T.; Midelfort, K. S.; Wittrup, K. D., Directed evolution of antibody fragments with monovalent femtomolar antigen-binding affinity. *Proceedings of the National Academy of Sciences of the United States of America* **2000,** *97* (20), 10701-5.
285. Evenson, W. E.; Lin, W. S.; Pang, K.; Czaja, A. T.; Jalali-Yazdi, F.; Takahashi, T. T.; Malmstadt, N.; Roberts, R. W., Enabling Flow-Based Kinetic Off-Rate Selections Using a Microfluidic Enrichment Device. *Anal Chem* **2020,** *92* (15), 10218-10222.
286. Jalali-Yazdi, F.; Corbin, J. M.; Takahashi, T. T.; Roberts, R. W., Robust, quantitative analysis of proteins using peptide immunoreagents, in vitro translation, and an ultrasensitive acoustic resonant sensor. *Anal Chem* **2014,** *86* (10), 4715-22.
287. Larsen, A. C.; Gillig, A.; Shah, P.; Sau, S. P.; Fenton, K. E.; Chaput, J. C., General approach for characterizing in vitro selected peptides with protein binding affinity. *Analytical chemistry* **2014,** *86* (15), 7219-7223.
288. Duarte, J. G.; Blackburn, J. M., Advances in the development of human protein microarrays. *Expert Rev Proteomics* **2017,** *14* (7), 627-641.
289. Weng, S.; Gu, K.; Hammond, P. W.; Lohse, P.; Rise, C.; Wagner, R. W.; Wright, M. C.; Kuimelis, R. G., Generating addressable protein microarrays with PROfusion covalent mRNA-protein fusion technology. *Proteomics* **2002,** *2* (1), 48-57.
290. Bentley, D. R.; Balasubramanian, S.; Swerdlow, H. P.; Smith, G. P.; Milton, J.; Brown, C. G.; Hall, K. P.; Evers, D. J.; Barnes, C. L.; Bignell, H. R.; Boutell, J. M.; Bryant, J.; Carter, R. J.; Keira Cheetham, R.; Cox, A. J.; Ellis, D. J.; Flatbush, M. R.; Gormley, N. A.; Humphray, S. J.; Irving, L. J.; Karbelashvili, M. S.; Kirk, S. M.; Li, H.; Liu, X.; Maisinger, K. S.; Murray, L. J.; Obradovic, B.; Ost, T.; Parkinson, M. L.; Pratt, M. R.; Rasolonjatovo, I. M.; Reed, M. T.; Rigatti, R.; Rodighiero, C.; Ross, M. T.; Sabot, A.; Sankar, S. V.; Scally, A.; Schroth, G. P.; Smith, M. E.; Smith, V. P.; Spiridou, A.; Torrance, P. E.; Tzonev, S. S.; Vermaas, E. H.; Walter, K.; Wu, X.; Zhang, L.; Alam, M. D.; Anastasi, C.; Aniebo, I. C.; Bailey, D. M.; Bancarz, I. R.; Banerjee, S.; Barbour, S. G.; Baybayan, P. A.; Benoit, V. A.; Benson, K. F.; Bevis, C.; Black, P. J.; Boodhun, A.; Brennan, J. S.; Bridgham, J. A.; Brown, R. C.; Brown, A. A.; Buermann, D. H.; Bundu, A. A.; Burrows, J. C.; Carter, N. P.; Castillo, N.; Chiara, E. C. M.; Chang, S.; Neil Cooley, R.; Crake, N. R.; Dada, O. O.; Diakoumakos, K. D.; Dominguez-Fernandez, B.; Earnshaw, D. J.; Egbujor, U. C.; Elmore, D. W.; Etchin, S. S.; Ewan, M. R.; Fedurco, M.; Fraser, L. J.; Fuentes Fajardo, K. V.; Scott Furey, W.; George, D.; Gietzen, K. J.; Goddard, C. P.; Golda, G. S.; Granieri, P. A.; Green, D. E.; Gustafson, D. L.; Hansen, N. F.; Harnish, K.; Haudenschild, C. D.; Heyer, N. I.; Hims, M. M.; Ho, J. T.; Horgan, A. M.; Hoschler, K.; Hurwitz, S.; Ivanov, D. V.; Johnson, M. Q.; James, T.; Huw Jones, T. A.; Kang, G. D.; Kerelska, T. H.; Kersey, A. D.; Khrebtukova, I.; Kindwall, A. P.; Kingsbury, Z.; Kokko-Gonzales, P. I.; Kumar, A.; Laurent, M. A.; Lawley, C. T.; Lee, S. E.; Lee, X.; Liao, A. K.; Loch, J. A.; Lok, M.; Luo, S.; Mammen, R. M.; Martin, J. W.; McCauley, P. G.; McNitt, P.; Mehta, P.; Moon, K. W.; Mullens, J. W.; Newington, T.; Ning, Z.; Ling Ng, B.; Novo, S. M.; O'Neill, M. J.; Osborne, M. A.; Osnowski, A.; Ostadan, O.; Paraschos, L. L.; Pickering, L.; Pike, A. C.; Pike, A. C.; Chris Pinkard, D.; Pliskin, D. P.; Podhasky, J.; Quijano, V. J.; Raczy, C.; Rae, V. H.; Rawlings, S. R.; Chiva Rodriguez, A.; Roe, P. M.; Rogers, J.; Rogert Bacigalupo, M. C.; Romanov, N.; Romieu, A.; Roth, R. K.; Rourke, N. J.; Ruediger, S. T.; Rusman, E.; Sanches-Kuiper, R. M.; Schenker, M. R.; Seoane, J. M.; Shaw, R. J.; Shiver, M. K.; Short, S. W.; Sizto, N. L.; Sluis, J. P.; Smith, M. A.; Ernest Sohna Sohna, J.; Spence, E. J.; Stevens, K.; Sutton, N.; Szajkowski, L.; Tregidgo, C. L.; Turcatti, G.; Vandevondele, S.; Verhovsky, Y.; Virk, S. M.; Wakelin, S.; Walcott, G. C.; Wang, J.; Worsley, G. J.; Yan, J.; Yau, L.; Zuerlein, M.; Rogers, J.; Mullikin, J. C.; Hurles, M. E.; McCooke, N. J.; West, J. S.; Oaks, F. L.; Lundberg, P. L.; Klenerman, D.; Durbin, R.; Smith, A. J., Accurate whole human genome sequencing using reversible terminator chemistry. *Nature* **2008,** *456* (7218), 53-9.
291. Svensen, N.; Peersen, O. B.; Jaffrey, S. R., Peptide Synthesis on a Next-Generation DNA Sequencing Platform. *ChemBioChem* **2016,** *17* (17), 1628-1635.
292. Blanco, C.; Verbanic, S.; Seelig, B.; Chen, I. A., EasyDIVER: A Pipeline for Assembling and Counting High-Throughput Sequencing Data from In Vitro Evolution of Nucleic Acids or Peptides. *J Mol Evol* **2020,** *88* (6), 477-481.